SAINT PETERSBURG STATE UNIVERSITY

As manuscript

Danilov Lavrentii Glebovich

Study of amyloid properties of nucleoporin proteins and the effect of their aggregation on the import of macromolecules into the nucleus in yeast *Saccharomyces cerevisiae cells*

Scientific specialty 1.5.7. Genetics

Dissertation for the degree of Candidate of Biological Sciences

Translation from Russian

Scientific supervisor: Candidate of Biological Sciences.
Stanislav Alexandrovich Bondarev

Saint Petersburg
2024

Table of contents

List of abbreviations and symbols

BME-β-mercaptoethanol

IPTG-isopropyl β-D-1-thiogalactopyranoside

bp — pairs of nucleotides

PCR-polymerase chain reaction

EDTA-Ethylenediaminetetraacetic acid

YAPK-nuclear Pore complex

BSA — *bovine serum albumin* (bovine serum albumin)

C-DAG-*curli-dependent amyloid generator* (a system for testing the amyloid properties of proteins in bacteria)

HTT-*huntingtin* (human protein huntingtin)

IPTG-Isopropyl-β-D-1-thiogalactopyranoside

LiAc — *lithium acetate* (ацетат лития)

LBa-LB medium with ampicillin

mQ — deionized water

SDS — *sodium dodecyl sulfate* (додецил сульфат натрия)

SC — *Synthetic Complete* (synthetic environment based on YNB)

Q / N-rich-enriched with glutamine and asparagine residues

v/v — *volume/volume* (volume to volume ratio)

w/v — *weight/volume* (mass to volume)

YNB— -Yeast Nitrogen Base

Standard single-letter designations of nucleotides, as well as single-letter and three-letter designations of amino acids are used in the work.

Introduction

Relevance of the topic. Amyloids can form ordered aggregates organized into unbranched fibrils enriched with β-layers. Such aggregates are prescribed for various amyloidosis, such as Alzheimer's, Huntington's, and Parkinson's diseases. These aggregates are poorly soluble and their accumulation in the cell leads to a violation of cellular homeostasis and cell death. At the same time, there are examples of accumulated amyloids considered as functional. For all amyloids, common properties can be distinguished. These properties include binding to amyloid-specific dyes (Congo red and Thioflavin T) and the formation of detergents and protease-resistant aggregates. Due to the increasing frequency of amyloid diseases, proteome analysis is becoming relevant in order to identify and analyze new amyloidogenic proteins. Such proteins can form aggregates themselves or be the part of already existing aggregates. One of the most important processes inside the cell is the exchange of molecules between the nucleus and the cytoplasm. Additionally, the nucleoporin proteins forming a specific structure, the nuclear pore, provide an essential function there. Previously, the presence of amyloid properties in yeast nucleoporins was shown, but how their aggregation affects the transport of molecules between the nucleus and the cytoplasm was not studied. On the other hand, the conservatism of these proteins' ability to aggregate from the view of evolution has been poorly understood, representing a significant gap towards the better comprehension about the physiological role of particular protein aggregation.

Objective: To evaluate the conservativeness of the amyloid properties of nucleoporins with FG repeats and their aggregation effect on nuclear cytoplasmic transport in model systems.

The following tasks within the objective were formulated:

1. Verification of the amyloid properties of the human protein NUP58 *in vitro* and in model systems.
2. Search for the NUP58 site responsible for aggregation using deletion analysis in the C-DAG system and yeast cells.
3. Validation of the conservativeness in amyloid properties of orthologs of yeast nucleoporins Nsp1 and Nup145 in the C-DAG system and yeast cells.
4. Evaluation of the nucleoporin aggregation effect on nuclear-cytoplasmic transport in yeast cells.

Scientific novelty of the work. In this study, we analyzed the amyloid properties of nucleoporin proteins, which are found in all eukaryotic organisms. Early studies have shown that some yeast nucleoporins, such as the Nup100 protein, have amyloid properties. This prompted us to conduct bioinformatics screening of nucleoporins to assess the

conservativeness of amyloidogenic properties. The analysis revealed that nucleoporins from various organisms exhibit amyloid properties in the yeast and C-DAG systems. Moreover, for the human protein NUP58 additional tests were also performed. It was found that the region from 1 to 213 amino acids is necessary for the formation of amyloid aggregates. We also analyzed the effect of aggregation of nucleoporin protein fragments on nuclear-cytoplasmic transport in the yeast system. As a result, we have shown that fragments of nucleoporins$_{spNup98\ 250\text{-}500}$, Nup58$_{60\text{-}320}$ *of Taeniopygia guttata* and Nup98$_{250\text{-}500}$ *of Drosophila melanogaster* lead to a decrease in the import of macromolecules into the nucleus.

Theoretical and practical significance of the work. The results obtained in the current study provide a wider insight into the frequency of amyloids occurrence. The study highlights the conservative amyloid properties of nucleoporin proteins based on bioinformatic data and partially confirms these properties using experimental methods. The effect of aggregation of nucleoporin proteins on the import of macromolecules into the nucleus is also shown.

Methodology and methods of research. In the course of the thesis, a large number of modern research methods were used, including molecular biological methods for working with nucleic acids and proteins, biochemical analysis methods, fluorescence, polarization and electron microscopy. Experiments were performed on various model systems, such as *the in vitro* system, bacteria, and yeast. The methods of nuclear-cytoplasmic transport analysis were also applied to assess the import of macromolecules into the nucleus. Bioinformatics methods were used to evaluate the amyloid properties of nucleoporin proteins.

The degree of reliability and approbation of the results. The main results of the dissertation work were reported at four international conferences.

The materials of the dissertation are presented in three publications:

1. **Danilov L.G.,** Moskalenko S.E., Matveenko A.G., Sukhanova X.V., Belousov M.V., Zhouravleva G.A., Bondarev S.A. The Human NUP58 Nucleoporin Can Form Amyloids *In Vitro* and *In Vivo*. // Biomedicines. — 2021. — Vol. 9 — P. 1451.
2. **Danilov L.G.,** Sukhanova X.V., Rogoza T.M., Antonova E.Y., Trubitsina N.P, Zhouravleva G.A., Bondarev S.A. Identification of New FG-Repeat Nucleoporins with Amyloid Properties. // International Journal of Molecular Science. — 2023. — Vol. 24 — P. 8571.
3. Barbitoff Y.A., Matveenko A.G., Matiiv A.B., Maksiutenko E.M., Moskalenko S.E., Drozdova P.B., Polev D.E., Beliavskaia A.Y., **Danilov L.G.**, Predeus A.V.,

Zhouravleva G.A., Chromosome-level genome assembly and structural variant analysis of two laboratory yeast strains from the Peterhof Genetic Collection lineage //G3 Genes|Genomes|Genetics. — 2021. — Vol. 11

Main scientific results. The thesis presents the main scientific results of the research in the form of the three publications performed by the applicant in co-authorship:

1. In the experimental article "The Human NUP58 Nucleoporin Can Form Amyloids *In Vitro* and *In Vivo*"[30], published in Biomedicines (Scopus) in collaboration with Moskalenko S.E., Matveenko A. G., Sukhanova K. V., Belousov M. V., Zhuravleva G. A. and Bondarev S. A. published results on the amyloid properties of the NUP58 protein and its fragment from 1 to 213 amino acids.
2. In the experimental article " Identification of New FG-Repeat Nucleoporins with Amyloid Properties "[31], published in the International Journal of Molecular Science (Scopus) In collaboration with Sukhanova K. V., Rogoza T. M., Antonova E. Yu., Trubitsina N. P., Zhuravleva G. A. and Bondarev S. A., the results of bioinformatic evaluation of the conservativeness of amyloid properties of nucleoporin proteins and experimental verification of amyloid properties in the C-DAG system and in yeast *Saccharomyces cerevisiae are published.* This article also contains information on the effect of the [PIN^+] factor on the frequency of aggregation of nucleoprotein fragments.
3. In the experimental article "Chromosome-level genome assembly and structural variant analysis of two laboratory yeast strains from the Peterhof Genetic Collection lineage" [13], published in the journal G3 Genes|Genomes|Genetics (Scopus), co-authored with Barbitov Yu. A., Matveenko A. G., Matiiv A. B., Maksyutenko E. M. Moskalenko S.E., Drozdova P. B., Polevy D. E., Belyavskaya A. Yu., Popov A.V. and Zhuravleva G. A. published results on the effect of mutations in the NUP100 gene *NUP100*on the tendency to aggregation in yeast protein Nup100 in various strains.

In the top two articles, the personal contribution of the author consisted of the study design development, collection of experimental material, statistical processing of the obtained data, preparing tables and figures, and writing the manuscript. In the last one article, the author made a contribution in the form of an analysis of the Nup100 protein’s amyloid properties in various yeast strains, a description of obtained statistical results, and the preparation of illustrations.

The main provisions submitted for defense.

1. The human protein NUP58 can form amyloid aggregates stabilized by disulfide bonds *in vitro* and demonstrates amyloid properties both in the C-DAG system and in *Saccharomyces cerevisiae* cells.
2. Aggregation of the NUP58 protein is performed in the region from 1 to 213 amino acid residues with FG repeats.
3. Nucleoporin fragments from different species exhibit amyloid properties in various test systems. These proteins include the nucleoporins *Nup98* of *Homo sapiens*, *Schizosaccharomyces pombe*, and *Drosophila melanogaster*.
4. Yeast factor [PIN^+] does not affect the aggregation frequency of Nup98 from *Homo sapiens*, *Schizosaccharomyces pombe*, and *Drosophila melanogaster* nucleoporin fragments.

Scope and structure of work. The thesis consists of an introduction, a literature review, materials and methods, research results, discussion, conclusions, and a list of references containing 165 references. The work is presented on 100 pages, contains 31 figures and 11 tables.

CHAPTER 1. LITERATURE REVIEW

1. General characteristics of amyloids

Amyloids are ordered protein fibrils in which β-folded sheets are formed by the formation of intermolecular hydrogen bonds. These bonds are formed with a certain regularity, since the same amino acid sequences of monomers are involved in the interaction [73]. Today, an amyloid is considered to be any protein with no associated components that is localized in any cell compartment and has one of the following structures: a super-folded β-structure (parallel or non-parallel), a β-solenoid, or a stack of globules ([73, 142]). In medicine, when making a diagnosis of amyloidosis, amyloid is more often understood not only as a protein fibrils with a certain structure, but as the entire complex of proteins that is associated with this structure [16, 79, 152]. To date, we can distinguish a number of properties that are inherent in all amyloids (according to [1,3]):

1. Interaction with specific dyes, such as Congo Red and Thioflavin T.
2. The presence of a transverse striation along the main axis of the fibrills, which occurs as a result of the transverse arrangement of protein monomers relative to the main axis of the fibrillum.
3. Resistant to detergents such as SDS.
4. Fibril growth is caused by the addition of a monomeric protein to the protofibril, which is accompanied by a change in conformation [99].

The amyloidogenic properties of a protein are determined by the composition of its amino acid sequence, and some algorithms for predicting the amyloid properties of a particular protein are based on this. It is believed that amino acid sequences enriched with hydrophobic amino acids such as valine, isoleucine, and phenylalanine, as well as the amino acids glutamine and asparagine, have the greatest amyloidogenic potential, while sequences containing highly charged amino acids are not capable of forming amyloid aggregates [7]. Most of the currently known amyloids have pathogenic properties and are characterized by an increase in the level of protein in the cell [3]. However, over the past 5 years, a number of functional amyloids have been identified that are constitutively formed in cells or begin to form aggregates in response to changes in environmental conditions [128, 150]. Inclusion of a monomeric protein in aggregates often leads to partial or complete inactivation of the protein, and in rare cases-to the acquisition of new functions (according to the review [163]).

The term "*Prion*" was first coined by Stanley Prusiner to describe a particular variant of the PrP protein structure that leads to mammalian neurodegenerative diseases, such as scrapie or

sheep scratching (Prusiner, 1987). The main reason for the development of such diseases is that the monomeric protein PrP^{C} (*cellular*) changes its conformation and passes into the prion conformation-PrP^{Sc}, which accumulates in cells in the form of protein aggregates. Protein aggregates of the PRP protein of amyloid nature are found in the brain and spinal cord, in secretions from the lymphatic system, as well as in other organs and tissues [5]. The main features of protein aggregates discovered by Stanley Prusiner were their resistance to treatment with various detergents (SDS, urea), proteolysis, heating, and ultraviolet radiation [122]. Testing most of these traits is one step in proving that the protein has amyloid properties. The presence of infectivity is the main difference between prions and amyloids. During aggregation, the conformation of the monomeric protein changes and attachment to the aggregate occurs, which ensures the growth of fibrils. At the initiation stage, the processes of prion and amyloid formation do not differ [1]. In the case of functional amyloid formation, the level of protein production is sufficient for the monomers to bind to each other due to the formation of intermolecular interactions [1]. The resulting seed adds new monomers, which leads to the formation of an oligomer and a protofibril. In the case of prions and pathological amyloids, this process is initiated by an increase in the concentration of amyloidogenic protein. It is important to emphasize that each new non-infectious amyloid aggregate is formed independently of the previous one, whereas in the case of prions, the aggregates are cleaved, which leads to a prion conversion cycle [1, 92]. Prion infectivity is ensured by fragmentation of aggregates, which occurs due to the interaction of protein aggregates with chaperone proteins, which perform non-specific cutting of aggregates into smaller ones [85].

2. Biological role of amyloids

Initially, it was assumed that amyloids can only be pathogenic and lead to diseases, but over the past decade, a number of amyloids have been described that perform various physiological functions in the body of both prokaryotic and eukaryotic organisms [128, 150].

2.1. Functional amyloids

Functional amyloids were first described as extracellular protein components in higher eukaryotes-the spidroin and fibroin proteins. These proteins are components of the web and silk, respectively. There is still no clear understanding of the structure of amyloid data. Due to the special sequence $(Gly\text{-}Ser\text{-}Gly\text{-}Ala\text{-}Gly\text{-}Ala)_{of\ n}$ (in fibroin) [129] or the presence of repeated alanine motifs (in spidroin), amyloid fibrils are formed during the secretion of these proteins from the salivary glands [66]. An interesting question is why there is no pathogenicity in the case of functional amyloids in the cell. Possible mechanisms that cause pathogenesis in the

development of amyloid diseases include the formation of extracellular amyloid formations (plaques in Alzheimer's disease) and intracellular formations (in Parkinson's and Huntington's diseases) [145], as well as the formation of protein oligomers, which are the most cytotoxic [76]. It is important to take into account the interaction of mature amyloid fibrils with cell membranes: such interaction can lead to disruption of the membrane integrity and its depolarization; splitting of the fibrils into toxic oligomers can lead to secondary nucleation of the amyloid protein, which will enhance pathogenesis [156]. To level the toxicity of amyloid fibrils and preserve the normal functioning of the cell, the following mechanisms can be identified in a cell with functional amyloids [70]:

- Regulation of the production of amyloidogenic proteins and peptides (control of transcription and translation, as well as control of proteolytic cleavage of proteins).
- Minimization of the lifetime of prefibrillary oligomers that have the greatest toxicity (this is often achieved due to a higher rate of mature fibrillation formation than the rate of oligomer formation).
- Use of molecules that regulate the cellular response to environmental conditions to control the assembly of functional amyloid fibrils.
- Assembly of amyloid fibrils in various cell compartments (endoplasmic reticulum).
- "Disassembly" of fibrils when changing environmental conditions or using chaperone systems of the cell.

Thus, the main difference between functional amyloids and pathological amyloids is that the cycle of assembling and disassembling fibrils is characterized by greater control by cellular systems and signals from the external environment, which, in turn, allows you to control the place, time and number of fibrils formed.

2.1.1. Functional amyloids of prokaryotes

To date, the most studied groups of prokaryotic functional amyloids are Curlins and Chaplins, and there are several other groups of functional amyloids (according to [128, 152], data are presented in Table 1). Most of the currently discovered functional bacterial amyloids most often perform a protective or adhesive function, which is undoubtedly due to the structural and biochemical features of amyloids [128].

Table 1 – Bacterial functional amyloids.

Species	**of Protein**	**Function in the cell**	**References**
Escherichia coli, Salmonella enteritidis	CsgA	Biofilm component, cell-substrate adhesion	[26, 53]
Pseudomonas sp.	FapC	Biofilm component, cell-substrate adhesion	[39]
Streptomyces coelicolor	Chaplins (ChpA-H)	Bacterial spore surface protein, air hyphae formation	[45]
Bacillus subtilis	TasA	Biofilm component, cell-substrate adhesion, bacterial spore surface protein	127]
Klebsiella pneumoniae	Microcin E492	Antimicrobial protection	[140]
Staphylococcus aureus	PSM	Biofilm component, cell-to-substrate adhesion	[137]
Streptococcus mutans	Adhesin P1	Biofilm component, cell-to-substrate adhesion	[113]
Mycobacterium tuberculosis	MTP	Lamin-associated pilae formation – host interaction	[11]
Xanthomonas axonopodis	HpaG	Cytotoxic activity, virulence	[111]

The CsgA protein is one of the first discovered and most studied of all functional bacterial amyloids. Initially, it was detected as a protein in a pathogenic strain *of E. coli* and described as fibronectin-binding "curled pili" [115]. At the first stage of the study of extra-clad formations using electron microscopy, it was shown that these protein fibrils, which at low magnification look like an amorphous matrix around bacteria, at high magnification are represented by single fibrils with a width of 6-12 nm. These fibrils are resistant to the effects of proteases and detergents, and also bind the amyloid-specific dyes Congo Red and Thioflavin T and have an ordered structure

enriched with beta-sheets [26].

CsgA protein encoded by the CsgA gene *csgA* (from English-*curlin subunit gene*) is the main structural protein of amyloid fibrils. Transcription *of the csgBAC operon* is triggered by the RNA polymerase sigma factor RpoS. This sigma factor is expressed in the stationary phase of bacterial growth, and its expression positively correlates with a decrease in temperature and osmolarity of the medium [114]. Thus, CsgA protein fibrils are formed as a response to unfavorable environmental conditions in the stationary phase of bacterial growth, which corresponds to the role of biofilms in the survival of microorganisms. Another important component of the system is the CsgB protein. It acts as a factor of CsgA protein nucleation and a minor component of the resulting amyloid fibrils [17, 60]. The CsgB protein is capable of forming small amyloid fibrils independently, but its main function is to initiate aggregation of the CsgA protein. The CsgA and CsgB protein sequences are 30% identical, which contributes to the formation of similar secondary structures, which leads to the initiation of aggregation [14]. The third protein that is necessary for the formation of fibrils and functions on the cell wall surface is the CsgF protein. This protein has chaperone activity and is responsible for the correct localization of amyloid fibrils on the cell surface. In strains with deletion of the csgF gene, the binding of fibrils to the cell surface is disrupted [108].

CsgG protein is also a component of the amyloid fibrillation system of the CsgA protein. It is a lipoprotein that binds to the outer cell membrane and regulates the intracellular concentration of CsgA and CsgB proteins. This regulation is carried out through the formation of a channel through which CsgA and CsgB proteins enter the cell surface. Before incorporation into the outer membrane, the CsgG protein forms soluble oligomers consisting of 16 subunits organized into 2 ring octameric complexes. Monomers contain 4 α-helices and 6 β-sheets in the structure. However, when the transition to the membrane-bound state occurs due to the attachment of a lipid anchor from the N-terminus of the protein, the transmembrane section of the channel assumes the structure of a β-barrel [56]. CsgA, CsgB, and CsgF proteins pass through the resulting channel and form amyloid fibrils on the cell surface.

2.1.2. Functional amyloids of eukaryotes

Lower and higher eukaryotes also have functional amyloids that perform various functions in the body. An example of functional amyloids in lower eukaryotes is the protein Bgl2, which is an important element of the cell wall in the yeast *Saccharomyces cerevisiae*. The main component of the cell wall is β (1-3)-and β(1-6) - glycans. Initially, glycans are synthesized as linear molecules, and then, due to glycosyltransferases, new β(1-3)- and β(1-6) bonds are formed. The Bgl2 protein, which has glycosyltransferase activity, has been shown to have amyloid properties

[75]. During cell wall formation, the Bgl2 protein in its amyloid conformation participates in the formation of β (1-6) glycosidic bonds between various glycans [8]. Another example of a functional amyloid is the Het-S protein in the fungi *Podospora anserina*. This type of fungi is characterized by the predominance of the syncytial stage in the life cycle. Syncytia of two different fungi can merge to form a heterokaryon. The fusion process is controlled by the Het locus. If these loci are the same in merging hyphae, the fusion process will be successful, and if there are differences, then due to vegetative incompatibility, the heterokaryon will die off. The key participant in the process of vegetative incompatibility is the prion [*Het-s*]. There are 2 alleles of the *het-s* gene*: het-s* and *het-S.* The product *o*f the *het-S* gene, the NO-S protein, does not adopt the prion conformation. *The P. anserina strain*carrying the protein in this form is designated [Het-S] [29]. When the hyphae of two strains [Het-S] and [Het-s] merge, a vegetative incompatibility reaction occurs and the heterokaryon dies at the fusion site. Thus, the amyloid form of the Het-S protein triggers programmed cell death [125].

Functional amyloids also include the protein CPEB (cytoplasmic polyadenylation element binding) of the mollusk *Aplysia californica*, as well as its ortholog *Orb2* in *Drosophila melanogaster*. The main function of the CPEB protein is mRNA transport in neurons [23]. In response to the release of serotonin, amyloid aggregates of the CPEB protein are formed, which also include RNA. The resulting aggregates maintain and stabilize synapses for several days, which ensures the formation of long-term memory [143]. Similar functions were demonstrated for the drosophila ortholog Orb2. Moreover, it was shown that a violation of the aggregation ability of the Orb2 protein led to a loss of the ability to remember information in drosophila flies. During the formation of aggregates of the Orb2 protein in complex with RNA, neural connections that are involved in memorizing new information are maintained [96]. Another protein whose aggregation is associated with memory in vertebrates is the FXR1 protein. This protein was found in amyloid aggregates in rat brains, and was practically undetectable in the monomeric state. The main function of the FXR1 protein is to bind to mRNA, protecting it from degradation. This mechanism allows you to regulate the level of expression of certain proteins, which in turn can be a mechanism for the formation of long-term memory. An important characteristic of FXR1 is its high conservativeness in mammals, which suggests a functional role for its orthologs [147].

Another functional amyloid is the Pmel17 protein, or rather its part, which is formed as a result of processing the primary protein product of the gene *pmel*. This protein in its aggregated form is localized in the cytoplasm of skin melanocytes. There is an assumption that the network structure of amyloid fibrils binds melanin and in this form the pigment accumulates and is stored in cells [47]. In 2017, a site was identified that is responsible for the transition of the PMEL protein to the amyloid form. This region with 148 to 223 amino acids was named CAF (from the

English CoreAmyloid Fragment). It was shown that 27 mutations in this region disrupted the formation of Pmel17 fibrils, including 9 completely. This was due to a violation of the stage of nucleation of fibrils. The important role of aromatic radicals of amino acids in this region for the formation of amyloid fibrils has been shown [62]. An example of functional amyloids that play an important role in cell signaling is the RIP family of proteins (from the English Receptor Interacting Protein kinase). The main function of the RIP1 signaling kinase is to determine the fate of the cell: if RIP1 is polyubiquitinated, the cell survives [160]; if it interacts with RIP3 kinase, the cell will embark on the path of necrosis or apoptosis in the case of ubiquitination with kinase (according to [46]). Kinases contain a homologous sequence called RHIM (from the English RIP Homotypic Interaction Motif), due to which they interact with each other. The presence of mutations in this sequence disrupts the interaction of kinases, thereby disrupting the function of the complex. It was shown that the complex of RIP1 and RIP3 kinases forms fibrils that exhibit amyloid properties, and it is in this conformation that it is a signal component that induces necrosis [89].

A certain group of functional amyloids is associated with reproductive function. One example is the presence of Balbiani bodies, specialized amyloid-like organelles that contain mitochondria, RNA, and the endoplasmic reticulum. Amyloid properties have also been demonstrated for proteins forming oocyte membranes in insects and mammals. One such example is the presence of amyloid structures in the chorion of the butterfly *Antheraea polyphemus* [67]. In the course of the experiments, it was shown that the X-ray scattering spectrum is similar to the spectrum characteristic of amyloids. It has also been shown for human protein fragments ZP1–ZP4 that they bind to amyloid-specific dyes, and also demonstrate the characteristic morphology of aggregates obtained *in vitro* [93]. Presumably, similar amyloid structures in the oocyte envelope in various organisms contribute to protection against various external influences, including mechanical pressure and temperature changes. Moreover, such amyloid aggregates have been described as structural elements of chicken oocytes and are also found in the egg shells *of D. melanogaster* [144].

Functional amyloids have also been described in another kingdom of living organisms – plants. The main function that they perform is to store nutrients in the form of proteins. One example of such amyloids is the protein Vicilin, aggregates of which are stored in *Pisum sativum seeds*. The study showed that the amount of aggregates increases during seed maturation and decreases during seed germination. It has also been shown that the resulting aggregates are resistant to digestion by gastrointestinal enzymes and exhibit toxicity to yeast and mammalian cells [12]. The functional amyloid CnAMP2 performs a different function, namely, it is an amyloid-like AMP (antimicrobial peptide). This protein was isolated from the liquid endosperm

of the coconut *Cocos nucifera*. Aggregates obtained in an aqueous buffer have such amyloid properties as binding to dyes (Congo red and Thioflavin T), and fibrils are also observed when visualized using TEM. However, there is no evidence that the CnAMP2 protein exhibits AMP properties in an aggregated form [55].

3. Pathological amyloids

To date, more than 30 diseases are known, the cause of which is the formation of amyloids. The type of treatment depends entirely on the type of protein being aggregated and, therefore, on the underlying pathogenesis. Proteins whose aggregation causes the development of amyloid diseases include: Aß, α-synuclein, tau protein, β-2-microglobulin, amylin, and many others [120].

3.1. Amyloid peptide β

Aß (Amyloid peptide β) is a product of enzymatic cleavage of the transmembrane domain of the APP protein under the action of β - and γ-secretase enzymes (Selkoe, 2011). To date, 2 Aß peptides are known, consisting of 40 and 42 amino acid residues, respectively. The most toxic is the peptide oligomers with 42 amino acid residues [43]. In Alzheimer's disease, aggregates of the Aß peptide accumulate, and there is evidence that aggregates can include various proteins, including the tau protein [32]. Moreover, the Aß protein has been shown to interact with the PrP protein in yeast cells [130]. Usually, the symptoms of Alzheimer's disease appear later in life due to changes in the ratio of β - and γ-secretase enzymes and the accumulation of the pathogenic form of the Aß protein in neurons [138]. However, mutations have been described that lead to an increased likelihood of Alzheimer's disease at an early age due to changes in the level of full-length APP production or an increase in the enzymatic activity of γ-secretase and an increase in the level of the Aß peptide [132]. To prove that this amyloid is a prion, experiments were conducted to prove the infectivity of aggregates. Injection *of in vitro-derived fibrils*or brain homogenate from a sick animal resulted in increased amyloidogenesis or induction of a prion transition [101, 106].

3.2. SSA protein

The protein determinant of amyotrophic lateral sclerosis is the protein SAA1 (Serum Amyloid A). *The Saa gene family* in humans encodes 4 proteins, one of which is expressed continuously (SAA4), while the others are expressed depending on environmental factors [162]. The level of SAA1 increases in response to a chronic bacterial infection, and during such an infection, amyloid aggregates, mostly consisting of SSA1 protein, can be detected in the blood

serum. However, there are some difficulties in proving the prion properties of the SAA1 protein. Despite the fact that the injection of fibrils obtained from a sick animal accelerates amyloidogenesis in the recipient, based on this alone, it cannot be said that this protein has infectious properties due to the fact that it itself is not capable of *de novo aggregation* [107].

3.3 tau protein

The main function of the tau protein is to stabilize microtubules in neurons. In the study of neurodegenerative diseases such as Alzheimer's disease and Parkinson's disease, it has been shown that the tau protein is included in the resulting protein aggregates (Aß or α-synuclein) or forms separate small aggregates. These aggregates can be transferred from cell to cell and are infectious when introduced into the brain. This was proved in an experiment in which oligomers of the tau protein isolated from the brain of a person who died from Alzheimer's disease led to the occurrence of the disease in mice [87,100].

3.4 Huntingtin protein

Aggregation of the huntingtin protein leads to the development of Huntington's disease. This is a hereditary disease caused by an increase in the number of repeats of the CAG code in *the HTT gene*encoding the amino acid glutamine. Currently, the HTT protein is considered to be involved in vesicle transport and intracellular transport. The HTT protein also acts as a transcription factor, in particular, it regulates the transcription *of the BDNF gene* (the protein encoded by this gene is responsible for regulating the formation of neurons during neurogenesis) [15].

In the human population, up to 34 a.c. glutamine residues are usually found in the HTT protein [88]. However, when the number of repeats is exceeded, these amino acid sequences assume a different conformation from the main one for the HTT protein, and form toxic amyloid aggregates that accumulate in various parts of neurons in the basal ganglia and other brain structures [133]. At first, this leads to a violation of shallow gait, the appearance of tremors and "dancing gait", and as the disease progresses, the functions of the cerebral cortex are disrupted and the striatum atrophies, which ends in a fatal outcome. [159]. At the cellular level, several processes occur at once, which lead to the death of neurons and disruption of brain function. Aggregates of both the full-length HTT protein and its poly-Q region can be formed both in the cytoplasm and in the nuclei of neurons. In the nuclei, these aggregates sequester other proteins, which leads to a violation of transcription regulation. In the cytoplasm of the cell, these aggregates involve other proteins of the cell, and the amount of soluble HTT protein decreases. The formation of aggregates in the cytoplasm leads to disruption of axonal transport in neurons

and destruction of synapses, which, in turn, leads to the development of Huntington's disease [15].

4. Methods for identifying amyloids

4.1. Experimental methods

4.1.1 Proteomic screening systems

Biochemical methods for identifying amyloids are based on their biochemical properties. Initially, in the 20th century, there were methods based on the detection of binding to Thioflavin T or S, resistance to proteases and detergents, which made it possible to determine the amyloidogenicity of one particular protein. Until recently, there were no experimental methods for detecting amyloidogenic proteins on the scale of whole proteomes. However, two methods have recently been developed, one of which has since been improved: TAPI (*Technique for Amyloid Purification and Identification*-protocol for purification and identification of amyloids) and PSIA (*Proteomic Screening and Identification of Amyloids* – Proteomic Analysis and identification of amyloids). Both are based on the resistance of amioloids to denaturing agents (SDS, sarcosylate) [3]. In the first method, TAPI, the following manipulations are performed to identify amyloids. At the first stage, the cells are destroyed, then the resulting solution is centrifuged in a gradient of 40% sucrose. As a result of these manipulations, cellular proteins are separated, and the sedimentary fraction contains proteins that are part of amyloid fibrils. The resulting fraction is selected and heated to 37°C in a 2% SDS solution to destroy non-amyloid protein formations. Then, on the SDD-PAGE, stable amyloid aggregates and soluble protein molecules are separated. Protein aggregates do not enter the polyacrylamide gel well and remain in its upper part, from where they are cut out and subjected to trypsinolysis to separate into smaller fragments. The resulting proteins are then identified by tandem mass spectrometry [82]. The PSIA method uses two-dimensional polyacrylamide electrophoresis for separation, which makes it possible to compare the molecular composition of two samples with high accuracy. Before applying to the gel, proteins from each sample are labeled with a fluorochrome specific to each sample. The protein fractions are then separated by two-dimensional electrophoresis. Then a fraction of detergent-resistant proteins is excised from the gel, and the proteins contained in it are subjected to trypsinolysis and determination by tandem mass spectrometry [109]. The latter method has been modified to improve the accuracy of predictions. In parallel with identification using two-dimensional polyacrylamide gel electrophoresis, liquid chromatography analysis is performed. To do this, a mixture of high-molecular protein aggregates is dissolved and treated with trypsin. The individual peptides are then separated by liquid chromatography and analyzed

using mass spectrometry [1]. It is important to note that the proteins detected by these methods are only candidates for the role of amyloids, and additional experimental evidence is required to prove their amyloid properties. These methods include testing for the formation of SDS-resistant aggregates in *in vivo* and *in vitro systems*, as well as testing for binding to amyloid-specific dyes, such as Thioflavin S or Congo red.

4.1.2. The C-DAG system

This experimental system was proposed in 2013. This system was based on the well-known functional amyloid *of E. coli bacteria*, which belongs to the Curli protein group. The N-terminal sequence of the CsgA protein is signaling and is involved in the export of proteins to the cell surface. When this signal sequence is attached to the N-terminus of the test protein, the protein is exported to the bacterial cell surface, where amyloid fibrils will already be assembled. A large number of methods that can confirm the amyloid nature of the resulting fibrils (determination of the colony phenotype binding to the Congo red dye, visualization of fibrils using TEM and analysis of birefringence) make this method very good for mass screenings of potentially amyloidogenic proteins (Figure 1).

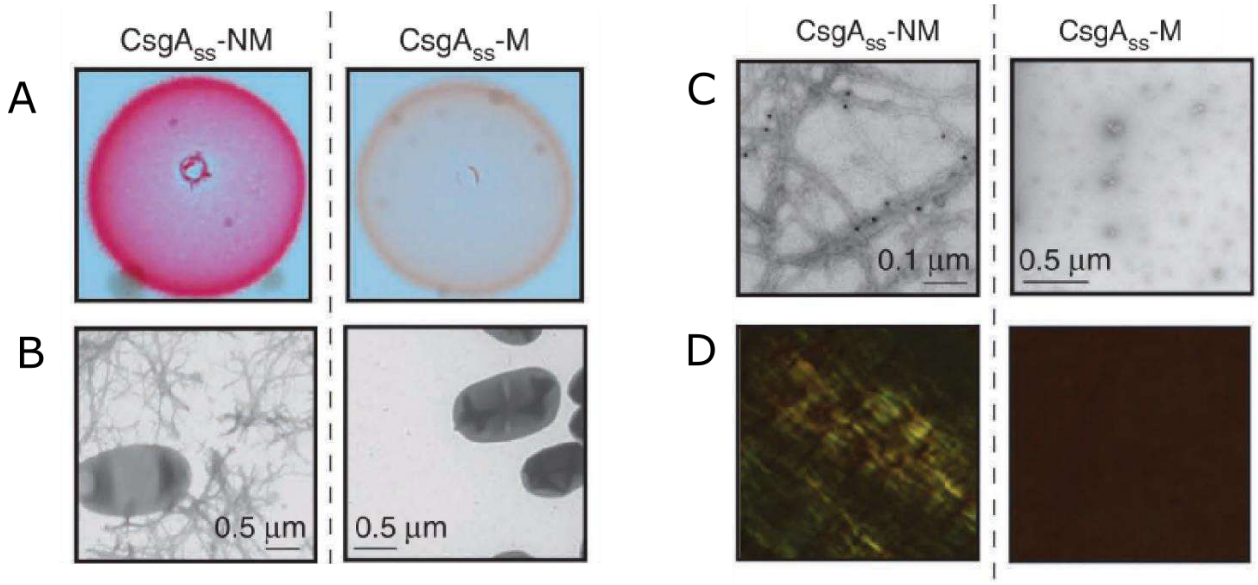

Figure 1 — C-DAG system. A. When grown on a medium with Congo red, colonies of bacteria that produce CsgAss-NM are colored red. **B.** CSGASS-NM secretion leads to the appearance of fibrillar aggregates that can be visualized using electron microscopy. **C.** Fibrillar aggregates formed by the CsgAss-NM protein, They can be detected by TEM after binding to labeled antibodies to the Sup35 protein. **D.** When the CsgAss-NM protein is overproduced, fibrillar aggregates also give an apple-green glow as a result of birefringence in polarized light (according to [146]).

4.1.3. Yeast systems

S. cereviseae yeast cells can be used to study the amyloid properties of proteins that are described as potential amyloids as a result of bioinformatic screenings*S. cereviseae*. For such

tests, constructs are used that allow the overproduction of proteins of interest crosslinked with fluorescent proteins in yeast cells. Detection of aggregates can be performed using fluorescence microscopy (the presence of luminous foci may indicate the presence of amyloid properties). Another property of amyloids that is tested in such systems is resistance to detergents, such as SDS. For this purpose, tests are performed using the SDD-AGE method to identify stable aggregates [25, 6, 124].

The ability of *Sup35* protein to form aggregates in yeast cells can be used to test various proteins whose amyloidogenicity is predicted using various algorithms. Previously, it was shown that overproduction of a chimeric protein consisting of the human amyloidogenic protein and the prion domain *of the yeast Sup35*protein leads to aggregation of the Sup35 monomeric protein and the appearance of the [*PSI*$^{+}$] factor in yeast cells in the absence of pre-existing prions, such as [*PIN*$^{+}$], which can serve as a matrix for aggregation of the Sup35 protein. As a positive control, the yeast test system uses a construct containing the Sup35 prion domain fused with the Aß peptide [25]. If the protein of interest is amyloidogenic, the prion [*PSI*$^{+}$] appears in the yeast cell (Figure 2). It is assumed that the prion domains of the Sup35 monomeric protein aggregate in the cell as a result of the formation of amyloid aggregates of the protein of interest. When the prion [*PSI*$^{+}$] is induced, cell growth will be observed on media that do not contain adenine, and they will be white on 1/4 YEPD medium, and after a series of passages on YEPD medium with HGH, they will lose the prion phenotype. This system uses a premature stop codon in the Ade1 gene. In cells that do not carry the [*PSI*$^{+}$] prion, the prematurely generated stop codon is not read, and as a result, the functional enzyme is not synthesized. This leads to the accumulation of red pigment in the cells in the case of growing cells on 1/4 YEPD medium and the absence of cell growth on medium without adenine. This verification system was proposed by Yuri Olegovich Chernov [25].

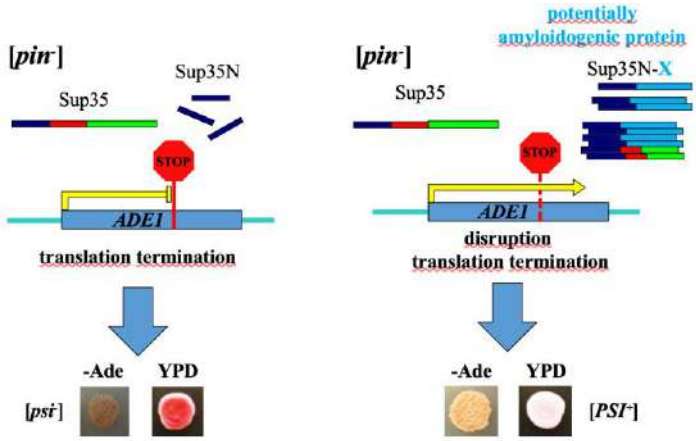

Figure 2-Yeast test system. In the case of potentially amyloidogenic protein crosslinked with the N-domain of Sup35 protein, protein aggregates are formed, which induces aggregation of Sup35 protein, which leads to the appearance of the prion [*PSI*$^{+}$]. Drawing provided by A. A. Zelinsky, personal message.

Another version of the system, which takes advantage of the yeast protein Sup35's ability to form amyloid aggregates, was proposed by Vaughn Der Haar in 2007. In this method, we proposed replacing the N-terminal domain of the Sup35 protein, which is necessary for the formation of the prion [PSI^{+}], with a potential amyloid protein. Using such system, prion formation can be detected using standard selective media for *S. cerevisiae yeast* [158]. An important advantage of this system is that the analysis of amyloid properties is carried out without the wild-type Sup35 protein, which can, although with a low frequency, spontaneously aggregate and give a false positive result. However, a common disadvantage of such methods is that the studied protein is overproduced, which increases the probability of aggregates forming. Also, it is worth noting that we over-produce human proteins in cells of another organism, and the absence of any post-translational modifications and chaperone systems can lead to both false positive and false negative results.

5. The nucleoporin family of proteins

5.1. Characteristics of nucleoporin proteins

Nucleoporins are an extensive family of proteins, with more than 3,000 known mammalian proteins [40]. These proteins form a structure called the nuclear pore (Figure 3). This pore is a symmetrical structure containing 8 identical components [9]. When studying the nuclear pore using cryo-electron microscopy, researchers distinguish 3 parts: (i) the nuclear basket, (ii) the cytoplasmic ring, and (iii) the central pore framework (Fig. It is worth noting that each nuclear pore is a unique set of different nucleoporin proteins, and each pore is responsible for the transport of certain molecules inside the cell. Proteins in the pore structure form various subcomplexes, which are formed on the basis of the biochemical affinity of various proteins [78].

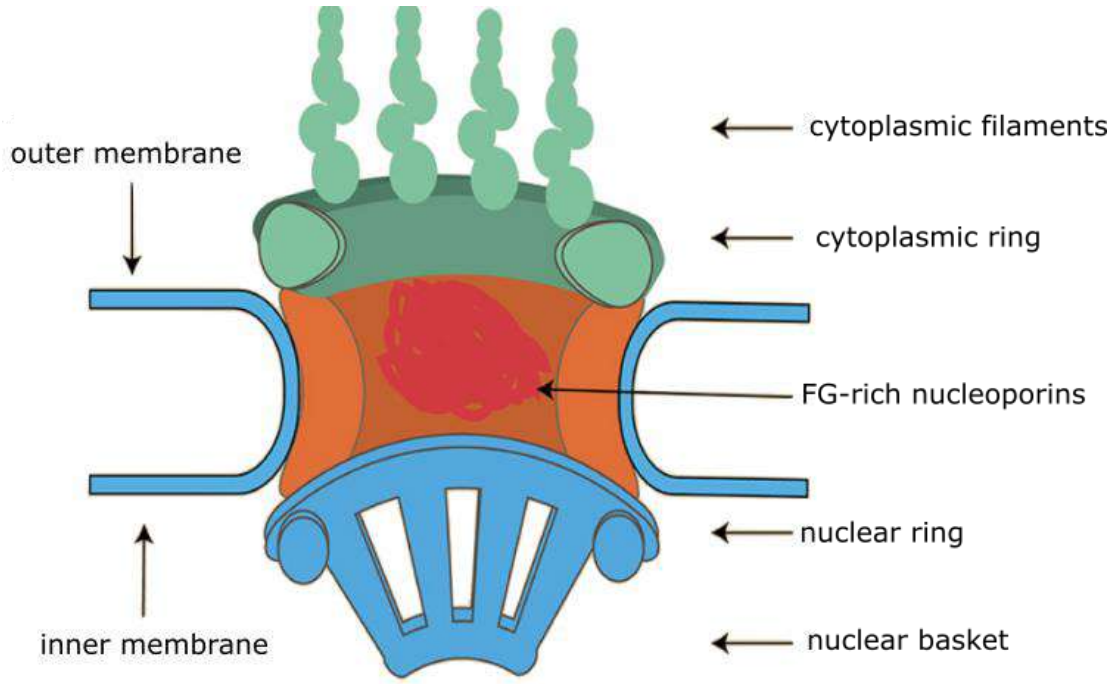

Figure 3-Structure of the eukaryotic nuclear pore. By [78]

Depending on the location of nucleoporins in the nuclear pore, they may contain different types of structural domains. Proteins contain α-helices, β-sheets, and special structural units – phenylalanine-glycine repeats (FG repeats) [63]. About a third of the nucleoporin proteins contain such FG repeats. Such structural elements are enriched in the nucleoporin sequences that are located in the middle part of the nuclear basket. It is assumed that these nucleoporins, having a disordered structure, form a gel in the center of the nuclear pore, which acts as a selective filter. FG repeats also play an important role in recognizing molecules for transport and binding to it [68, 78]. The structure of the nuclear pore complex is highly conserved. A study conducted in yeast compared with other eukaryotes showed similarities in the localization and function of nucleoporin proteins. However, the amino acid sequence of these proteins has not been shown to be sufficiently conserved [78]. Due to the fact that different nucleoporins can be expressed in different tissues, mutations in them can lead to various disorders in the development of organ systems or even the whole organism [78]. The functions of nucleoporins also include transcription regulation, both mediated through the regulation of transcription factor transport into the nucleus and through interaction with chromatin adjacent to the inner membrane of the nucleus near the nuclear pores [91, 164]. A complex system of interaction between nucleoporins, signal proteins, and transport targets is involved in regulating cell differentiation and maintaining their functions [78, 165].

NUP58 protein

Human protein NUP58 is a protein of the middle part of the nuclear pore and contains a large number of FG repeats [78]. In the nuclear pore, this protein functions as a tetramer due to its C-terminus [80]. FG-repeat-rich regions interact with other proteins involved in nuclear pore transport, in particular with complex partners (NUP54 and NUP62 proteins), as well as with importin-β and Cariferin β-1 [94]. The NUP58 protein forms homotetramers or heterotetramers with the NUP54 protein in the central channel of the pore. In the NUP58 protein itself, a region with α-helices (239-415 a.s.) can be distinguished, which is flanked by unstructured regions rich in FG repeats [80]. The complex of NUP54 and NUP58 interacts with the NUP62 protein, which forms a complex of three proteins that is anchored in the cell membrane [141]. The NUP54 and NUP58 proteins play a key role in the "opening-closing" cycle of the nuclear pore. Namely, the dimer consisting of the NUP58 protein is shifted relative to another similar dimer and the nuclear pore channel opens [141]. It should be noted that sites enriched with FG repeats also participate in nuclear cytoplasmic transport. It has been shown that importin proteins bind to these regions and transport importin-carrying molecules to and from the nucleus [80]. Another function of the NUP58 protein is to interact with the fission spindle and centrosomes during mitosis. It has been shown that a decrease in the amount of NUP58 protein leads to abnormal centrosome formation and mitotic anaphase disturbances [61].

5.2 Amyloid properties of nucleoporins

An important function of barrier nucleoporins, as basic components of the nuclear pore complex, is to ensure the selective exchange of macromolecules between the nucleus and cytoplasm. The implementation of this complex task is achieved due to the peculiarities of the amino acid sequence of these proteins. The primary structure of barrier nucleoporins is characterized by the presence of extensive internally disordered regions of FG repeats, which are replaced by segments enriched in glutamine and asparagine (Q/N) [33]. Nevertheless, the features under consideration are also found in the structure of yeast infectious amyloids. In this case, the presence of such regions contributes to internal reorganization and the formation of a stable β-folded conformer, which is formed after [157]. In other words, the same structural features are involved in the functioning of the nuclear pore complex along with the formation of amyloid fibrils.

Under in *vitro conditions*, many FG-nucleoporins form hydrogels in a certain concentration, actually reproducing the structure of the permeability barrier of the nuclear pore complex [49, 105]. This phase separation is caused by amyloid-like interactions between nucleoporins. Based on this, it can be assumed that the aggregation of nucleoporins can

participate in the regulation of transport. It is known that about 200 proteins of the yeast *Saccharomyces cerevisiae* have similar fragments to amyloid proteins in their amino acid sequence [10, 103]. Most yeast nucleoporins have been shown to have amyloid properties, such as the formation of detergent-resistant aggregates [10]. Among them, there are barrier nucleoporins enriched in FG and Q/N regions, as well as proteins containing aromatic and hydrophobic amino acid residues (Fig.59 Hydrophobic interactions between FG motifs are extremely important and necessary for creating a size-selective barrier for protein diffusion in the nuclear pore complex [118].

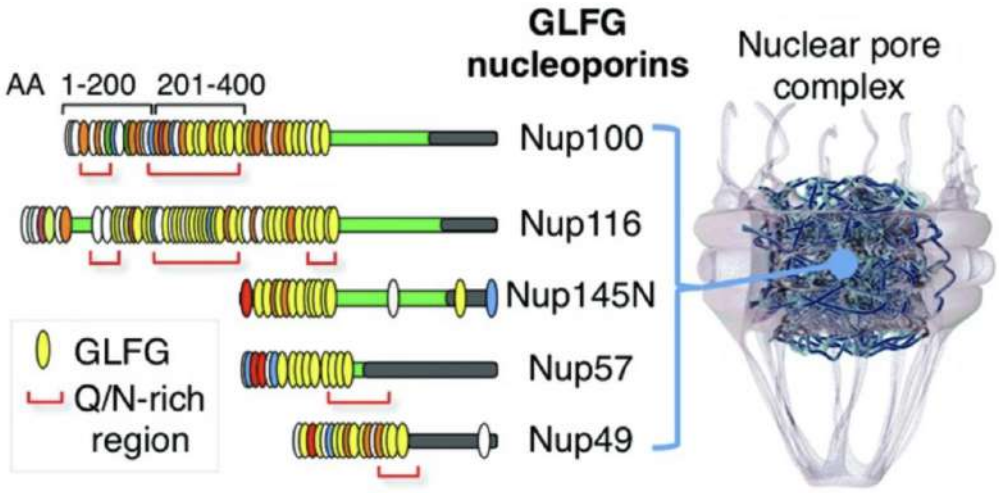

Figure 4-Diagram of the complex of the nuclear pore and internally disordered GLFG nucleoporins that make up its central region

During experimental tests, it was shown that the Q/N-enriched region of FG-nucleoporin fused with CFP Nup100 *S. cerevisiae*, namely amino acids (201st to 400th), forms glow foci when overexpressed in wild-type yeast cells. The formation of such foci leads to a violation of the localization of other FG nucleoporins, as a result of which they are found in the zone of glow points, and not in the region of the nuclear pore [59].

In addition, the Nup100 fragment, which has the greatest similarity to yeast prions, was tested for its ability to form aggregates in *vitro*. It was found that the amino acid sequence from 300 to 400 has seven FG repeats and consists of 38% of residues Q and N. It was shown that this fragment can form fibrils *in vitro.* Even if Nup100 $aggregates_{300\text{-}400\ \text{are added}}$ to the protein fragment solution, a significant lag phase is detected in the complete absence of pre-existing fibrils. However, when preformed Nup100 300-400 aggregates are added to the reaction $medium_{300\text{-}400}$, no increase in the aggregation rate is observed. At the same time, when adding $Nup100_{201\text{-}400}$ in *vivo*, there is a clear dependence on the presence of a pre-existing factor [PIN^{+}]. Thus, the obtained aggregates revealed a fluorescent glow when interacting with Thioflavin T, as well as a morphology characteristic of amyloids under electron microscopy.

It should be noted that not only individual regions of Nup100 nucleoporin are capable of aggregation. For example, a full-length protein fused with GFP overexpressed in yeast cells showed multiple foci of fluorescence. The isolated aggregates proved to be resistant to SDS treatment, and also had the ability to induce changes in the structure of soluble Nup100 to an amyloid-like one [59].

Most of the yeast nucleoporins, including the Nsp1 protein, can also be attributed to yeast amyloids [10]. Studies were conducted for this protein, which showed that it can form hydrogels [4]. According to the two-dimensional NMR spectrum, mobile segments do not have a constant structure [71]. In the course of the conducted studies, it was shown that in the case of hydrogels formed by the Nsp1 protein, an interaction between phenylalanine residues is observed. Most likely, such hydrophobic interactions are necessary for gel formation, since mutant FG domains without hydrophobic residues do not form hydrogels [49]. The predominance of the β-folded structure was also shown for fragments enriched with NQTS amino acid residues [161].

According to other experiments, the nucleoporin fragment $Nsp1_{2\text{-}277}$ can be assumed to form intermolecular β-sheets, which act as the main structural element of the hydrogel [4]. It is also known that the FG / FxFG domain of the Nsp1 protein forms a hydrogel with permeability properties that are similar in nature to the barrier of the nuclear pore complex [49]. It is important to note that inter-stranded β-sheets are also characteristic of amyloid fibrils [27]. In earlier studies, some nucleoporins were characterized as Q/N-rich ([103] and associated with such amyloid-forming proteins as huntingtin and its variants or yeast translation terminators Sup35 [34].

An example of an amyloid-forming Q/N-rich domain is residues 2 to 41 of yeast protein Sup35 [83]. Two-dimensional NMR spectroscopy of the Nsp1 protein shows that FG repeats with Q/N-enriched inserts interact through intermolecular β-sheets in the same way as in individual Sup35 protein molecules [4]. Based on this similarity, interactions between the Nsp1 and Sup35 domains are possible. This fact was confirmed by studying hydrogels from the N-terminal ($FG^{Nsp11}_{2-175-175}$) or full FG/FxFG domain of Nsp1 ($FG\ /\ FxFG^{Nsp11}_{2-601-601}$) and fluorescently labeled $Sup35_{2\text{-}140}$. During the experiment, the fluorescence level inside the FG hydrogel increased 100-fold. These results allow us to state the fact that proteins enriched with FG repeats can interact with protein fragments $Sup35_{2\text{-}140}$. Based on this, it can be suggested that proteins rich in FG repeats may be part of aggregates of known amyloids.

5.3 Effect of protein aggregation on nuclear cytoplasmic transport

One of the characteristic features of neurodegenerative diseases is the accumulation of protein aggregates. As a result of the formation of such aggregates, cascading disturbances in the functioning of the highly conservative mechanism of nuclear cytoplasmic transport in the cell also occur. [19]. As you know, the process of exchanging molecules between the nucleus and cytoplasm is necessary for the normal functioning of the cell. For long-lived cells, such as neurons, this process is particularly important. This is due to the fact that proteins associated with DNA maintenance and repair enter the nuclear structures of postmitotic nondividing cells precisely through the mechanism of nuclear-cytoplasmic transport [110]. In the case of neurodegenerative processes, the nuclear pore complex is damaged by accumulating protein aggregates, which can lead to cell death [28]. In addition, protein and RNA aggregates may affect the functioning of certain nucleoporins [57]. In medical diagnostics, protein fibrils are characteristic biomarkers of the progression of various neurodegenerative pathologies: amyotrophic lateral sclerosis, frontotemporal dementia, Alzheimer's disease, Huntington's disease, and Parkinson's disease [154]. For example, in modern medical practice, amyotrophic lateral sclerosis is usually considered as a neurodegenerative disease with a fatal outcome. The pathogenesis of the disease is characterized by the loss of motor neurons in the brain and spinal cord [153]. Patients with progressive amyotrophic lateral sclerosis have behavioral and cognitive impairments due to atrophy of the frontotemporal cortex [151]. In this regard, such symptoms are often diagnosed as frontotemporal dementia. The difficulty in making an accurate diagnosis provokes the need to consider the symptoms characteristic of the diseases listed above, together to determine the overall clinical picture.

According to a number of studies, most patients with amyotrophic lateral sclerosis show the amyloidogenic protein TDP-43, which is characterized by an altered subcellular localization and partially disappears from the nucleus in neurons and glial cells [95]. The nuclear RNA binding protein TDP-43 is known to be encoded by the TARDBP gene. In addition to its nuclear functions, TDP-43 takes part in processes occurring in the cytoplasm: for example, it maintains stability, provides transport and translation of mRNA [18]. In other words, the presence of this protein, which freely moves through the nuclear pore complex, is necessary for the normal functioning of neurons. On the other hand, this protein undergoes phase separation in the cell cytosol in *in vivo models* after overexpression or exposure to amyloid-like TDP-43 fibrils [51]. Drops of cytosolic TDP-43 recruit importin-α and Nup62, provoke incorrect localization of RanGAP1, Ran, and Nup107 genes, which contributes to the inhibition of nuclear-cytoplasmic transport.

Another example of impaired nuclear cytoplasmic transport is Huntington's disease. The development of the disease is caused by an extended CAG trinucleotide repeat in *the HTT gene*, which encodes the huntingtin protein. Patients carrying the mutation are characterized by the formation of abnormally long polyglutamine sequences in the huntingtin structure, which together affects toxic enhancement of protein function and aggregation and ultimately leads to neuronal death [15]. The indirect mechanism *of HTT interference* in the nuclear pore complex is confirmed by the presence of GLE1 among other proteins sequestered by polyglutamine formations in Huntington's disease [52]. When modeling the disease in *vivo*, several proteins important for nuclear cytoplasmic transport, including RanGAP1, Nup62, and Nup88, form intranuclear inclusions that colocalize with *HTT aggregates* in neurons of the striatum and cerebral cortex [57].

Thus, to date, medical diagnostic data indicate a relationship between the formation of aggregates in nerve tissue cells and the presence of structural and functional damage to the nuclear pore complex. However, the functional role of impaired nuclear cytoplasmic transport in the development and progression of neurodegenerative diseases remains unclear. On the one hand, nuclear cytoplasmic transport dysfunction may underlie a common pathogenetic mechanism that precedes the progression of neurodegenerative diseases. On the other hand, this disorder can occur already due to the functioning of specific pathological aggregates in neurological disorders of various etiologies. For this reason, a wide field opens up for a more detailed study of the mechanism of the relationship between the dysfunction of nuclear cytoplasmic transport and the formation of protein aggregates in various models of pathological conditions.

CHAPTER 2. MATERIALS AND METHODS

2.1 Strains and plasmids

The S. cerevisiae strains used in this study are listed in Table 2.

Table 2* - *S. cerevisiae yeast strains*used in the study

Strain	Genotype	Source
2-74-D694	*MAT* a *ade1-14(UGA) trp1-289(UAG) ura3-52 his3-200 leu2-3, 122* [*psi*$^{-}$] [*pin*$^{-}$]	[35]
74-D694	*MAT* a *ade1-14(UGA) trp1-289(UAG) ura3-52 his3-200 leu2-3, 122* [*psi*$^{-}$] [*PIN*$^{+}$]	[35]
OT56	*MAT* a *ade1-14(UGA) trp1-289(UAG) ura3-52 his3-200 leu2-3,112* [*PSI*$^{+}$]^{S} [*PIN*$^{+}$]	[35]
1-OT56	MATa ade1-14 (UGA) trp1-289(UAG) ura3-52 his3-200 leu2-3,112 [*psi*$^{-}$] [*PIN*$^{+}$]	[98]
2-OT56	MATa ade1-14 trp1-289 his3-Δ200 leu2-3,112 ura3-52 [*psi*$^{-}$] [*pin*$^{-}$]	[98]
OT56-NLS-GFP	*MAT* a *ade1-14(UGA) trp1-289(UAG) ura3-52 his3-200 leu2-3,112* [*psi*$^{-}$] [*PIN*$^{+}$]	provided by A. G. Matveenko
1-OT56-NLS-GFP	*MAT* a *ade1-14(UGA) trp1-289 (UAG) ura3-52 his3-200 leu2-3,112* [*psi*$^{-}$] [*pin*$^{-}$]	Obtained in this work

** Standard designations are used for mating loci and mutations. Alleles of the mating locus are designated MAT a and MAT α. The mutant alleles ade1-14 and lys2-87 contain the premature stop codon UGA [2], while the trp1-289 allele contains UAG [24]. These mutations lead to auxotrophy of strains (lack of growth) on media that do not contain adenine, tryptophan, and lysine, respectively.*

Table 3 - *E. coli bacterial*strains used in the study

Strain	Genotype	Application	Source
DH5a	*supE44 ΔlacU169 (φφ80 lacZΔM15) hsdR17 recA1 endA1 gyrA96 thi-1 relA1*	Plasmid development and routine bacterial transformation	[131]
DB3. 1	F-*gyrA462 endA1 glnV44 Δ(sr1-RecA) mcrB mrr hsdS20 (rB -, mB-) ara14 galK2 lacY1 proA2 rpsL20 (Smr) xyl5 Δleu*	mtl1 Plasmid lifetime with ccdB cassette	Thermo Scientific
BL21(DE3)	F- *ompT gal dcm lon hsdSB(rB- mB-) λ(DE3 [lacI lacUV5-T7 gene1 ind1 sam7 nin5])*	Operating time Production of recombinant proteins	[149]
VS39	F- *[araD139] B/r Δ(argF-lac)169 λ-e14-flhD5301 Δ(fruK-yeiR)725(fruA25) relA1 rpsL150(strR) rbsR22 Δ(fimB-fimE) 632(::IS1) deoC1 Δ(csgBAC)(:: KanR)*	Conducting experiments in the C-DAG system	[146]

The plasmids used in this study are listed in Table 4.

Table 4-Plasmids used in the study.

Plasmids of the pDONR221 series (excluding the plasmid with the NUP58 gene) were constructed as follows. The product obtained during PCR reactions was cloned into the pDONR221-ccdB vector (primers are shown in Table 5) during the BP cloning reaction. Plasmids of the pVS-GW, pAG416GPD-EGFP, and pAG415GPD-Cerulean series were obtained by performing LR reactions, where the sequence for cloning was cut from plasmids of the pDONR221-ccdB series.

The name of the plasmid	Markers	Source
pDONR221-NUP58	*KanR*	TermoFisher(Scientific)

		Ultimate ORF Clone
pDONR221-ccdB	*KanR*	TermoFisher(Scientific) #12536017
pDONR221-NUP58-1-213	*KanR*	[30]
pVS105	*AmpR*	[146]
pVS72	*AmpR*	[146]
pVS-GW-Sup35M	*AmpR*	[30]
pVS-GW-Sup35NM	*AmpR*	[30]
pVS-GW-ccdB	*AmpR*	[30]
pVS-GW-NUP58	*AmpR*	[30]
pVS-GW-NUP58-1-213	*AmpR*	[30]
pDONR221-NUP58-1-95	*KanR*	Obtained in this work
pDONR221-NUP58-215-599	*KanR*	Obtained in this work
pVS-GW-NUP58-215-599	*AmpR*	Obtained in this work
pVS-GW-NUP58-1-95	*AmpR*	Obtained in this work
pAG416GPD-EGFP-NUP58-1-95	*AmpR, URA3*	Obtained in this work
pAG416GPD-EGFP-NUP58-215-599	*AmpR, URA3*	Obtained in this work
pAG416GPD-EGFP-ccdB	*AmpR,CmR, URA3*	Provided by S. Lindquist (Addgene plasmid # 14316)
pAG416GPD-EGFP-NUP58	*AmpR, URA3*	Obtained in this work
pDEST527-ccdB	*AmpR*	Provided by D. Esposito (Addgene plasmid # 11518)
pDEST527-His_6-NUP58	*AmpR*	[30]

pVSGW-NSP1-1-136	*AmpR*	[31]
pVSGW-Nup145-1-152	*AmpR*	[31]
pVSGW-hs-Nup62-1-175	*AmpR*	[31]
pVSGW-dm-Nup62-1-175	*AmpR*	[31]
pVSGW-tg-Nup58-60-320	*AmpR*	[31]
pVSGW-sp-Nup45-1-220	*AmpR*	[31]
pVSGW-Nup100-1-400	*AmpR*	[31]
pVSGW-dm-Nup98-250-500	*AmpR*	[31]
pVSGW-sp-Nup98-250-500	*AmpR*	[31]
pVSGW-hs-Nup98-250-500	*AmpR*	[31]
pDONR221-NSP1-1-136	*KanR*	[31]
pDONR221-Nup145-1-152	*KanR*	[31]
pDONR221-hs-Nup62-1-175	*KanR*	[31]
pDONR221-dm-Nup62-1-175	*KanR*	[31]
pDONR221-tg-Nup58-60-320	*KanR*	[31]
pDONR221-sp-Nup45-1-220	*KanR*	[31]
pDONR221-Nup100-1-400	*KanR*	[31]
pDONR221-dm-Nup98-250-500	*KanR*	[31]
pDONR221-sp-Nup98-250-500	*KanR*	[31]
pDONR221-hs-Nup98-250-500	*KanR*	[31]
pAG416GPD-EGFP-NSP1-1-136	*AmpR, URA3*	Obtained in this work

pAG416GPD-EGFP-Nup145-1-152	*AmpR, URA3*	Obtained in this work
pAG416GPD-EGFP-hs-Nup62-1-175	*AmpR, URA3*	Obtained in this work
pAG416GPD-EGFP-dm-Nup62-1-175	*AmpR, URA3*	Obtained in this work
pAG416GPD-EGFP-tg-Nup58-60-320	*AmpR, URA3*	Obtained in this work
pAG416GPD-EGFP-sp-Nup45-1-220	*AmpR, URA3*	Obtained in this work
pAG416GPD-EGFP-Nup100-1-400	*AmpR, URA3*	Obtained in this work
pAG416GPD-EGFP-dm-Nup98-250-500	*AmpR, URA3*	Obtained in this work
pAG416GPD-EGFP-sp-Nup98-250-500	*AmpR, URA3*	Obtained in this work
pAG416GPD-EGFP-hs-Nup98-250-500	*AmpR, URA3*	Obtained in this work
pAG415GPD-ccdB-Cerulean	*AmpR, LEU2*	Provided by S. Lindquist (Addgene plasmid # 14386)
pAG415GPD-Cerulean-dm-Nup62-1-175	*AmpR, LEU2*	Obtained in this work
pAG415GPD-Cerulean-NSP1-1-136	*AmpR, LEU2*	Obtained in this work
pAG415GPD-Cerulean-Nup145-1-152	*AmpR, LEU2*	Obtained in this work
pAG415GPD-Cerulean-tg-Nup58-60-320	*AmpR, LEU2*	Obtained in this work
pAG415GPD-Cerulean-dm-Nup98-250-500	*AmpR, LEU2*	Obtained in this work
pAG415GPD-Cerulean-sp-Nup98-250-500	*AmpR, LEU2*	Obtained in this work

2.2 Cultivation medium and conditions

To grow yeast cells under nonselective conditions, we used a complete YEPD medium

[72]. To conduct experiments on the cultivation of crops and transformants, as well as to test the phenotype using selective markers, we used a synthetic SC medium based on YNB [72]. The complete SC medium contained additives in the following concentrations: 20 mg/l adenine sulfate (for solid) or 40 mg/L mg/L (for liquid), 20 mg/L L-histidine, 20 mg/L L-lysine, 60 mg/L L-leucine, 20 mg/L L-methionine, 150 mg/l L-threonine, 20 mg/l L-tryptophan, 20 mg/l uracil. All *S. cerevisiae cells* were grown at 30°C.With and at a mixing speed of 200 rpm [72].

When conducting experiments in which it was necessary to estimate the optical density of the culture, we used an iMark flatbed photometer (BioRad) with a light filter. The optical density of the yeast culture was recorded at an analytical wavelength of 595 nm. The measurements were carried out in a volume of 200 μl, and we used a medium similar to that in which the cells were grown as a control liquid.

To grow *E. coli cells*, we used LB medium: liquid – for plasmid production, solid-for seeding transformants and maintaining bacterial strains, respectively [131]. To grow *E. coli cells*containing plasmids or select transformants, we added antibiotics to the LB medium: 100 mg/l ampicillin or 50 mg/l kanamycin. All *E. coli* cells were grown at a temperature of 37°C, with constant stirring at a speed of 250-300 rpm (in the case of growing cells in a liquid medium). For experiments in the C-DAG system, LB solid medium with the following additives was used: L-arabinose (0.2% (w/v)), IPTG (0.1 mM), Congo red dye (10 micrograms/ml), ampicillin (200 mg/L) and chloramphenicol (50 mg / ll).

To conduct experiments in the C-DAG (Curli-dependent amyloid generator) system, we transformed *E. coli* strain VS39 cells with target plasmids and grew a night culture in LB medium with the addition of ampicillin and chloramphenicol at 37°C. The resulting crops were sown on a series of plates:

- experimental plate (L-arabinose (0.2% (w/v)), IPTG (0.1 mM), Congo red dye (10 mcg / ml), ampicillin (200 mg / L) and chloramphenicol (50 mg/L)),
- a cup with inducers (L-arabinose (0.2% (v/w)), IPTG (0.1 M), ampicillin (200 mg/L) and chloramphenicol (50 mg / L)),
- a control cup that contains only antibiotics.

The resulting plates were incubated at different temperatures, namely 22°C, 26°C and 30°C (according to [146]). In the course of the work, variants with 0.5 x, 1x, and 2x concentrations for the Congo red dye, L-arabinose, and IPTG in various combinations were experimentally tested. Modified protocols were used for the final experiments in the C-DAG system. Modified plasmids pVS-GW Sup35M and pVS-GW-Sup35NM and classical plasmids pVS72 and pVS105 from the original paper [146].

2.3 Bacterial transformation

To develop plasmids in *the E. coli strain*, we performed bacterial transformation of chemically competent cells [131]. To do this, we added plasmid DNA to the competent cells in the amount of 50 to 100 ng. per reaction, depending on the experiment. The cells were then incubated in ice for 30 minutes. The cells were then subjected to thermal shock in a water bath at 42°C for 1 minute. After that, we added an antibiotic-free LB medium to the cell suspension, bringing the total volume to 1 ml. The resulting mixture was then incubated by stirring in a thermostat at 37°C. At the end, we seeded the cells on a selective medium and grew the transformants for 12-16 hours at 37°C.

To develop the recombinant protein, we performed chemical transformation of BL21(DE3) cells of *the E. coli strain*. To do this, we grew the cells overnight in a non-selective LB medium. Stationary cell culture was diluted 100 times and grown to the logarithmic stage. After that, we deposited the cells, washed them with 0.1 M $CaCl2,_2$ and left them to incubate in ice for an hour. After that, plasmid DNA was added to the cells in an amount of 100 to 200 ng per reaction. The cells were then incubated in ice for 30 minutes. Next, the cells were subjected to thermal shock in a water bath at 42°C for 1 minute. After that, we added an antibiotic-free LB medium to the cell suspension, bringing the total volume to 1 ml. The resulting mixture was then incubated by stirring in a thermostat at 37°C. At the end, we seeded the cells on a selective medium and grew the transformants for 12-16 hours at 37°C.

2.4 Yeast transformation

In this study, we used standard methods for working with yeast strains [72]. When performing yeast cell transformation, the protocol using lithium acetate (hereinafter referred to as LiAc) was followed [72]. By the beginning of transformation, the cell concentration in the culture should be approximately^{107} cells/ml. The required number of cells was deposited from the culture in a 1.5 ml tube (centrifugation for 1.5 min, 3000-5000 rpm, 3 times), the medium was drained after each round of precipitation. The cell sediment was resuspended in 1 ml of water. Then the cells were again deposited and drained of water. 0.5 ml of 100 mM LiAc was added to the cell sediment. The cells were resuspended in LiAc and centrifuged for 1.5 minutes at a speed of 5000 rpm, the remaining LiAc was drained. 0.5 ml of 100 mM LiAc was added to the cell sediment, resuspended, and left for 20-30 minutes at 30°C. Most of the LiAc was then drained, leaving approximately 50-100 µl. Cells were resuspended in this volume. The resulting suspension was divided into the required number of eppendorfs and components of the transformation mixture were added to them in the following amounts:

- water (up to the final volume of 360 µl) - 40 µl

- PEG 50% (w/v) - 240 µl
- plasmid (based on the fact that the reaction requires 1.5 mcg of plasmid DNA) - 5 mcl
- ssDNA (5 mcg / ml) - 24 mcl
- 1M LiAc - 36 µl

After adding all the components, the mixture was mixed to a homogeneous state and incubated for 20-30 minutes at room temperature. Then we subjected the cells to thermal shock by incubating them in a water bath at 42°C for 12 minutes (the time indicated for strain 74-D694). After that, the cells were precipitated by centrifugation for 5 minutes at a speed of 5000 rpm and the remaining transformation mixture was drained. Then the cells were diluted in 100 µl of water and seeded on a selective medium. The plates were incubated in a thermostat at 30°C for 4-10 days before the appearance of colonies [131].

2.5. Prion loss [*PIN*$^+$]

For prion loss, cells were grown on a medium containing guanidine hydrochloride at a final concentration of 4 mM. This chemical agent leads to disruption of the Hsp104 chaperone, which is responsible for the fragmentation of aggregates and, as a result, the possibility of transmission to daughter cells. The strain was grown for a long time and replanted four times in order to increase the probability of prion loss [*PIN*$^+$]. To test prion elimination, we analyzed the presence of Rnq1 aggregates in cells using the SDD-AGE method [81].

2.6. Microscopy

2.6.1 Fluorescence microscopy

Temporary preparations for confocal and fluorescence microscopy were prepared by depositing 500 µl of a liquid culture of yeast cells in a selective medium at a logarithmic growth stage (at an optical density of 0.3-0.4 according to iMark (BioRad)). The resulting precipitate was then resuspended in 100 µl of water. Then we mixed 5 µl of the resulting suspension with 50% (v/v) glycerol in a 1:1 ratio.

The Zeiss AxioScope A1 was used in this work. To visualize the sequences of proteins crosslinked with EGFP, filter 46 (excitation maximum — 500 nm, emission maximum — 535 nm) was used, and filter 74HE (excitation maxima — 483 nm and 569 nm; emission maxima — 526 nm and 636 nm) was used to separate autofluorescence from fluorescence. Photos were taken using a Zeiss Axiocam ERc s5 camera for a Zeiss Primostar microscope. The ImageJ program was used for image processing [136].

2.6.2 Transmission electron microscopy

To study protein fibrils obtained *in vitro* and in the C-DAG system *in vivo*, we used transmission electron microscopy. Electron microscopy copper meshes (EMS G200-Cu) coated with a formvar film were used to prepare the preparations. 5 µl of a solution with a solution of fibrils or a suspension of VS39 bacterial cells was applied to the mesh from a cup with Congo red dye, after 30 seconds the excess was removed with filter paper. After that, the mesh was incubated with a solution of 1% (w/v) uranyl acetate for 30 seconds, then the preparation was washed with water [146]. The obtained preparations were analyzed in the Resource Center "Development of Molecular and Cellular Technologies" of St. Petersburg State University using a JEM-1400 microscope (Jeol).

2.6.3 Polarizing microscopy

To prove the binding of the Congo Red dye to the fibrils of the studied protein in *in vivo* and *in vitro* systems, we used polarization microscopy. In the case of *in vivo* preparations, bacterial cells were removed from a solid medium containing inducers (L-arabinose and IPTG), as well as a Congo red dye, and applied to a slide. Next, the resulting preparation is covered with a cover glass. In the case of *in vitro* fibrils, the sample was applied to a clean slide (approximately 20 µl of solution), after which the sample was allowed to dry completely. Then a solution of Congo Red dye was applied to the dried film (2.5 mg / ml in water; to remove crystals, the solution was previously filtered through an antibacterial filter) so that it covered the

entire film. After that, we expected 5 to 15 minutes, depending on the protein. For Sup35NM and BSA proteins, the incubation time with Congo red is 5-10 minutes (personal message from Yu. V. Sopova, for the NUP58 protein, the incubation time was selected experimentally and was 10-15 minutes). Then we selected a solution of Congo red and washed off the remaining 70% alcohol. After that, we applied 5 µl of glycerol and covered it with a cover glass. The obtained preparations were analyzed in both cases in the RC "Development of Molecular and Cellular Technologies" of St. Petersburg State University using a DMI6000 microscope (Leica).

2.7 Methods of working with nucleic acids

2.7.1 Isolation and purification of DNA

We isolated plasmid DNA using a GeneJET Plasmid Miniprep Kit (Fermentas or Thermo Scientific). A GeneJET PCR purification kit (Thermo Scientific) was used to purify PCR products. All manipulations were performed according to the manufacturer's protocol.

2.7.2 PCR (polymerase chain reaction)

For PCR, we used the pDONR221-NUP58 plasmid as a template and primers: NUPL1-F-1-213 and NUPL1-R-1-213 for amplification of the amyloidogenic region of the NUP58 protein (Table 4). For PCR preparation, we used Taq polymerase (Sibenzyme) in the amount of 0.5-1 activity units per 10 µl of the reaction, a mixture of deoxynucleotide triphosphates at a final concentration of 2 mM, 10^x buffer for PCR (Sibenzyme), and primers at a final concentration of 2-4 pmol/µl.

Amplification reaction program:

1. DNA denaturation – 30 seconds, 95°C.
2. Fragment amplification – 25 cycles: DNA denaturation – 30 seconds, 95°C. Primer annealing – 1 minute 57°C. DNA synthesis – 1 minute, 72°C.
3. Completion of DNA synthesis – 10 minutes, 72°C.

Table 5-Primers used in the study.

Bold text indicates attB recombination sites. The annealing temperature of the primers was selected experimentally by gradient PCR.

Name primer	**Sequence primer**	**Application in the work of**	**$T_{annealing}$**
NUPL1-F-1-213	gggg**ACAAGTTTGTACAAAAAAGCAGGCT**ccatgtccacaggg	Cloning of a portion of a gene *NUP58*	58°C

NUPL1-R-1-213	ggggg**ACCACTTTGTACAAGAAAGCTGGGT**ctaattgcctgcagttg	Cloning of a portion of a gene *NUP58*$_{1-213}$	58°C
M13rev_20-mer	TCACACAGGAAACAGCTATGAC	PCR from colinies	54°C
M13F_(-20)18-mer	GTAAAACGACGGCCAGTG	PCR from colinies	54°C
pBAD_f	ATGCCATAGCATTTTTATCC	PCR from colinies	54°C
HS_Nup58-215-end-F	**GGGGACAAGTTTGTACAAAAAAGCAGGCT**caatgCTTGGTGGTATAGATTTCAGTAGCTCC	Amplification of a fragment 215-599 with matrix pDONR221-Nup58	62,9°C
HS_Nup58-215-end-R	**GGGGACCACTTTGTACAAGAAAGCTGGGT**cgTTACTATCTTTTTCCTCTTTTGTTTCC	Amplification of fragments 215-599 and 468-599 with matrix pDONR221-Nup58	61,7°C
HS_Nup58-468-end-F	**GGGGACAAGTTTGTACAAAAAAGCAGGCT**caatgACACTTACACAGCAGCAACAGCCTGCTacaggg	Amplification of a fragment 468-599 with matrix pDONR221-Nup58	65.4°C
HS_Nup58-1-95-R	**GGGGACCACTTTGTACAAGAAAGCTGGGT**cgTTACAGAGTTAATCCTGTAGTTATAG	Amplification of a fragment of 1-95 with matrix pDONR221-Nup58	59,6°C
HS_Nup58-175-F	**GGGGACAAGTTTGTACAAAAAAGCAGGCT**ccatgGCTGGTTTGGGAGGTTCACTTTTCC	Amplification of a fragment 175-213 with matrix pDONR221-Nup58	61.1°C
HS_Nup58-1-213-F	**GGGACAAGTTTGTACAAAAAAGCAGGCT**ccATGTCCACA	Amplification of a fragment of 1-95 with	61.1°C

	GGG	matrix pDONR221-Nup58	
HS_Nup58-213-R	**GGGACCACTTTGTACAAGAAAGCTGGGT**ctAATTGCCTGCAGTTG	Amplification of a fragment 175-213 with matrix pDONR221-Nup58	62,9°C
attb1-Nup100-1-400-F	**GGGGACAAGTTTGTACAAAAAAGCAGGCT**caacaATGTTTGGCAACAATAGACCAATGTTTgg	Amplification a fragment of $Nup100_{1-400}$ with genomic DNA *of S. cerevisiae* strain 1B-D1606	61°C
attb2-Nup100-1-400-R(stop)	**GGGGACCACTTTTGTACAAGAAAGCTGGGT**cgTTATGCTGGTTTGGCTCCAAACAAACCTGTAG	Amplification a fragment $Nup100_{1-400}$ with genomic DNA of *S. cerevisiae* strain 1B-D1606	61°C
attb1-Nup145-1-152-F	**GGGGACAAGTTTGTACAAAAAAGCAGGCT**caacaATGTTTAATAAAAGTGTAAATAGTGG	Amplification *S. cerevisiae* $Nup145_{1-152}$ fragment with S. cerevisiae genomic DNA of strain 1B-D1606	59°C
attb2-Nup145-1-152-R(stop)	**GGGGACCACTTTTGTACAAGAAAGCTGGGT**cgTTAATTTTGCGTGGTAGAAGTTATATTG	Amplification *S. cerevisiae* $Nup145_{1-152}$ fragment with S. cerevisiae genomic DNA of strain 1B-D1606	59°C
attb1-Nsp1-1-136-F	**GGGGACAAGTTTGTACAAAAAAGCAGGCT**caacaatgaactt	Amplification of a fragment of $Nsp1_{1-136}$	63°C

	caatacacctcaacaaaacaaaacgccc	with genomic DNA *of S. cerevisiae* strain 1B-D1606	
attb2-Nsp1-1-136-R(stop)	**GGGGACCACTTTGTACAAGAAAGCTGGGT**cgTTAattgctattagtactgttattgaataaggatg	Amplification of a fragment of $Nsp1_{1-136}$ with genomic DNA *of S. cerevisiae* strain 1B-D1606	63°C
attB1-hsNup98-1-F	**GGGGACAAGTTTGTACAAAAAAGCAGGCT**caATGTTTAACAAATCATTTGGAACACCC	Amplification of a fragment of $Nup98_{1-250}$ with cell line cDNA *H. sapiens* IMR-32	60°C
attB2-hsNup98-stop-250-R	**GGGGACCACTTTGTACAAGAAAGCTGGGT**cgTTAAAAGCCTGAATTAGTGGTGGAGG	Amplification of a fragment of $Nup98_{1-250}$ with cell line cDNA *H. sapiens* IMR-32	60°C
attB1-spNup98-250-F	**GGGGACAAGTTTGTACAAAAAAGCAGGCT**caAATCAAGGACGACGTTTTGGC	Amplification of a fragment of $Nup98_{250-499}$ with cDNA *Sh. pombe*	61°C
attB2-spNup98-stop-499-R	**GGGGACCACTTTGTACAAGAAAGCTGGGT**cgTTAATTAGCATTTTGCCCAAAAGAAAAACCtcc	Amplification of a fragment of $Nup98_{250-499}$ with cDNA *Sh. pombe*	61°C
attB1-spNup45-1-F	**GGGGACAAGTTTGTACAAAAAAGCAGGCT**caATGTTCGGGTTAAATAAAACACCC	Amplification of a fragment $Nup45_{1-220}$ with cDNA *Sh. pombe*	60°C
attB2-spNup45-220-R	**GGGGACCACTTTGTACAAGAAAGCTGGGT**cgTTACTTCCCAAACAAAGAACCAGTAC	Amplification of a fragment $Nup45_{1-220}$ with cDNA *Sh. pombe*	60°C

attB1-dmNup62-1-F	**GGGGACAAGTTTGTACAA AAAAGCAGGCT**caATGGTAT TCCAGTTGCCAACAAC	Amplification of a fragment of $Nup62_{1-175}$ with cDNA *D. melanogaster*	61°C
attB2-dmNup62-175-R	**GGGGACCACTTTGTACAA GAAAGCTGGGT**cgTTACTGC GTGGAGGCTATGGC	Amplification of a fragment of $Nup62_{1-175}$ with cDNA *D. melanogaster*	61°C
attB1-hsNUP62-1-F	**GGGGACAAGTTTGTACAA AAAAGCAGGCT**caATGAGTG GATTTAACTTTGGAGGC	Amplification of a fragment of $NUP62_{1-175}$ with cell line cDNA *H. sapiens* IMR-32	61°C
attB2-hsNUP62-175-R	**GGGGACCACTTTGTACAA GAAAGCTGGGT**cgTTATGAG CCAATGTTGAAACCGG	Amplification of a fragment of $NUP62_{1-175}$ with cell line cDNA *H. sapiens* IMR-32	61°C
attB1-dmNup98-250-F	**GGGGACAAGTTTGTACAA AAAAGCAGGCT**caGCGGGC GCAAGGGTCCAC	Amplification of a fragment of $Nup98_{1-250}$ with cDNA *D. melanogaster*	61°C
attB2-dmNup98-500-R	**GGGGACCACTTTGTACAA GAAAGCTGGGT**cgTTAGCAC ATATAGTCTTCCAGGCGG	Amplification of a fragment of $Nup98_{1-250}$ with cDNA *D. melanogaster*	61°C
attB1-tgNup58-60-320-F	**GGGGACAAGTTTGTACAA AAAAGCAGGCT**caATGGGA CTTAATTTTGGAGCTCTGGG CTCTtcc	Amplification of a fragment of $Nup58_{60-320}$ with cDNA *T. guttata*	61°C
attB2-tgNup58-60-	**GGGGACCACTTTGTACAA**	Amplification of a	61°C

320-R	**GAAAGCTGGGT**cgTTATAGC TCCTGTGCAGTTTCCACTTTC AGcttgtc	fragment of Nup58$_{60\text{-}320}$ with cDNA *T. guttata*	

2.7.3. PCR from colonies

For PCR, we selected bacterial colonies from a selective medium, resuspended them in 20 µl of water, and incubated them at 100°C for 5 minutes. The resulting mixture was then centrifuged for 10 minutes at 14,000 rpm at 4°C and 2 µl was used for PCR. In PCR, we used Taq polymerase (Sibenzyme) in the amount of 0.5-1 activity units per 10 µl of the reaction, a mixture of deoxynucleotide triphosphates in a final concentration of 2 mM, a 10x buffer for PCR (Sibenzyme), and primers in a final concentration of 2-4 pmol/µl. The primers used in this study are NUPL1-F-1-213, NUPL1-R-1-213, M13rev_20-mer, M13F_(-20) 18-mer, pBAD_f, and PROEX_R (Table 5).

Amplification reaction program:

1. DNA denaturation – 30 seconds, 95°C.
2. Fragment amplification – 30 cycles: DNA denaturation – 30 seconds, 95°C. Primer annealing – 1 minute 58°C. DNA synthesis – 1 minute, 72°C.
3. Completion of DNA synthesis – 10 minutes, 72°C.

2.7.4 Nucleic acid electrophoresis

To assess the size of DNA in the sample, we performed electrophoresis in 0.5^{x} multiple TBE buffer (10.8 g-Tris, 5.5 g-Boric acid, 4 ml-0.5 M EDTA pH 8.0, mQ-up to 100 ml, the composition is given for 1^{x} buffer) in agarose gel (1% (w/v) agarose for fragments larger than 500 base pairs and 1.5% (w/v) for smaller fragments) for 40 minutes at 80 V. Application buffer-5^{x} Sample buffer DNA (0.25% (w/v) bromphenol blue, 0.25% (w/v) xylenedianol, 30% (v/v) glycerol) [131]. After the electrophoresis was completed, we stained the gel in ethidium bromide solution for 5-10 minutes and visualized the DNA fragments using a transilluminator. They were photographed using a Canon PowerShot G12 digital video camera.

2.7.5 Obtaining cDNA

Total RNA was isolated using the TRIzol reagent (Fermentas) according to the manufacturer's protocol. Strain 972 was used to isolate RNA from S. pombe cells. An IMR-32

cell culture (provided by D. V. Kachkin) was used to isolate human RNA. cDNA synthesis was synthesized using the RevertAid RT Kit (Thermo Scientific, K1691), according to the manufacturer's recommendations.

2.7.6 Restriction and ligation of fragments

During the restriction reaction, we used PstI restrictase in Orange buffer to test plasmids where the gene of interest is crosslinked with EGFP*PstI* . The fragments were ligated using the enzyme T4 DNA ligase in a buffer for this enzyme (Fermentas).

2.7.7 Gateway reaction cloning

To perform the recombination cloning reaction, we mixed 100 ng of the plasmid containing the gene sequence of interest and 150 ng of the insertion vector in a 10^x TE buffer (1 ml of 1 M Tris – HCl pH 8.0 per 100 ml of buffer, 200 µl 0.5 M EDTA) in a final volume of 7 µl. We added 1 µl of LR clonase mix (Thermo Scientific) to the resulting mixture and incubated it for 3 to 12 hours at 26°C. After that, to stop the reaction, we added 0.5 µl of proteinase K solution and incubated for 10 minutes at 37°C according to the manufacturer's protocol (Thermo Scientific). Then, with the resulting mixture, we transformed competent cells of the TOR10 strain according to the standard bacterial transformation protocol.

2.7.8 DNA sequencing

Sequencing of PCR products and the resulting plasmids was performed by A. S. Masharsky and A. S. Samarina at the St. Petersburg State University Resource Center "Development of Molecular and Cellular Technologies" on an ABI Prism 310 capillary sequencer using a standard M13 primer, as well as primers specific to the sequences of the studied genes and plasmids. The obtained chromatograms were analyzed using the UGENE program using the “Sanger Sequencing Analysis" function to check the correctness of the obtained plasmid sequences [112].

2.8 Methods of working with proteins

2.8.1 Protein denaturing electrophoresis in polyacrylamide gel (SDS-PAGE)

To prove protein aggregation in *in vivo* and *in vitro systems*, as well as to check the presence of protein in samples, we used the polyacrylamide gel protein electrophoresis technique [131]. We applied to the gel samples mixed with a buffer for application (buffer composition in final concentrations: 0.6 M Tris-HCl pH 6.8, 2% (w/v) SDS, 0.002% (w/v) bromphenol blue, 2%

(v/v) β-mercaptoethanol, 5%(v/ v) glycerol), then a current of up to 60 V was applied before the samples entered the separating gel. After that, we performed electrophoresis at 180 V until the paint came out of the gel. For electrophoresis, we used polyacrylamide gels 10% separating and 5% concentrating [131]. To test the SDS stability of the resulting aggregates, we also used the SDS-PAGE method with gel boiling. In the course of this procedure, a standard SDS-PAGE was performed, but after 40-50 minutes from the beginning of the cut, it stopped, and 1-x Samle-buffer was applied to the wells, after which we poured 10% polyacrylamide gel into the wells so that the contents of the wells did not boil away. After that, this gel was sealed in a film and boiled for 5 minutes. Further, the phoresis was continued until the paint came out of the gel [84].

2.8.2 Coloration of proteins with Coomassie dye

To color all proteins in polyacrylamide gel, it was boiled in Coomassie dye (0.25% (w/v) Coomassie R-250 (the original protocol used Coomassie R-350), 10% (v/v) acetic acid, 50% (v/v) ethanol) for 1.5 min. Then we removed the excess dye by boiling it in water [131].

2.8.3 Semi-denaturing electrophoresis of protein aggregates in agarose gel (SDD-AGE)

We performed electrophoresis in a gel containing 1.5% agarose, which was dissolved in a single TAE buffer under heating (composition per 1 liter of buffer: Tris-242 g, glacial acetic acid-57 ml, 0.5 M EDTA-18.6 ml, pH 8.0). After the agarose was dissolved, we added SDS to 0.1% (v/v) and stirred quickly, as agarose can precipitate. For electrophoresis, we used a 1x TAE buffer with the addition of SDS. We added 300 μl of 10% (w/v) SDS to 300 ml of buffer. Then we mixed the lysates with the application buffer (buffer composition: 2x TAE, SDS-8% (w/v) by weight, glycerol-20% by weight, bromphenol blue) and incubated for 5 minutes at room temperature. We applied samples to the gel and performed electrophoresis at a specific field voltage of 3 V / cm of gel (21 V for 4 hours) [81].

2.8.4 Semi-dry transfer of proteins to the membrane

To transfer proteins from the gel to the polyvinylidene fluoride membrane after SDS-PAGE, we used the semi-dry transfer method (according to [131] with changes). For the transfer, we built the structure (from bottom to top):

- transfer sponge;
- Whatman sheet.
- polyvinylidene fluoride membrane (pre-activated in methanol for 1-2 minutes);
- polyacrylamide gel;
- Whatman sheet.
- transfer sponge.

All components were impregnated with transfer buffer (composition per 1 liter of buffer: Tris-6.06 g, glycine-28.8 g, methanol-400 ml). The transfer was performed at 10-15 V for 90 minutes using a Trans-Blot SD Semi-Dry Transfer Cell (BioRad) device.

2.8.5 Capillary transfer

For protein transfer after SDD-AGE, we used the capillary transfer technique [58]. We prepared a stack of filter paper and several sheets of whatman cut to fit the size of the gel, as well as a" wick " (a strip of whatman whose width corresponds to the size of the gel, and the length is several times larger than it). Then we activated the polyvinylidene fluoride membrane in methanol for a few minutes. Next, we washed the membrane in TBS buffer (composition per 1 liter: 1 M Tris-15 ml, NaCl-9 g) for several minutes. After that, the capillary transfer system was assembled (assembly order from bottom to top):

- a stack of dry filter paper;
- Three or more dry sheets of Whatman.
- two moistened sheets of whatman paper;
- polyvinylidene fluoride membrane;
- agarose gel with the test proteins;
- two moistened sheets of whatman paper;
- a wetted wick, the ends of which are placed in containers with a TBS buffer located above the gel level;
- cargo at the rate of 10 grams per 1^{cm2} of gel.

After assembly, we placed this structure in 4°C for the night.

2.8.6 Western blot hybridization

Western blot hybridization was performed according to the described procedure [131]. To identify proteins fused with EGFP, we used commercial antibodies G(CY) FP (Evrogen AB121). To identify the proteins fused with His6, we used commercial His6 antibodies (GE27-4710-01 Sigma). For hybridization, we used a 1:3000 solution of primary antibodies in 1% (w/v) Blocking agent (ECL Plus Western Blotting Detection System (Amersham)) (for G(CY)antibodiesFP and His6) based on TTBS buffer (9 g-NaCl, 15 ml - 1 M Tris-HCl pH 7.6, 0.5 ml-Tween 20 per 1 liter of water). The membrane was then washed in TTBS buffer 3 times for 10 minutes. Then hybridization was performed with secondary anti-rabbit antibodies (ECL Plus Western Blotting Detection System (Amersham)) for G(CY)detectionFP и anti-mouse (ECL Plus Western Blotting Detection System (Amersham)) to detect His6, a 1:20000 antibody dilution in a 1%(w/v) Blocking agent based on TTBS buffer was performed and the membrane

was washed as previously done. When conducting experiments to obtain antibodies to the test protein, we used a solution of 5% milk based on TTBS buffer in various dilutions with rabbit serum. For the development of antigen-antibody complexes, we used branded sets of ECL Plus Western Blotting Detection System (Amersham) secondary antibodies and ECL Plus Western Blotting Reagent Pack (Amersham) reagents. The signal was detected using a GeneGnome device (Syngene).

2.8.7 Purification of recombinant proteins

To purify and develop the recombinant NUP58 protein from bacteria, we selected the bacterial strain *E. coli* BL21(DE3). This strain was transformed with the pDEST527-His_6-NUP58 construct. The transformants were then grown overnight in LB medium with ampicillin added. The night culture was diluted 100 times to a certain final volume (up to 200 ml in a separate 2-liter flask) and incubated for three hours at a temperature of 37°C. Then, an IPTG inducer (Isopropyl-β-D-1-thiogalactopyranoside) was added to the cell culture to a final concentration of 1 mM and the cells were incubated for 4 hours. For trial induction, cells were grown in a volume of 10 ml under the same conditions. After this time, the cells were precipitated by centrifugation at a speed of 5000 rpm for 10 minutes, the remaining medium was removed and frozen. To purify the NUP58 protein under denaturing conditions, a lysing buffer containing 20 mM Tris-HCl (pH 8.0) and 8 M urea at the rate of 3 ml of buffer per 1 g of cells was added to the cells and incubated at room temperature for 1-1.5 hours with constant stirring. After that, the resulting lysate was centrifuged at an acceleration of 30,000 g for 20 minutes at 4°C and the supernatant fraction was collected in separate microtubes [139]. The efficiency of protein isolation was checked by comparing total cell lysate, sedimentary and supernatant fractions using SDS-PAGE. A stationary column with Ni-NTA agarose (Invitrogene) and a peristaltic pump (Bio-Rad) were used for preparative purification of the NUP58 protein. At the beginning, we washed the column with 50 ml of mQ, and then with 50 ml of washing buffer (buffer composition-20 mM Tris-HCl (pH 8.0), 8 M urea) at a rate of 1 ml/min. The cell lysate supernatant fraction was then passed through the column at a rate of 1.5 ml / min, after which the column was washed with a washing buffer at a rate of 1.5 ml / min (the volume of the washing buffer was 50 ml, an imidazole gradient from 0 to 8 mM was used for washing). The protein was then eluted using a linear gradient of imidazole concentration (from 8 mM to 400 mM imidazole, elution volume 50 ml) at a rate of 1.5 ml / min. Fractions were collected using an automated fraction collector (Econo Pump, Bio-Rad). Each fraction contained 2 ml of buffer with the protein dissolved in it. Subsequently, the obtained fractions were analyzed using SDS-PAGE and fractions containing the maximum amount of the target protein were selected in separate micro-

samples. We added 5 volumes of 100% methanol to these eluate fractions. The solution was then incubated overnight at 4°C. The precipitated protein was collected in micro tubes. Subsequently, the protein preparation was stored at a temperature of -80°C.

2.8.8 Proteinase K

Proteinase K (Helicon) was added to the monomeric and aggregated protein at a concentration of 0.5 mcg / ml. The resulting solutions were incubated for 60 min at 26 °C. The reaction was stopped by adding PMSF to the final concentration of 8.3 mM.

2.9 Statistical processing

In the course of this work, the analysis of variance and the analysis of the Wilcoxon criterion adjusted for multiple comparisons were calculated using the statistical processing environment R [123].

2.10 Analysis of nuclear cytoplasmic transport

Evaluation of the efficiency of nuclear transport was carried out according to one of the methods proposed in the article [77]. The N / C method used involves obtaining images of cells carrying the studied structures using fluorescence microscopy and processing them in the ImageJ program using the ROI Manager tool. According to the method, the transport intensity was estimated by calculating the ratio of the average value of the fluorescence intensity in the region of the cell nucleus (N) to the average value of the fluorescence intensity of its cytoplasm (C):

$$N/C = \frac{\text{Average nuclear fluorescence intensity}}{\text{Average cytoplasmic fluorescence intensity}}$$

Before measuring the N/C ratio of cells in ImageJ, we subtracted the background fluorescence intensity from the image, since the background can dramatically change the calculated N/C value. We used the pseudo-flat - field correction method (Process - > Filters -> Gaussian Blur). This method involves creating a duplicate image (Image -> Duplicate), which is blurred to such an extent that it loses the detail of the cells and maintains only the overall intensity of the background fluorescence. This blurry image is subtracted from the first one (Process - > Image Calculator). The resulting image has more uniform illumination and less background fluorescence. In the image of the selected cell, using the Rectangle tool, the area (ROI) of the nucleus and cytoplasm was manually selected in the form of a square with a side from 10 to 13 pixels. Then we used the ROI Manager tool (Analyze - > Tools -> ROI Manager). In the window that appeared, click the Add button (or “t " on the keyboard), after which the

coordinates of the selected area appeared in the ROI Manager window. After all the regions were selected, Measure was clicked and a table was obtained with the average values of the fluorescence intensity of the nucleus and cytoplasm for each cell. The obtained values were transferred to the Microsoft Excel program, where the N/C ratio was calculated. For each studied construct, three or more photographs were taken, on which up to 100 cells were measured. Statistical processing was performed in the R medium [123].

2.11 Bioinformatic methods

To assess the amyloidogenicity of the protein, we used the ArchCandy program, which predicts all possible beta-arches that can form in the protein [6]. To estimate the boundaries of unstructured sections, we used the IUPred program [38]. In the final analysis, we took arches that were completely located in unstructured areas of the protein. Further, the cumulative score for each position was calculated by summing the score of all β-arches in which this amino acid was present. To evaluate the conservativeness of the sequence, we used the MUSCLE alignment algorithm for constructing protein alignment [42]. Further, the proportion of matching amino acids for each position is calculated using scripts written in the R language available at the link (https://github.com/sukhanovaxenia/Evolutionary_conservatism_of_amyloidogeinc_properties_of_nucleoporins_with_FG_repeat

CHAPTER 3. RESULTS

3.1. Human protein NUP58 demonstrates amyloid properties in various systems

Earlier studies have shown that there are a large number of proteins that can potentially be included in the composition of amyloid aggregates [21]. In our laboratory, we analyzed proteins that interact with the human Htt protein (aggregation of this protein leads to the development of Huntington's disease) according to the BioGRID database [117]. This analysis identified a new potential human amyloid protein, NUP58. ArchCandy predicts that the human protein NUP58 contains several regions that are prone to aggregate formation. One of these regions is a protein fragment with 1 to 213 amino acid residues (Fig. 5). The choice of the program is associated with its high accuracy [6]. The presence of at least one beta-arch is used as a criterion for amyloid properties in this program. Since it is known that protein regions capable of forming amyloids are usually not structured, the obtained predictions were supplemented by modeling unstructured protein regions in the IUPred program [38].

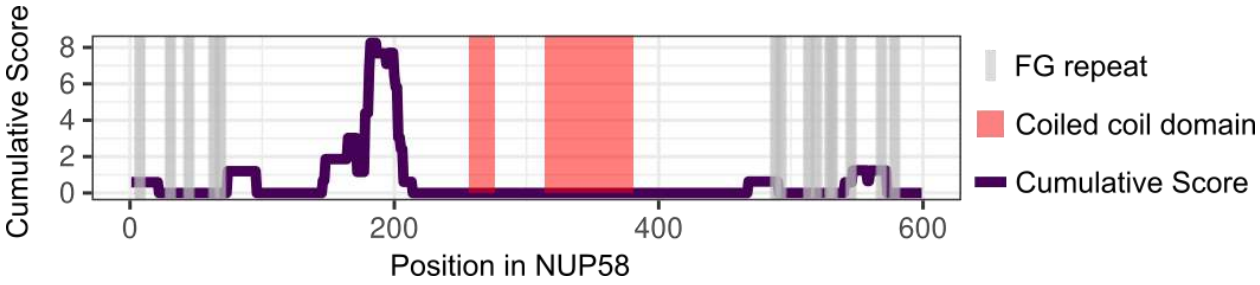

Figure 5-Amyloidogenic regions in NUP58. The cumulative ArchCandy score reflects the protein's ability to form beta-arches, which are a characteristic feature of amyloids. FG repeats - repeats of phenylalanine and glycine, coiled coil domain-coiled coil domain.

The conservativeness of the amyloid properties of human protein orthologs NUP58 was evaluated (101 protein sequences belonging to organisms from the Chordata group were taken for analysis). All the analyzed proteins had amyloidogenic properties. An important result is that the conservativeness of amyloid properties was higher than the conservativeness of the protein sequence (Fig. 6).

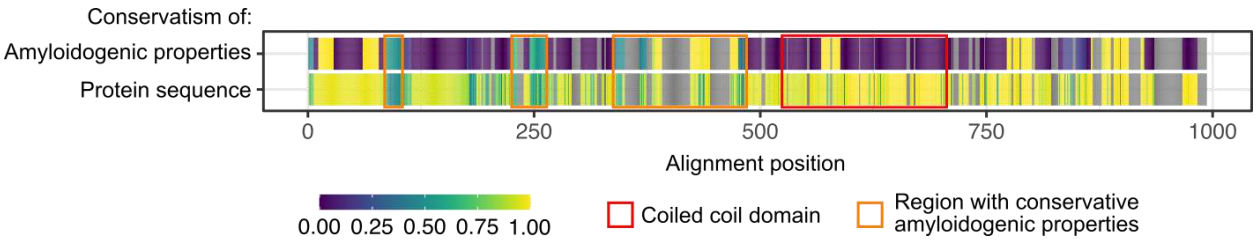

Figure 6-Conservativeness of amyloid properties of NUP58 protein orthologs. The heat map shows the conservativeness of the sequence of NUP58 orthologs (alignment columns containing a large number of gaps are indicated in gray) and the proportion of amyloidogenic sequences in a certain alignment position. Orange rectangles indicate regions with conservative amyloidogenic properties.

3.1.1 Amyloid properties of the NUP58 protein in *vitro*

To analyze the amyloidogenic properties of the NUP58 protein in *vitro*, we purified it from *E. coli* bacterial cells. For this purpose, we took strain BL21 (DE3) (see Materials and methods), which was transformed with plasmid pDEST527-His_6-NUP58. On this plasmid, a sequence of six histidines is encoded before the gene sequence that encodes the NUP58 protein. The resulting transformants were selected on a selective medium with ampicillin. Then, for the obtained transformants, we performed a test induction in a small volume (10 ml of LBa medium) at 37°C. Using SDS-PAGE, we were able to detect an increase in the amount of protein in bacterial cell lysate in the region of 60 kDa, which corresponds to the expected protein size. After preliminary testing, the night culture of transformants grown in liquid LB with the addition of ampicillin was diluted 100 times and increased in large volumes (200 ml in 2-liter flasks) for induction (see Materials and Methods). Protein elution from the column was performed using an imidazole gradient from 8 to 400 mM (samples were taken in 4 mM increments), followed by elution at 400 mM of imidazole (Figure 7). As a result, we obtained a protein preparation NUP58, which can later be used to stage protein aggregation to produce amyloid fibrils *in vitro*. We can also say that the protein elutes best from the column at an imidazole concentration of 40 to 96 mM. The experiments were performed together with Svetlana E. Moskalenko.

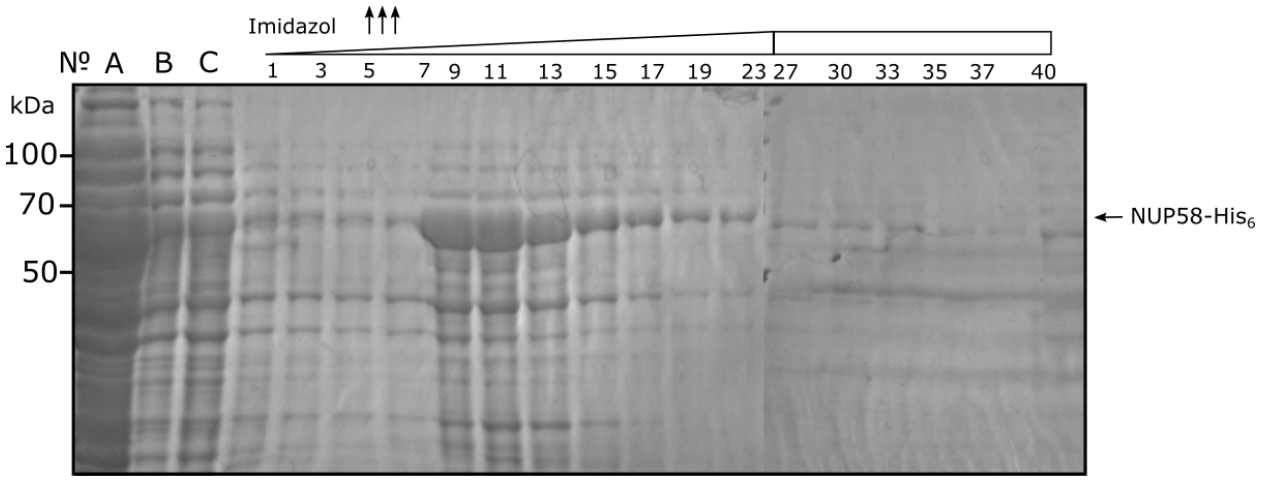

Figure 7-Purification of the NUP58 protein with His6 tag from bacterial cell lysates.
The figure shows a polyacrylamide gel after SDS-PAGE, painted with Coomassie dye. The results of analysis of various fractions after affinity chromatography using Ni-NTA agarose and imidazole concentration gradient are presented. A is the initial lysate, B is the supernatant fraction after centrifugation, and C is the precipitate after centrifugation. Numbers from 1 to 40 – sequentially collected elution fractions with an imidazole gradient of 8 to 400 mM (a step of 4 mM was from 1 to 23 samples, and then the imidazole concentration was 400 mM).

To test the amyloid properties of the protein, we needed to test its ability to aggregate. To do this, we analyzed various aggregation conditions. Initially, we incubated the samples in the following buffer (150 mM NaCl, 5 mM potassium phosphate buffer, pH 7.0) at 37°C. To check for aggregates, we checked the samples using SDS-PAGE. However, according to the results of testing, we did not observe any differences in the protein level in boiled and non-boiled samples. Because of this, we made a selection of the pH values of the solution. As a starting point, we used a buffer with a pH of 6.6, since a buffer with this pH value was used for yeast nucleoporin [59]. We also analyzed three buffers with different pH values, namely 5,8; 7,0; 8,0. All samples were incubated for 96 hours and then tested using SDS-PAGE (Figure 8). In the unboiled sample, the amount of monomeric protein is less than in the boiled sample, since the fibrils are not included in the polyacrylamide gel.

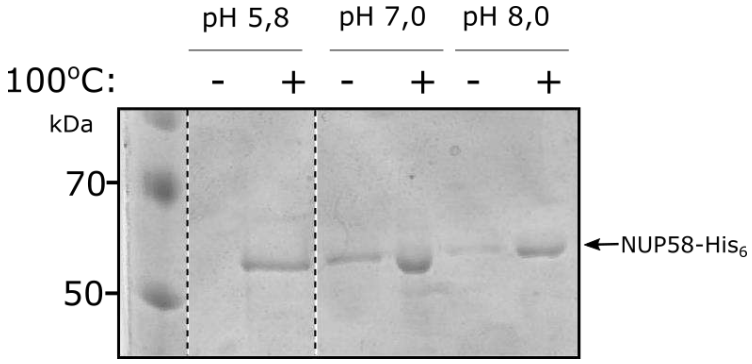

Figure 8-Optimization of NUP58 protein aggregation conditions. The figure shows a polyacrylamide gel after SDS-PAGE, painted with Coomassie dye. The difference in aggregation efficiency can be observed by the difference in protein level between the boiled

and non-boiled samples, depending on the pH of the buffer used. The numbers on the left indicate the molecular weights of the marker in kilodaltons. The arrow indicates the NUP58 protein molecules.

The highest amount of SDS-resistant protein aggregates was obtained at 37°C in the following buffer (150 mM NaCl, 5 mM potassium-phosphate buffer, pH 5.8) at a protein concentration of 1 mg/ml after 96 hours (Figure 8). To obtain the preparative amount of NUP58 protein aggregates, we used these conditions. We checked the presence of these aggregates using the SDS-PAGE method, which compared the amount of protein in boiled and unboiled samples on a Coomassie-colored gel (Fig. 9). In the unboiled sample, the amount of monomeric protein is less than in the boiled sample, which indicates the resistance of the obtained aggregates to detergents (SDS).

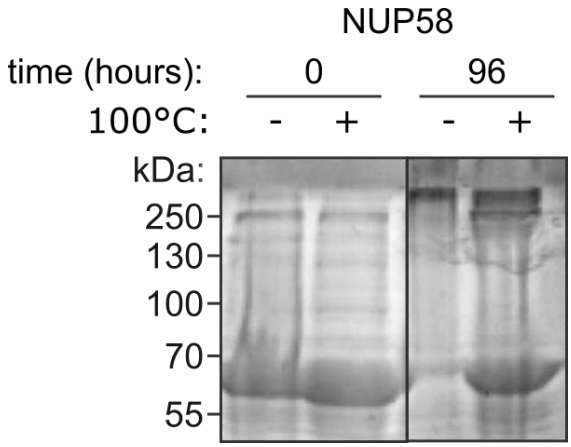

Figure 9-NUP58 protein forms SDS-stable aggregates. The figure shows a polyacrylamide gel after SDS-PAGE, painted with Coomassie dye. After 96 hours of incubation, the difference in protein level between the boiled and non-boiled samples can be observed in comparison with the zero point. The numbers on the left indicate the molecular weights of the marker.

To prove that the resulting aggregate solution consists of fibrils, we analyzed it using transmission electron microscopy. For this purpose, we made preparations (see Materials and Methods) and detected the presence of small fibrils on them (Fig. 10). This allows us to say that the resulting SDS-stable aggregates have a morphology characteristic of amyloid fibrils. The received photos are kindly provided by Mikhail Vladimirovich Belousov.

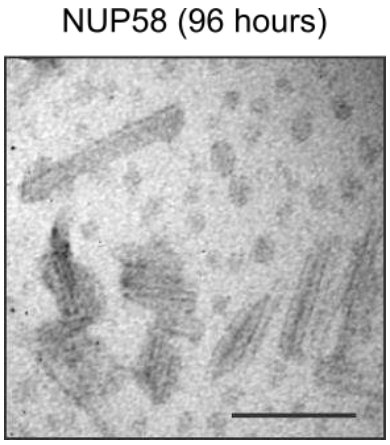

Figure 10 - NUP58 protein forms fibrils *in vitro*. Micrographs of NUP58 protein fibrils prepared using transmission electron microscopy. The scale ruler is 50 nm.

We also used a modification of SDS-PAGE with gel pre boiling [84] to further confirm the detergent stability of the obtained fibrils. We detected the presence of the protein using primary antibodies to His_6 (see Materials and methods). At the first stage of SDS-PAGE, monomeric proteins are added to the gel after boiling. After additional boiling of the gel, the aggregates remaining in the wells fall apart, and we can detect the protein of which they are composed. In the sample without initial heating, we can observe a protein strip in the upper part of the gel, which indicates the presence of SDS-stable aggregates. Using this method, we showed the presence of SDS-resistant aggregates of the NUP58 protein (Fig. 11).

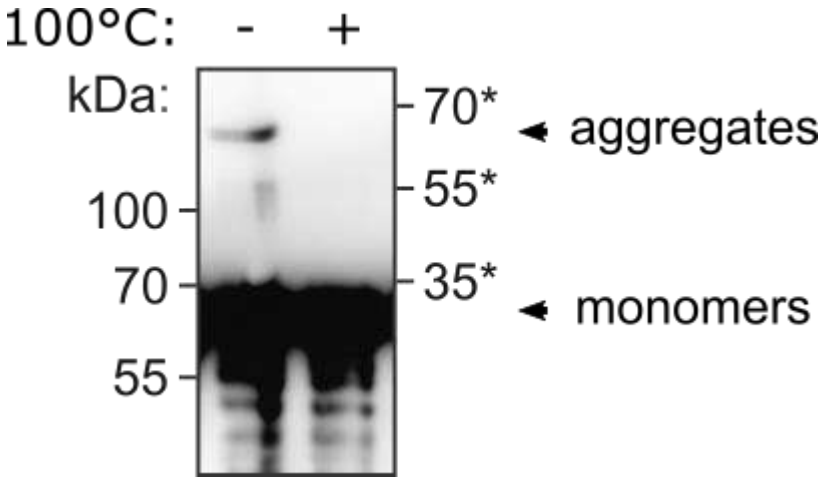

Figure 11-NUP58 protein fibrils are resistant to SDS. When using the SDS-PAGE method with gel boiling, we can detect a small fraction of protein that is part of SDS-stable aggregates. Primary antibodies to the His_6 tag were used for detection in both cases. The numbers on the left indicate the molecular weights of the marker in kilodaltons. Numbers marked with * – a marker added after boiling the gel.

The final stage was visualization of amyloid fibrils using the SDD-AGE method. This

method allows the separation of monomeric proteins and large protein aggregates. Detailed analysis of the NUP58 solution revealed two aggregate forms that differ in size and resistance to BME. We tested the resistance of NUP58 fibrils to "cold" SDS in the absence of BME in the boot buffer for SDD-AGE (Figure 12). Surprisingly, we found large aggregates that were resistant to boiling in SDS, but after heating, we observed the accumulation of smaller aggregates in the sample with BME without boiling (Fig. 12). Since BME leads to the destruction of disulfide bonds, we conclude that these aggregates are rather polymers stabilized by disulfide bonds. A similar situation was previously described for the protein β2-microglobulin, whose amyloid aggregates are also stabilized by disulfide bonds [120]. These studies were carried out with S. A. Bondarev.

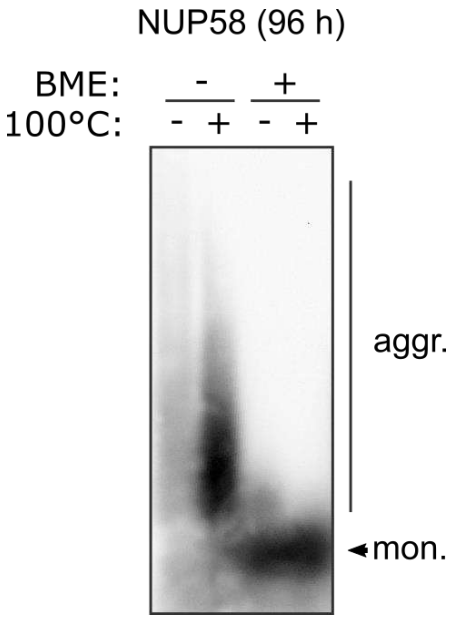

Figure 12-NUP58 protein aggregates are destroyed in the presence of BME. The addition of BME is necessary for the destruction of intramolecular and intermolecular disulfide bonds. In the case of boiling in the presence of BME, we observe the destruction of aggregates. For detection, primary antibodies to His_6 were used.

Another property of amyloid aggregates is their resistance to various proteases. In the course of this work, we analyzed the obtained NUP58 protein fibrils for their resistance to protease K. Previously, PRP protein aggregates were shown to be resistant to this protease [121]. We exposed NUP58 protein fibrils to proteinase K to prove their resistance to proteases. The NUP58 monomeric protein was taken as a control that resistance to proteinase K occurs as a result of the formation of aggregates, and not due to the amino acid sequence of the NUP58 protein. As a result, after incubation with proteinase K for 90 minutes, we observed no proteolysis of the NUP58 protein fibrils, while the monomeric protein was completely degraded (Fig. 13). This figure shows one repetition, and we can observe an increased protein concentration in sample 4, which suggests that protein fibrils are resistant to proteinase

treatment. This provides further evidence that the NUP58 protein forms amyloid aggregates.

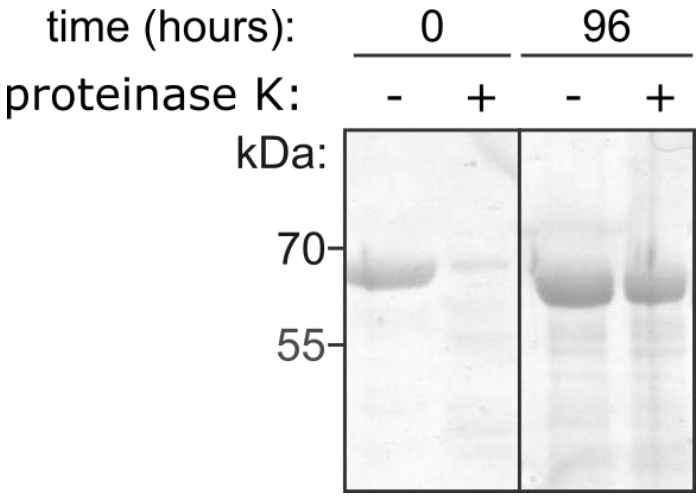

Figure 13-NUP58 protein fibrils are resistant to treatment with proteinase K. The results of the SDS-PAGE are presented. When proteinase K is added to the fibrils of the NUP58 protein, their degradation does not occur in contrast to the monomeric NUP58 protein. The size of the NUP58 protein is 60 kDa. The numbers indicate the molecular weights of the marker in kilodaltons.

In parallel, their ability to bind to specific amyloid dyes was analyzed for the obtained fibrils. One of these dyes is Congo Red. Congo preparations were stained red according to the protocol obtained from Yu. V. Sopova (for more details, see Materials and Methods). Sup35NM protein fibrils provided by S. A. Bondarev were used as a positive control, and BSA (Fermentas) was used as a negative control. As a result, we observed an apple-green glow on the preparations when the Congo red dye binds to the NUP58 protein fibrils (Fig. 14). For positive control of Sup35NM protein fibrils, we also observed an apple-green glow in polarized light, and in the case of BSA, where we expected the absence of amyloid fibrils, we did not observe such a glow.

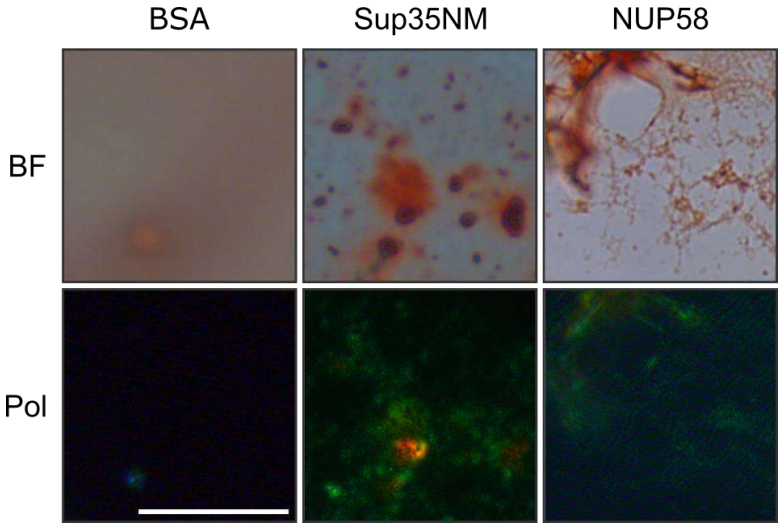

Figure 14-NUP58 protein fibrils bind to the Congo red dye. The figure shows micro-preparations of a protein solution stained with Congo red dye. When the Congo red dye

binds to the fibrils of the NUP58 protein, an apple-green glow can be observed in polarized light. Sup35NM protein was used as a positive control, BSA – as a negative one. The figure shows photos in transmitted light (BF) and polarized light (Pol). The scale ruler is 20 microns.

Another amyloid-specific dye is the Thioflavin T dye. When this dye binds to fibrils, we can observe fluorescence. In the course of our analysis, we found that in the presence of BME, the obtained NUP58 protein fibrils do not show fluorescence. At the same time, the preparation of fibrils without the addition of BME showed fluorescence when bound to the Thioflavin T dye, as well as a positive control – Sup35NM protein fibrils (Fig. 15). The results obtained suggest that the NUP58 protein is an amyloid.

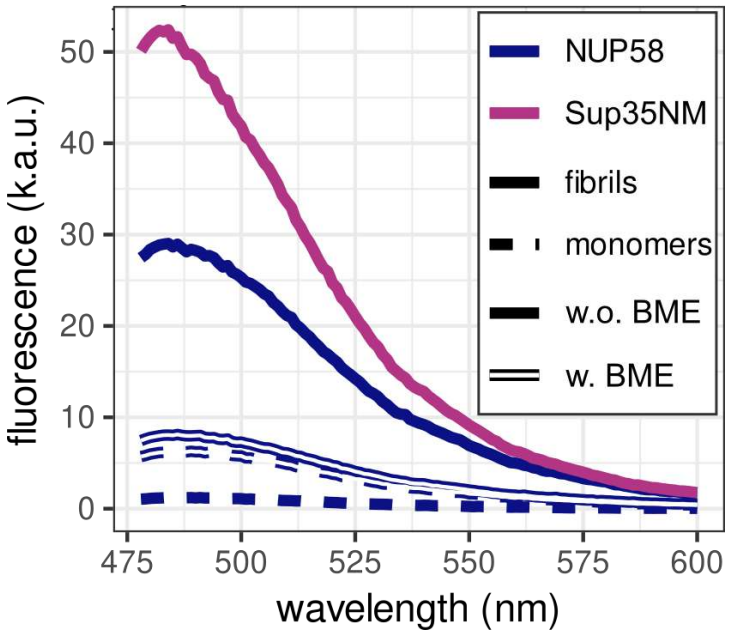

Figure 15-NUP58 protein fibrils bind to the dye Thioflavin T. The figure shows a graph of the fluorescence intensity of Thioflavin T bound to NUP58 protein fibrils. Sup35NM protein fibrils were used as a positive control.

3.1.2 Amyloidogenic properties of NUP58 protein in model systems

A large number of different systems are used to test amyloid properties, including yeast and bacterial cells (for more information, see Literature review). To test the amyloidogenic properties of the NUP58 protein, we constructed the pAG416GPD-EGFP-NUP58 and pVS-GW-NUP58 plasmids carrying the full-length human NUP58 protein. For experiments in the C-DAG system, the bacterial strain VS39 was transformed with the plasmid pVS-GW-NUP58. The bacteria selected after transformation were seeded into three LB-based media, one of which was simply selective, the second contained the Congo Red dye, and the third contained the amyloid-specific Congo Red dye and inductors (Arabinose and IPTG). As a result, after 5 days of growing bacteria on special media containing plasmids with the *NUP58* gene sequence at 26°C, we observed separate red colonies (Fig. 16). This was due to the fact that large proteins in the C-

DAG system lead to cell death (personal message of Yu.V. Sopova). To obtain a more explicit result, we obtained the pVS-GW-NUP58-1-213 plasmid, which contained the first amyloidogenic protein region from 1 to 213 a.a.. Bacterial cells carrying this construct also showed the red color of the colonies. We used Sup35NM and Sup35M proteins as positive and negative controls, respectively.

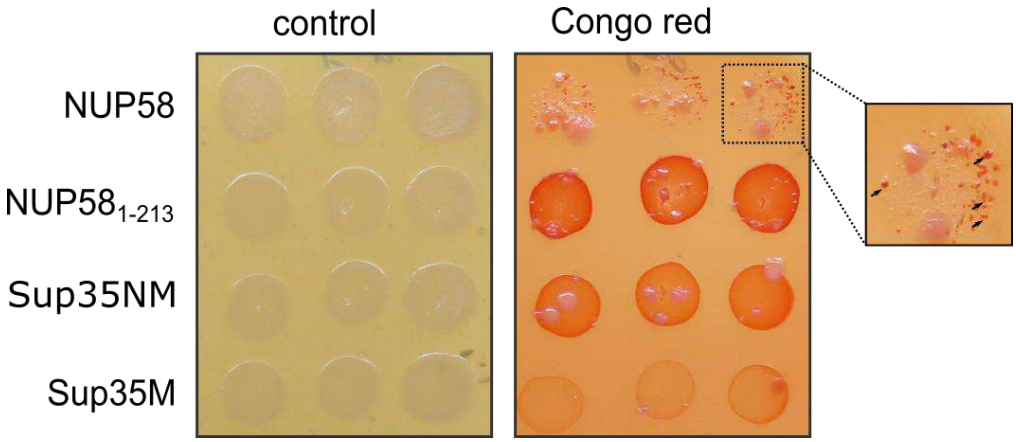

Figure 16-Bacteria with plasmid pVS-GW-NUP58 and pVS-GW-NUP58-1-213 red on medium with Congo red and inducers. The arrows in the removed areas indicate red colonies with NUP58 protein production. Sup35NM and Sup35M proteins were used as positive and negative controls, respectively. Designations: control - selective medium with antibiotics, Congo red-medium with antibiotics, Congo red dye and inducers. Photos of the plates are presented on day 5.

Then, we analyzed the bacteria that were grown on plates containing the inductor and the Congo red dye using transmission electron microscopy. As a result, we observed the presence of fibrils on the surface of cells in which the NUP58 protein and its fragment $NUP58_{1-213}$ were overproduced (Fig. 17). As a positive and negative control, we also used the Sup35NM and Sup35M proteins, respectively, in which we observed the formation of fibrils or smooth bacterial cells.

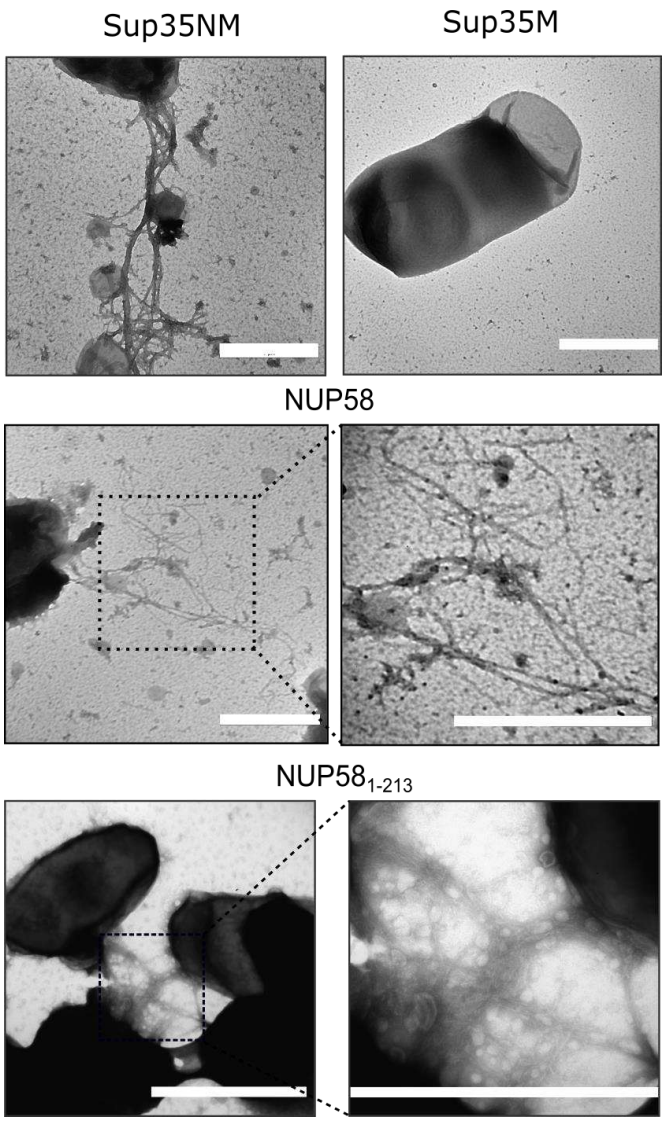

Figure 17-The NUP58 protein and its NUP58 fragment$_{1-213}$ form fibrils in the C-DAG system. The figure shows TEM micrographs. Sup35NM and Sup35M proteins were used as positive and negative controls. The scale ruler is 1 micrometer.

The number of bacterial cells in which the full-size NUP58 protein was super-produced did not allow conducting experiments on polarization microscopy, and for this experiment, cells producing the NUP58$_{1-213}$ fragment were used. The colonies were analyzed using a polarizing microscope. We observed an apple-green glow in the case of NUP58$_{1-213}$ and Sup35NM proteins, which indicates that the NUP58 protein has amyloidogenic properties (Fig. 18).

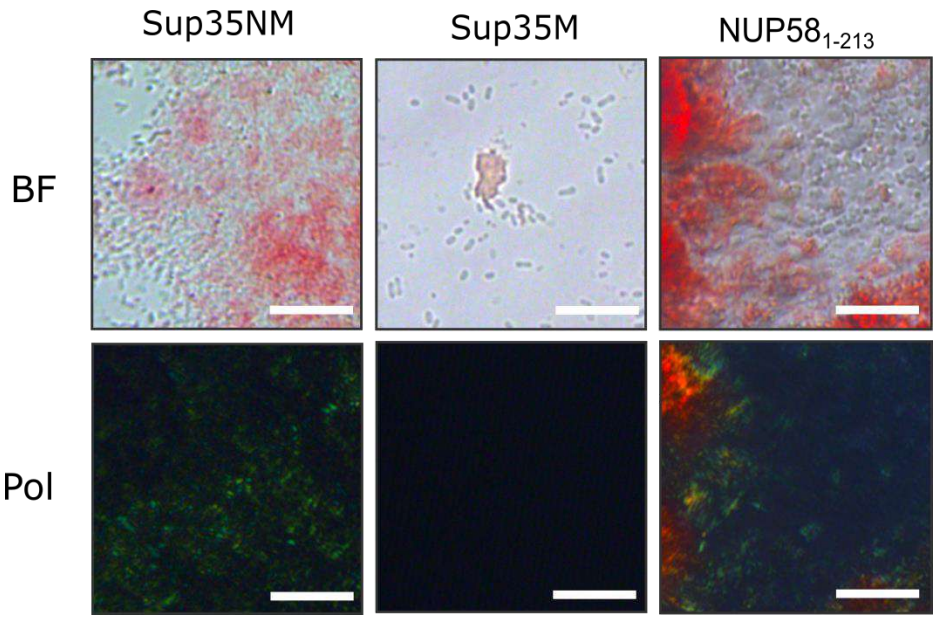

Figure 18-When the NUP58$_{1-213}$ protein is overproduced in bacteria, its fibrils have an apple-green glow in polarized light. Micrographs of cells from Figure 16 are presented.Sup35NM and Sup35M proteins were used as positive and negative controls, respectively. The figure shows photos in transmitted light (BF) and polarized light (Pol). Scale ruler of 50 microns.

Yeast is a convenient model object due to the simplicity of introducing various constructs into cells, the simplicity of cultivation, as well as the presence of the described prions and developed systems for testing protein aggregation (see literature review). Therefore, we used them as a model system to test the amyloidogenic properties of the NUP58 protein. To do this, we introduced a chimeric construct encoding the NUP58 protein fused with the fluorescent GFP protein under the GPD promoter into *S. cerevisiae* yeast cells using transformation. This promoter provides constitutive protein overproduction. In our analysis, the NUP58 protein was selected as a protein that can coagulate with the huntingtin protein. One of the Q-rich proteins of *S. cerevisiae* yeast is Rnq1, the aggregation of which leads to the appearance of the prion [*PIN*$^+$]. Aggregates of the Rnq1 protein can induce aggregation of other polyQ proteins [102]. To test whether the presence of the [*PIN*$^+$] prion affects NUP58 protein aggregation, we transformed 2 isogenic yeast strains 74-D694 and 2-74-D694, which differed in [*PIN*$^+$] status, with the pAG416-EGFP-NUP58 plasmid. After that, 6 transformants of each strain were analyzed using fluorescence microscopy. In yeast cells, we could observe fluorescent foci of luminescence of the NUP58 protein cross-linked with GFP. This is another proof of the amyloidogenic properties of this protein. However, as a result, we did not reveal any visual differences between [*PIN*$^+$] and [*pin*$^-$] strains either in the number of cells with aggregates or in their morphology (Fig. 19).

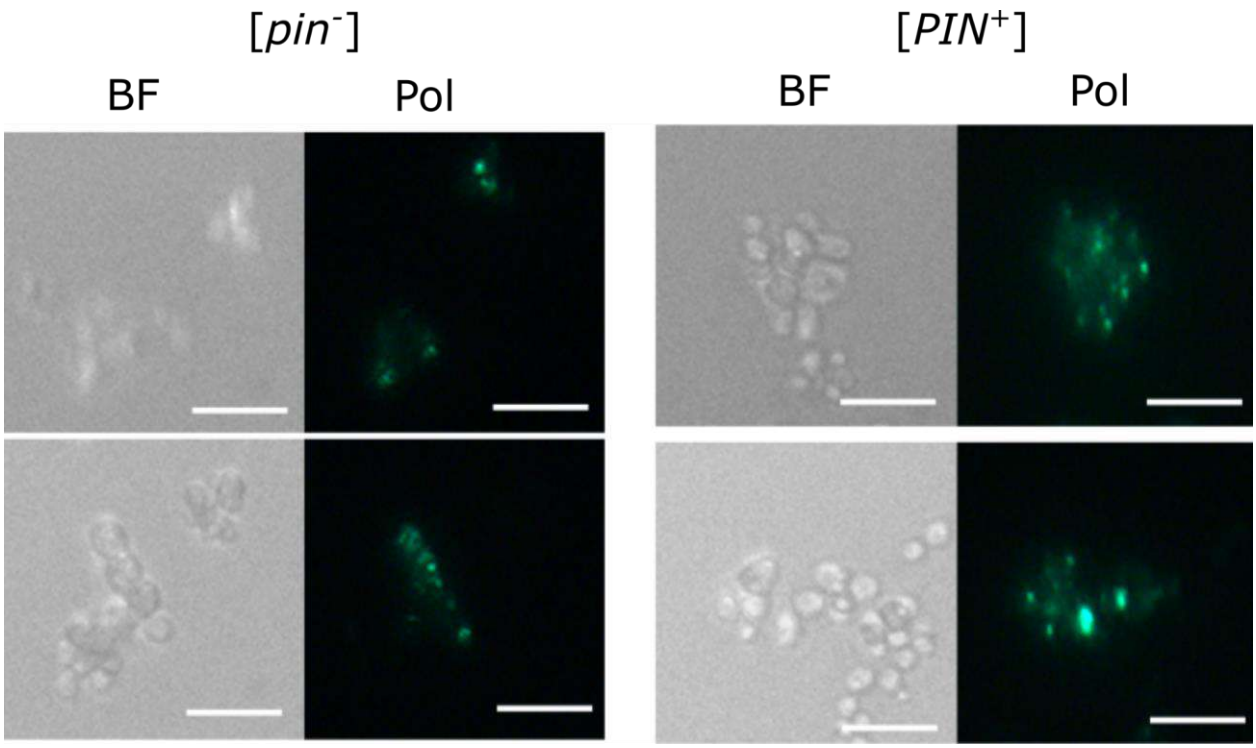

Figure 19-Aggregation of the NUP58 protein is independent of the presence of the yeast prion [*PIN*$^+$]. Strain 2-74-D694 – [*pin*$^-$], strain 74-D694 – [*PIN*$^+$]. The figure shows images in transmitted light (BF), and GFP. The scale ruler is 5 microns.

3.2. Fragments of nucleoporin NUP58 have amyloidogenic properties

To determine the NUP58 site responsible for its aggregation, we performed a deletion analysis of the NUP58 protein. Based on the predictions of the ArchCandy program (Figure 5), we selected potential fragments of the NUP58 protein for further evaluation of their amyloidogenicity, namely, fragments NUP58$_{1\text{-}95}$ and NUP58$_{215\text{-}599}$. To obtain shortened variants, fragments were amplified from the pDONR221-NUP58 matrix using PCR, the program of which is described in the corresponding section " Materials and Methods", primers are listed in Table 4. Subsequent preparation of plasmids is described in the section Materials and Methods. Experiments in this section were conducted jointly with Ekaterina Antonova.

3.2.1 Verification of aggregation of NUP58 protein fragments in the C-DAG system

Bacterial transformation of *E. coli* strain VS39 by plasmids pVS-GW-NUP58-215-599 and pVS-GW-NUP58-1-95 was performed using the C-DAG system to check the aggregation of fragments. For bacteria containing plasmids with fragments of the NUP58 gene at 30°C, we observed red coloration of colonies (Fig. 20) on plates containing inducers and Congo red.

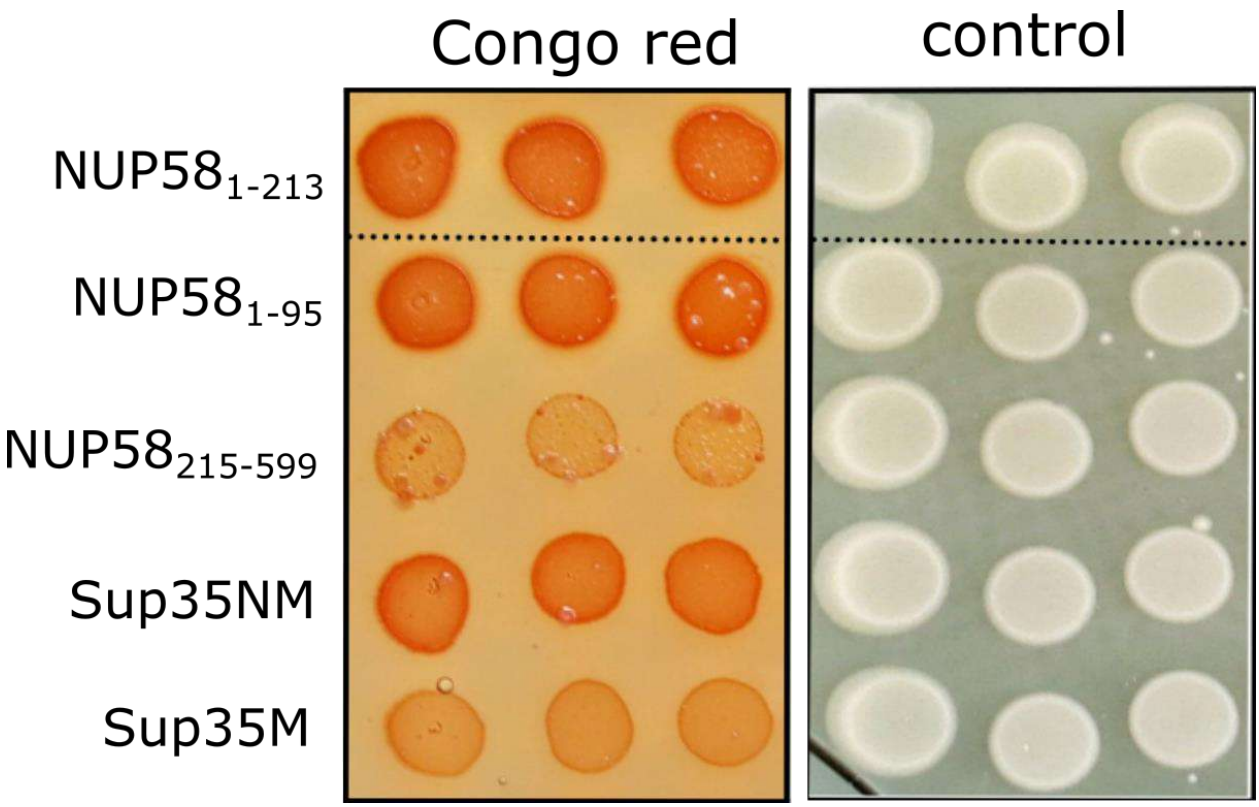

Figure 20-Fragments of the NUP58 protein bind to the Congo red dye. Designations: control - selective medium with antibiotics, Congo red-medium with antibiotics, Congo red dye and inducers. Sup35NM and Sup35M proteins were used as positive and negative controls. The bacterial growth time is 5 days.

Sup35NM was used as a positive control, and $NUP58_{1-213}$ was also used as an additional positive control due to the fact that its aggregation was shown earlier [30]. In the case of positive controls, we observed a red coloration of the colonies; in the case of negative controls, the Sup35M protein, there was no red coloration of the colonies. Comparing the color of the studied colonies containing fragments of the NUP58 protein with positive and negative controls, the following observations were made: staining of Congo amyloid fibrils with red is observed in the $NUP58_{1-95}$ fragment, and the NUP58 215-599 fragment does not have this property. Then, bacteria grown on plates (Figure 20) containing an IPTG inducer and a Congo red dye were analyzed using transmission electron microscopy (Figure 21). As a positive and negative control, we also used the Sup35NM and Sup35M proteins, respectively, in which we observed the formation of fibrils or smooth bacterial cells. As a result, we observed the presence of fibrils on the cell surface of only one fragment, namely, $Nup58_{1-95}$.

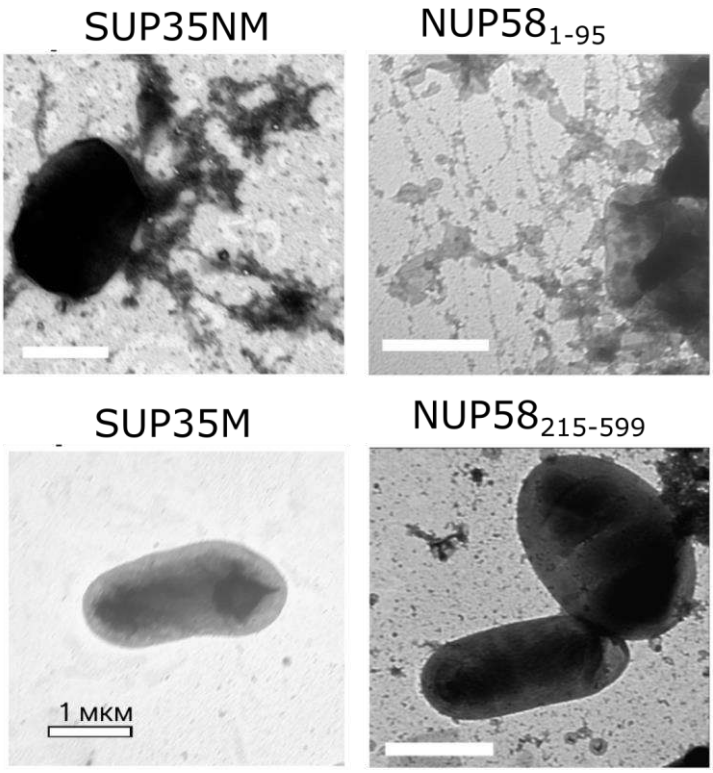

Figure 21-The NUP581-95 protein fragment is formed by fibrils in the C-DAG system. The figure shows TEM micrographs. Sup35NM and Sup35M proteins were used as positive and negative controls. The scale ruler is 1 micrometer.

Then we analyzed the same cells using a polarizing microscope (Fig. 22). We observed an apple-green glow in the NUP58$_{1-95}$ protein fragment, which indicates its amyloid properties. No luminescence was observed for the fragment NUP58 215-599, which indicates the absence of amyloid properties in this system.

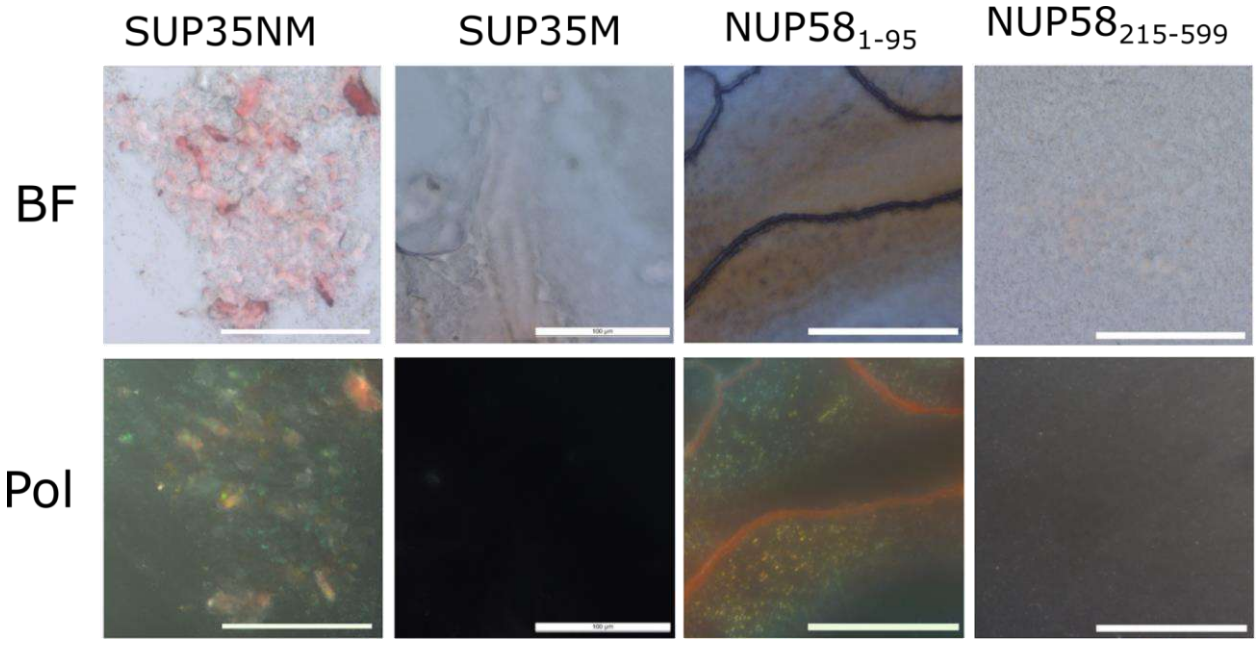

Figure 22-When the NUP58 1-95 protein is overproduced in bacteria, its fibrils have an apple-green glow in polarized light. Micrographs of cells from plates from Figure 20 are

presented. Sup35NM and Sup35M proteins were used as positive and negative controls, respectively. The figure shows photos in transmitted light (BF) and polarized light (Pol). Scale ruler of 50 microns.

The generalized results of the verification of fragments of the human protein NUP58 in the C-DAG system are presented in Table 6. Thus, we can say that the main amyloidogenic region is located from 1 to 213 amino acid residues, which is in good agreement with the predictions of the ArchCandy program (Fig.5).

Table 6 - Results of testing the amyloid properties of the human protein fragment NUP58 in the C-DAG system

Protein	**Red color of colonies**	**Polarization**	**Fibrils on TEM**
$NUP58_{1-213}$	Yes	Yes	Yes
$NUP58_{1-95}$	Yes	Yes	Yes
$NUP58_{215-599}$	No	No	No

3.2.2 Checking aggregation of NUP58 protein fragments in the yeast system

We used *S. cerevisiae yeast* as an additional model system to test the amyloidogenic properties of NUP58 protein fragments. For this purpose, we introduced chimeric constructs with fragments of the human protein NUP58 under the GPD promoter into *S. cerevisiae yeast cells* using transformation. This promoter provides constitutive protein overproduction. To test whether the presence of the prion [PIN^+] affects aggregation of NUP58 protein fragments, we transformed 2 isogenic yeast strains 1-OT56 and 2-OT56, which differed in [PIN^+] status, with plasmids pAG416GPD-EGFP-NUP58-215-599 and pAG416GPD-EGFP-NUP58-1-95. After that, the transformants of each strain were analyzed using fluorescence microscopy. According to the results of the experiment, luminescence foci were found for the constructs $NUP58_{1-95}$ and $NUP58_{215-599}$ (Fig. 23), which is due to aggregation of protein fragments. This means that the constructs $NUP58_{1-95}$ and $NUP58_{215-599}$ are able to aggregate in yeast cells.

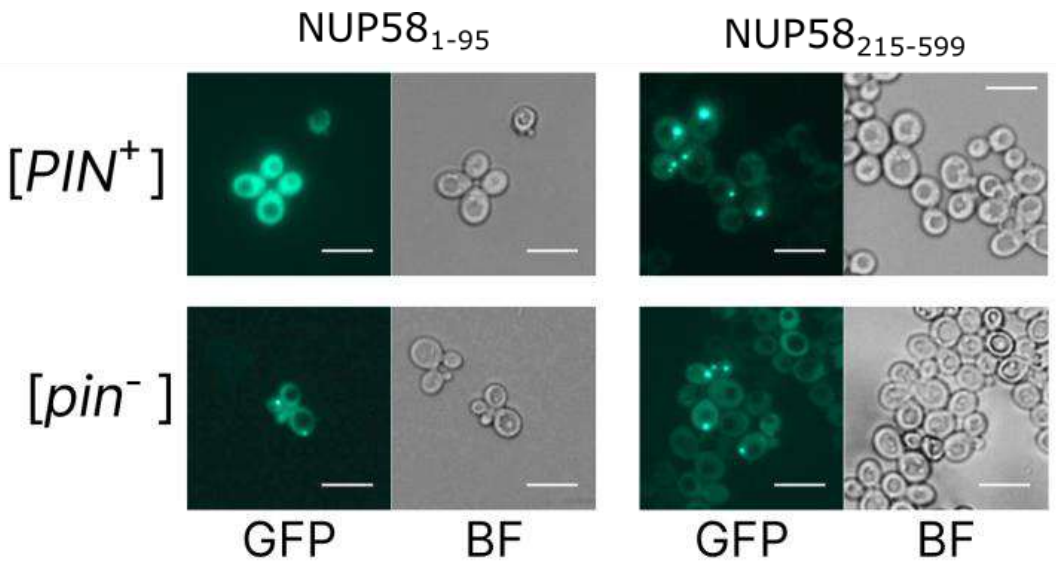

Figure 23-Aggregation of NUP58 protein fragments depends on the presence of yeast prion [*PIN*$^+$], fluorescence microscopy photos. In yeast cells, we could observe fluorescent foci of luminescence of the NUP58 protein crosslinked with GFP — this is another proof of the amyloid properties of this protein. Diffuse luminescence means that the protein is produced by yeast cells, but does not form fibrils. Strain 2-OT56 – [*pin*$^-$], strain 1-OT56 - [*PIN*$^+$]. The figure shows images in transmitted light, and GFP. The scale bar is 5 microns

3.3. Orthologs of human protein NUP58 and yeast protein Nup100 demonstrate amyloidogenic properties

Regulation of nuclear-cytoplasmic transport is an essential process that supports cellular homeostasis. The presence of amyloid properties in the human protein NUP58, as well as in yeast nucleoporins, suggests that amyloid properties may be the same and occur in nucleoporins from different taxonomic groups. To solve this problem, we performed a bioinformatic assessment of the amyloid properties of these proteins in the ArchCandy program with an additional filter applied to unstructured protein regions. The choice of the program was based on a series of articles that demonstrated its high accuracy in comparison with its analogues [6, 22, 126]. These studies were carried out jointly with Sukhanova K. V. and Bondarev S. A.

3.3.1 Bioinformatic analysis of amyloid properties of orthologs of nucleoporin proteins

Nucleoporins with FG repeats were used in the analysis, since experimental evidence of their aggregation was previously obtained for two proteins of *S. cerevisiae* yeast (Nup100 and Nsp1) [58, 86]. In addition, earlier in our work, we showed amyloid properties for aggregates of the human human protein NUP58, which also contains a similar domain. The list of proteins for analysis was formed on the basis of review articles (for example, [155]). We searched for orthologs using the EggNOGG database (http://eggnog5.embl.de/) [65] for the Opisthokonta

group. First of all, we analyzed *S. cerevisiae* proteins, since amyloid properties were shown for a large number of yeast proteins [10]. The list of proteins and the corresponding orthogroups are presented in Table 7.

Table 7-Proteins taken for analysis and their orthogroups.

* – *nucleoporins that do not contain FG repeats*

Белок *S. cerevisiae*	**protein Eggnogg**	**Vertebrate homologue**	**orthogroup Vertebrate homologue Eggnogg orthogroup for a vertebrate homologue (if it does not match column 2)**
Nup42	ENOG5039YMU	hCG1/NLP1	
Nup159	ENOG5039SKI	Nup214	
Nup49	ENOG5039TYE	Nup58, Nup45	ENOG5039TBQ
Nup57	ENOG5038C34	Nup54	ENOG503988N
Nsp1	ENOG5038HQQ	Nup62	
Nup100, Nup116, Nup145	ENOG5038I30	Nup98	
Nup1	ENOG5038UZQ	Nup153	ENOG5039R35
Nup2	ENOG5038HDP	Nup50	ENOG503969S
Nup60	ENOG503A52U	-	
Nup84*	ENOG5038BZM	Nup107	
Nup192*	ENOG5038B8H	Nup207	

Before further analysis, the sequences were additionally checked for repetitions (more than one sequence for one species), as well as for sequences that were mistakenly included in the set when compiling the database. Multiple alignment was constructed for each group of sequences based on the MUSCLE algorithm [42], which is the most widely used one to date. The algorithm built into the UGENE program [112] was started with an additional "refine" step to improve the alignment quality. During the analysis of the obtained alignment and filtering, we deleted sequences in the case of (1) if the protein records were deleted from NCBI databases, (2) if they captured only the C-terminal part of the protein (devoid of FG repeats), (3) if they were significantly shorter compared to another sequence of the same type. In several cases, we changed the sequences obtained from EggNOGG, if in the NCBI database, they contained updated versions.

To clarify the position of the fragments of interest, we created a set of functions that allowed us to superimpose data on amyloidogenic regions of proteins on their multiple alignment. This allowed us to trace how conserved the amyloid properties and amino acid composition of aligned protein fragments are. We estimated the conservativeness of amyloid properties at a particular alignment position as the proportion of sequences in which the corresponding amino acid is included in the amyloidogenic region from all sequences where there is no "gap" in a particular position. In order to avoid biasing the calculations towards the most represented taxonomic groups, we randomly left only a part of the sequences from the groups in the analysis. At the same time, this procedure was repeated 10 times for each set of proteins (these additional calculations were carried out during the second stage of the project). During the analysis, we also collected data on the presence of tertiary structures in nucleoporins (PDB database) and superimposed these data on alignments. For the formation of amyloid aggregates, an important requirement is the disordered nature of the aggregation-prone protein region. In the future, we excluded areas with a known structure from consideration.

When analyzing the results, we paid attention to homologous, according to alignment, sequences with high conservativeness of amyloid properties, which are present in more than half of the analyzed sequences, and are located outside the structured protein domains. Among the homologues of Nup84 and Nup192 proteins (proteins without FG repeats) we didn't find any such candidates. We made similar conclusions for the Nup42, Nup1, Nup153, Nup2, Nup50, Nup58, Nup54, Nup145, and Nup60 proteins. In the case of Nup49 and Nup57, such fragments were found. For Nsp1 and Nup159, we were able to detect regions with conservative amyloid properties only for certain taxonomic groups: Chordata and Ascomycota, respectively (Figure 24). Separately, I would like to note that in some cases the conservativeness of the amyloid properties of some of these sequences was higher than the conservativeness of the amino acid sequence. This may indirectly indicate that in the course of evolution, when the protein sequence changes, its tendency to aggregation may have been preserved. It is also important to note that Nup49 and Nup57, as well as Nsp1 and Nup159, are proteins that are located directly in the nuclear pore channel and are directly involved in the formation of a selective barrier. Thus, it can be assumed that the aggregation of these proteins may be important, since the corresponding property is preserved in many species.

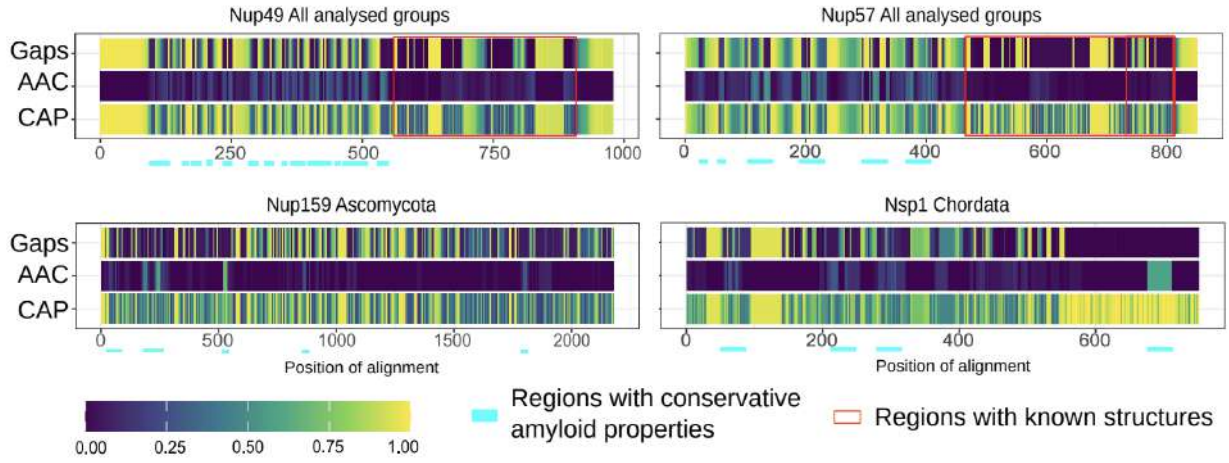

Figure 24 – Some of the nucleoporins with FG repeats have regions with conserved amyloid properties. Gaps — frequency of gaps in the position of alignment. AAC (Amino Acids Conservatism) — rate of most frequent amino acids. CAP (Conservatism of Amyloidogenic Properties) — frequency of cases when corresponding position is located inside amyloidogenic region. Regions with known structures are highlighted by red frames. Light cyan corresponds to potential conservative amyloidogenic regions.

Separately, we analyzed the sequences of the yeast protein Nup100 in several yeast strains: strain SC288C (this strain is a classic reference in research), as well as 2 strains 74-D694 and 15V-P4. The Nup100 protein is a protein determinant of the well-described prion [*NUP100*$^{+}$] [59]. According to the results obtained, we can observe that a large number of amino acid substitutions are located after 400 amino acids (Fig. 25). According to experimental data, the site from 200 to 400 aa is directly responsible for aggregation [59]. It should also be noted that we found two structurally different alleles of the gene *NUP100*. Moreover, strain 74-D694 contains a unique chimeric allele, in which the sequence near the N-terminus of the protein is identical to the reference S288C allele, and the middle and C-terminal parts of the protein originate from the ancestral allele of another strain (15V-P4). The set of mutations found in these strains has different effects on the tendency of the $NUP100_{1\text{-}400}$ nucleoporin fragment to aggregate, but the overall effect is still aimed at preserving the amyloid properties of the NUP100 protein. This may serve as further evidence that the aggregation of nucleoporins may be necessary in the case of the organization of nuclear-cytoplasmic transport [13].

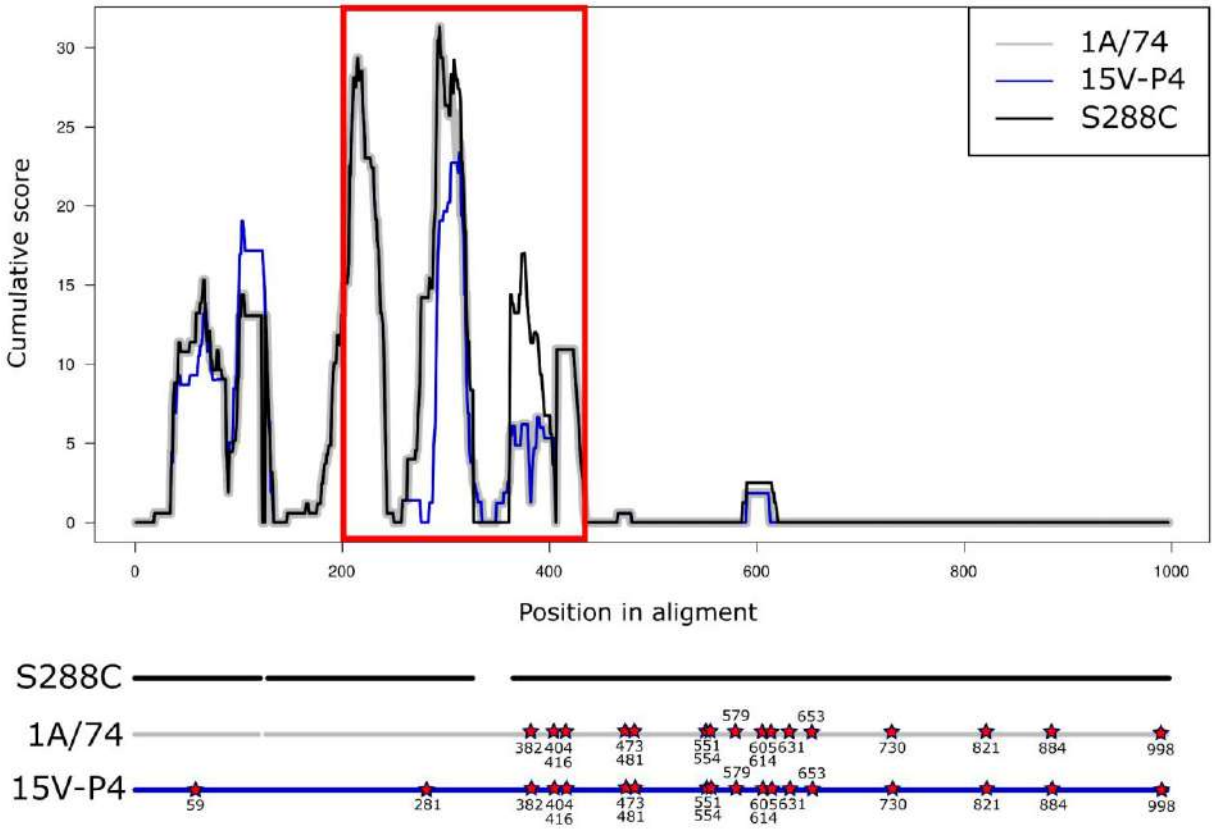

Figure 25. Yeast protein Nup100 demonstrates conservative amyloid properties in various yeast strains. The cumulative ArchCandy score reflects the protein's ability to form beta-arches, which are a characteristic feature of amyloids. The red border represents the prion domain required for aggregate formation. Breaks in the lines indicate the positions of deletions in the corresponding alleles of the NUP100 gene*NUP100*.

3.3.2 Nucleoporin proteins of various organisms exhibit amyloidogenic properties in the C-DAG system

In the course of our bioinformatic analysis, we identified a large number of nucleoporins with amioloid properties. For experimental tests, we selected individual representatives of orthologs from various organisms. We selected orthologs that had the highest level of predicted amyloidogenicity and also belonged to any model organisms. The corresponding experiments were conducted jointly with Rogoza Tatyana Mikhailovna. Then, potentially amyloidogenic fragments of these proteins were cloned into pVS-GW plasmids for subsequent testing in the bacterial C-DAG system (see Materials and Methods). The experiment was performed in each case for six independent transformants and in two independent replicates.

According to the results obtained, cells producing fragments of hsNup62$_{1\text{-}175}$, tgNup58$_{60\text{-}320}$, dmNup98$_{250\text{-}500}$, and spNup98$_{250\text{-}500}$ are red on a medium with Congo red (Fig.

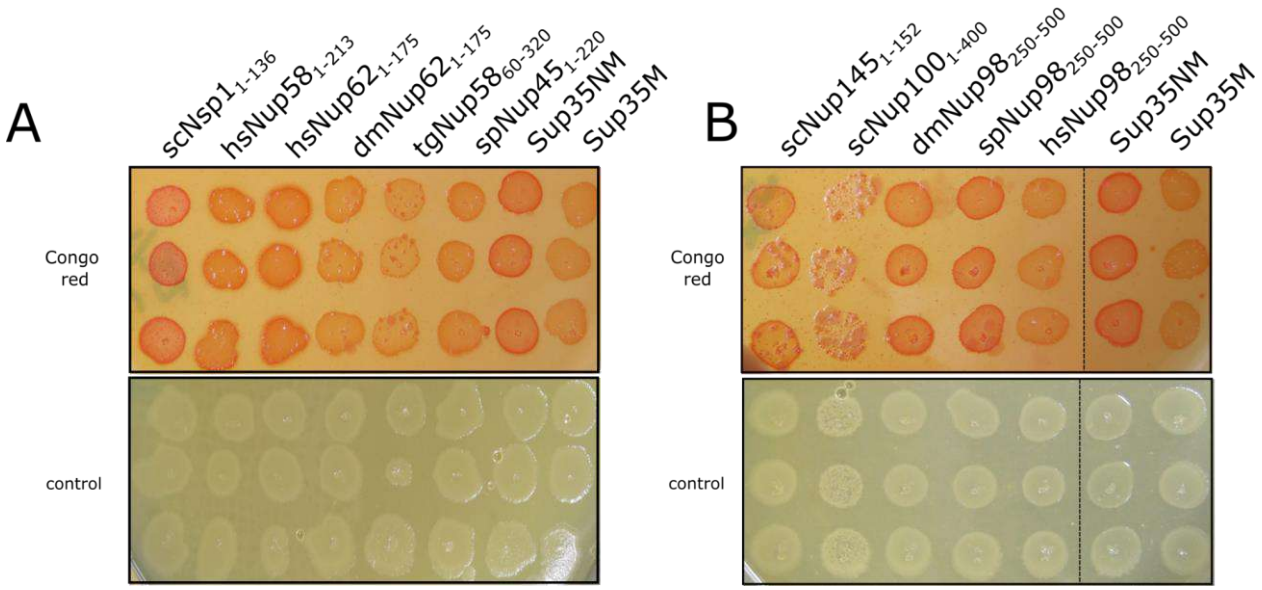

Figure 26-Overproduction of nucleoporins of various types leads to staining of bacterial cells on a medium with Congo red. Panel A shows the results for orthologs of the yeast protein Nsp1, and for orthologs of the yeast protein Nup145 (Nup100, Nup116) – panel B. Congo red-medium with antibiotics, Congo red dye and inducers. Sup35NM and Sup35M proteins were used as positive and negative controls. The bacterial growth time is 5 days.

The presence of apple-green birefringence aggregates colored with Congo red is important evidence for the presence of amyloids. We were able to show this feature only for bacterial cells producing fragments of the nucleoporins tgNup58$_{60-320}$, dmNup98$_{250-500}$, and spNup98$_{250-500}$ (Fig. 27)

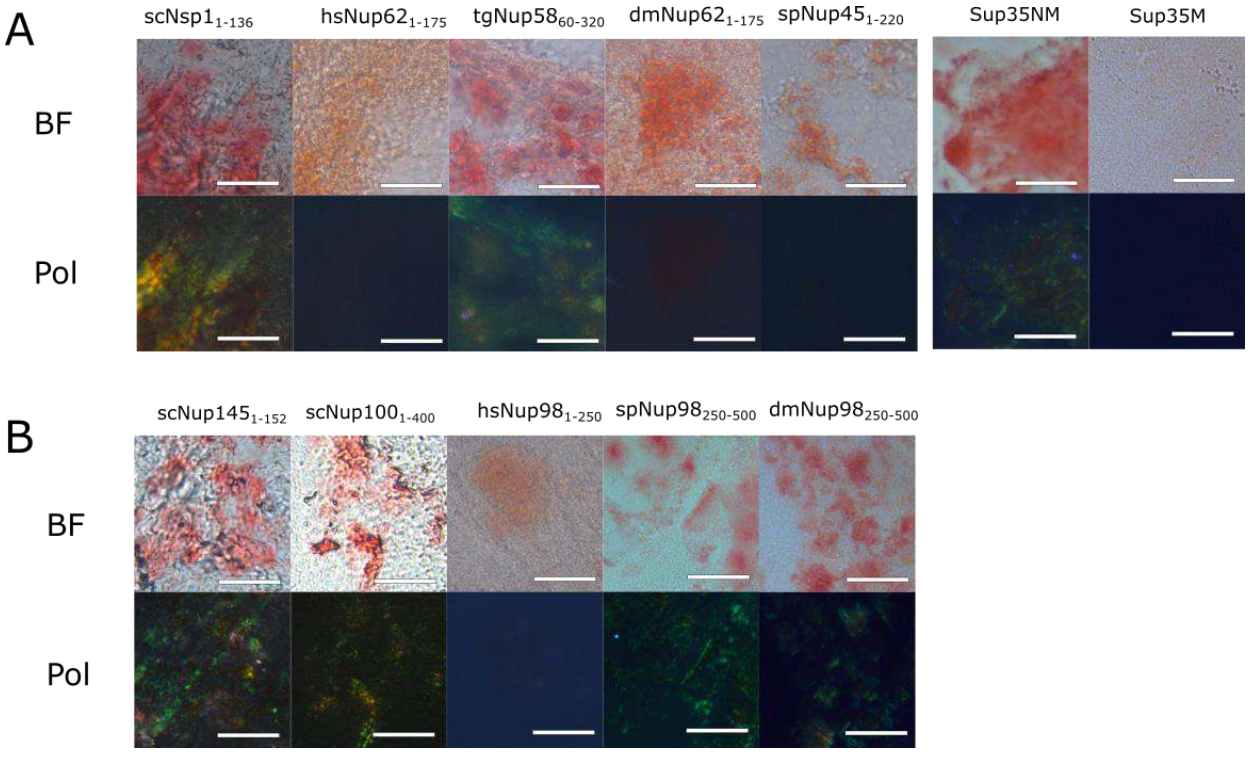

Figure 27-Bacteria producing fragments of the tgNup58$_{60-320}$, dmNup98$_{250-500}$, and spNup98$_{250-500}$ proteins show an apple-green glow in polarized light. Panel A shows the

results for orthologs of the yeast protein Nsp1, and for orthologs of the yeast protein Nup145 (Nup100, Nup116) - in panel B. The figure shows photos in transmitted light (BF) and polarized light (Pol) of bacteria from the plates shown in Figure 26. The Sup35NM and Sup35M proteins are taken as positive and negative control. Scale bar is equal 25 microns.

At the next stage of our work, we checked the presence of fibrils on the surface of the obtained transformants. For this purpose, we used transmission electron microscopy. The preparations were prepared in the same way as in the experiments with yeast nucleoporins. As a result of the analysis of the preparations, we were able to detect fibrils on preparations with bacteria producing the proteins tgNup58$_{60\text{-}320}$, dmNup98$_{250\text{-}500}$, and spNup98$_{250\text{-}500}$ (Fig. 28), which coincides with the data of polarization microscopy. Similar results were obtained for two independent transformants.

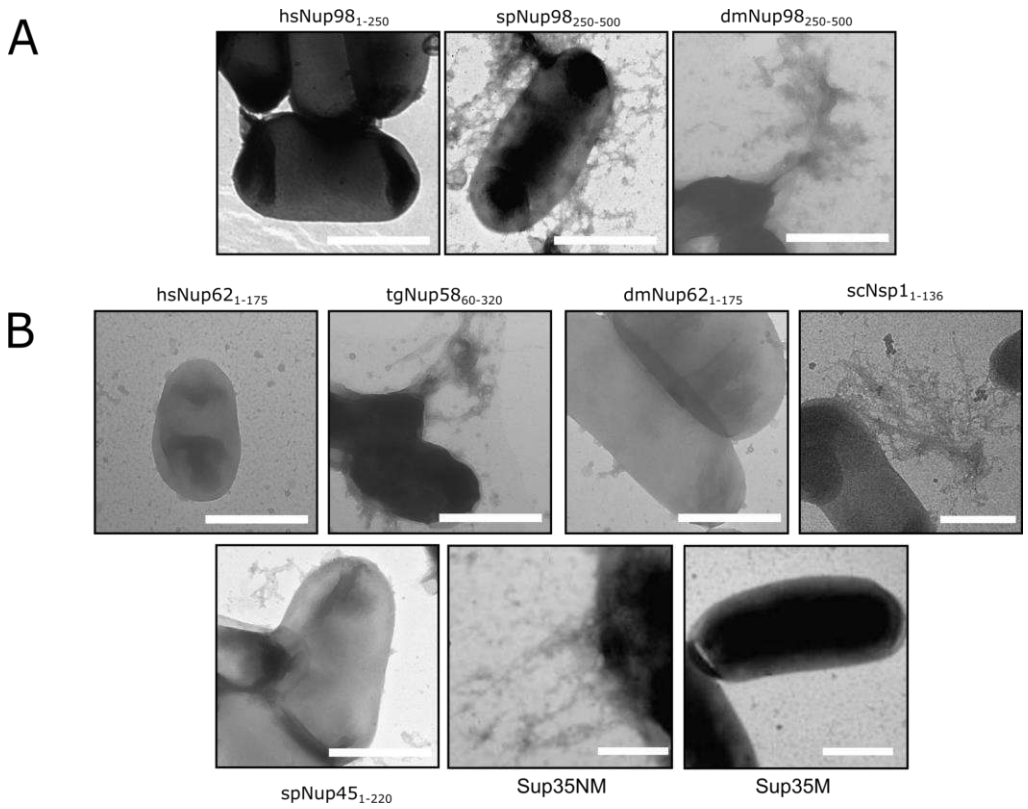

Figure 28-Fragments of the nucleoporins tgNup58$_{60\text{-}320}$, spNup98$_{250\text{-}500}$, and dmNup98$_{250\text{-}500}$ form amyloid aggregates on the cell surface. Panel A shows the results for orthologs of yeast protein Nsp1, and for orthologs of yeast protein Nup145 (Nup100, Nup116) - in panel B.

Summarizing the results obtained in the bacterial C-DAG system, it can be concluded that the tgNup58$_{60\text{-}320}$, spNup98$_{250\text{-}500}$, and dmNup98$_{250\text{-}500}$ proteins form amyloid aggregates. Such results were obtained for the first time.

3.3.3 Nucleoporin proteins from various organisms exhibit amyloidogenic properties in the yeast system

In the bacterial C-DAG system, not all of the studied proteins showed amyloid properties, which contradicted the results of bioinformatic analysis. In this regard, we decided to conduct an additional test of the ability of the studied proteins to aggregate using a yeast model system. For this purpose, we obtained a set of constructs based on pAG416-EGFP-ccdB for the overproduction of the studied proteins fused with EGFP. Using these constructs, we transformed the 74-D694 strain and analyzed the localization of proteins inside cells. For tgNup58$_{60\text{-}320}$ spNup45$_{1\text{-}220}$ hsNup98$_{1\text{-}250}$ spNup98$_{20\text{-}500}$ dmNup98$_{250\text{-}500}$, we were able to detect fluorescent protein clusters. However, in the cases of tgNup58$_{60\text{-}320}$ and spNup45 1-220, we rather observed amorphous protein accumulations (Fig. 29).

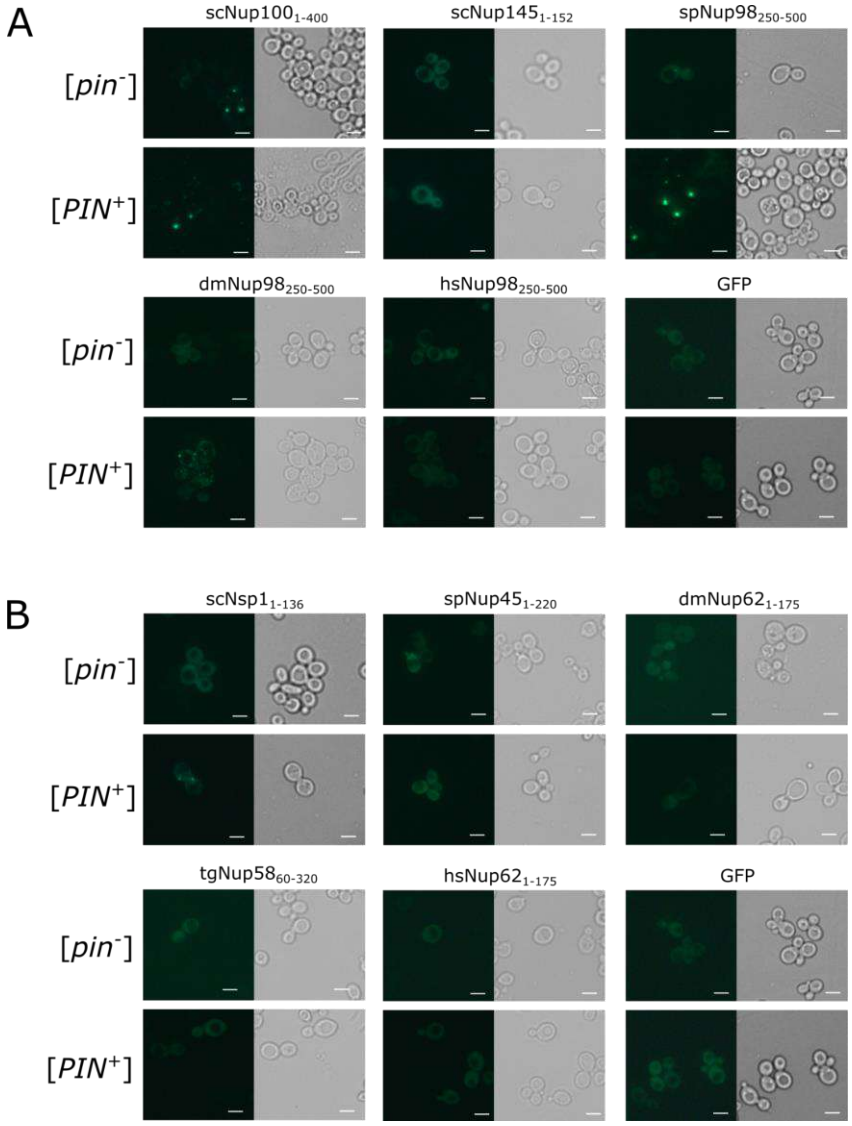

Figure 29 – Some nucleoporin proteins aggregate in yeast cells: Micrographs of orthologous proteins Nup100 (A) and Nsp1 (B) fused with GFP, on which fragments of nucleoporins fused with GFP were obtained. Only GFP was used as a negative control. Scale bar is equal 25

microns.

The generalized results of the tests performed in the bacterial and yeast model systems are presented in Table 8. The first thing we have to pay attention to is that the criterion used to predict amyloid properties did not work in all cases. According to the original paper [6], the presence of at least one beta-arch is a criterion for potential amyloidogenicity. All the protein regions analyzed by us satisfy this criterion, but not all of them demonstrate at least the possibility of aggregation. This fact, on the one hand, can serve as a reason to question the accuracy of ArchCandy. On the other hand, the tests performed in the two model systems are not sufficient to completely exclude the possibility that the protein is capable of forming amyloids. And it cannot be ruled out that the studied proteins are amyloidogenic, but under different conditions.

Table 8-Verification of amyloid properties of Nsp1 and Nup145 orthologs.

Construct name	**Red color of cells on a medium with Congo red**	**Apple green birefringence**	**Fibrils on the cell surface**	**Aggregation in yeast**
$cells_{scNup100\ 1\text{-}400}$	Yes	Yes	No	Yes
$scNup145_{1\text{-}152}$	Yes	Yes	Yes	No
$scNsp1_{1\text{-}136}$	Yes	Yes	Yes	Yes
$hsNup62_{1\text{-}175}$	Yes	No	No	No
$dmNup62_{1\text{-}175}$	No	No	No	No
$spNup45_{1\text{-}220}$	No	No	No	Yes
$tgNup58_{60\text{-}320}$	Yes	Yes	Yes	Yes
$hsNup98_{250\text{-}500}$	No	No	No	Yes
$dmNup98_{250\text{-}500}$	Yes	Yes	Yes	Yes
$spNup98_{250\text{-}500}$	Yes	Yes	Yes	Yes

Abbreviations in the names of constructs: dm – D. melanogaster, hs – H. sapiens, sc – S. cerevisiae, sp – S. pombe, tg-Taeniopygia guttata. After the protein number, the borders of the corresponding section are shown. For example, $hsNup62_{1\text{-}175}$ denotes amino acid fragment 1 to 175 of the human protein Nup62.

Data on the tendency of a particular protein to aggregate do not always coincide for different model systems. In particular, the proteins $spNup145_{1\text{-}220}$ and $hsNup98_{1\text{-}250}$ cannot be attributed to amyloids according to C-DAG results, but they aggregate in yeast cells. Such

observations are probably due to differences in models: different levels of protein production, localization of proteins (in bacteria they are imported from the cell, in yeast they remain in the cytoplasm), as well as a fundamentally different set of tests of amyloid properties that are carried out in these systems. From our point of view, an integrated approach is optimal in this situation. Following this logic, it is most likely that the tgNup58$_{60\text{-}320}$, dmNup98$_{250\text{-}500}$, and spNup98$_{250\text{-}500}$ proteins can form amyloid aggregates.

3.3.4 Evaluation of the effect of the [*PIN*$^+$] prion on nucleoporins aggregation

Aggregates of various QN-rich proteins can interact with each other in yeast cells. In particular, Rnq1 aggregates bound to the [*PIN*$^+$] prion are required for *de novo* aggregation of the Sup35 protein and inductionof the [*PSI*$^+$] prion [36]. Aggregation of some yeast nucleoporins also requires the prion [*PIN*$^+$] [59]. In this study, we performed experiments to evaluate the effect of the [*PIN*$^+$] prion on aggregation of yeast nucleoporin fragments NSP1$_{1\text{-}136}$ and Nup145$_{1\text{-}152}$. The construct with the Nup100$_{1\text{-}400}$ fragmen$_t$ also served as a positive control, since aggregation of this protein was previously described in the literature [59]. Two isogenic strains 1-OT56 and 2-OT56, which differ in the presence of the prion [*PIN*$^+$], were transformed by plasmids of the pAG416-EGFP series previously obtained in our laboratory. In these constructs, the sequences encoding fragments of nucleoporins are controlled by the constitutive GPD promoter (the use of this promoter allows increasing the amount of protein in the cell) and are fused with EGFP. To assess the effect of the [*PIN*$^+$] status on the aggregation of nucleoporin proteins, cells were grown in a selective medium, and then the number of cells with luminescence foci that were considered aggregates was analyzed. EGFP protein was used as a negative control (no aggregation). In the case of nucleoporin fragments Nup100$_{1\text{-}400}$ and Nsp1$_{1\text{-}136}$, we could observe the luminescence foci, in particular (Fig. Further, the frequency of occurrence of aggregates was analyzed using the exact Fisher criterion (the results are shown in Table 9). According to the results obtained, we can say that the presence of the prion [*PIN*$^+$] has a significant effect on the frequency of occurrence of aggregates of the NSP1$_{1\text{-}136}$ protein fragment, while for the Nup145$_{1\text{-}152}$ protein fragment and other fragments, such a dependence is not observed (Table 9).

Table 9 – Yeast factor [*PIN*$^+$] increases the aggregation frequency of protein fragments for yeast nucleoporins Nup100$_{1\text{-}400}$ and NSP1$_{1\text{-}136}$.

The table contains information on the proportion of cells with fluorescent aggregates. To compare the proportion of cells with aggregates and without aggregates, the exact Fisher test is used.

Construction	% of cells with glow foci in [*PIN*$^+$] strain	% of cells with glow foci in [*pin*$^-$] strain	Statistical significance (p-value <0.05)
scNSP1$_{1\text{-}136}$	4.99 ± 0.835	0.0 ± 0.162	yes
scNup100$_{1\text{-}400}$	52.11 ± 2.055	31.94 ± 1.687	yes
scNup145$_{1\text{-}152}$	0.32 ± 0.227	0.16 ± 0.162	no
hsNup62$_{1\text{-}175}$	0.0 ± 0.498	0.7 ± 0.312	No
dmNup62$_{1\text{-}175}$	0.29 ± 0.211	0.0 ± 0.161	No
spNup45$_{1\text{-}220}$	0.0 ± 0.16	0.16 ± 0.165	no
tgNup58$_{60\text{-}320}$	0.0 ± 0.152	0.0 ± 0.139	no
hsNup98$_{250\text{-}500}$	1.29 ± 0.455	0.48 ± 0.28	no
dmNup98$_{250\text{-}500}$	2.75 ± 0.622	1.83 ± 0.525	no
spNup98$_{250\text{-}500}$	3.50 ± 0.675	3.41 ± 0.699	no

3.4. Effect of nucleoporin aggregation on nuclear-cytoplasmic transport

Since the nucleoporin proteins are rather conservative, and some of them retain their amyloid properties [31], we decided to analyze the effect of aggregation of their fragments on nuclear-cytoplasmic transport. To perform the analysis, we constructed specialized constructs based on the pAG415GPD-ccdB-Cerulean vector. The coding sequences of fragments of nucleoporins of various species, which are orthologs of yeast nucleoporins Nsp and Nup145, as well as human nucleoporin NUP58, were transferred to it by recombination cloning. It is worth noting that there are no direct orthologs for human nucleoporin NUP58 in yeast. This ortholog is the NUP62 protein. However, the NUP58 and NUP62 proteins are paralogs and perform similar functions. Such orthologs were Nup58 *Taeniopygia guttata* (fragment from 60 to 320 a.a.), Nup98 *Schizosaccharomyces pombe* (fragment from 250 to 500 a.a.), and Nup98 *Drosophila melanogaster* (fragment from 250 to 500 a.a.). To compare the effect of overproduction of nucleoporin fragments on nuclear cytoplasmic transport In [*PIN*$^+$] and [*pin*$^-$] strains, we used OT56-NLS-GFP and 1-OT56-NLS-GFP strains, and then performed the experiment according to

the description in Materials and Methods. The results of the experiment conducted for strain 1-OT56-NLS-GFP showed that a significant decrease in nuclear cytoplasmic transport compared to the control (ccdB) is observed for the following fragment of the nucleoporin protein – spNup98$_{250-500}$ (p-value = 2.4*10-5^{-5}) (Table 10). At the same time, we do not observe any differences for the dmNup98$_{250-500}$ and tgNup58$_{60-320}$ constructs (Figure 30), as well as for yeast protein fragments.

Table 10-Results of the Wilcoxon test with the Benjamin Hochberg correction for comparing the effect on nuclear cytoplasmic transport in a strain with the [*pin*$^{-}$]prion

Comparing pair	**p-value**
ccdB – dmNup98$_{250-500}$	0.39918
ccdB – spNup98$_{20-500}$	2.4*10^{-5}
ccdB – tgNup58$_{60-320}$	0.11838
ccdB-scNsp1$_{1-136}$	0.11838
ccdB-scNup145$_{1-152}$	0.11838
Nsp1 – dmNup98$_{250-500}$	0.62691
Nsp1 – spNup98$_{20-500}$	0.00417
Nsp1 – tgNup58$_{60-320}$	0.80221
Nup145 – dmNup98$_{250-500}$	0.63569
Nup145 – spNup98$_{20-500}$	0.00019
Nup145 – tgNup58$_{60-320}$	0.67122

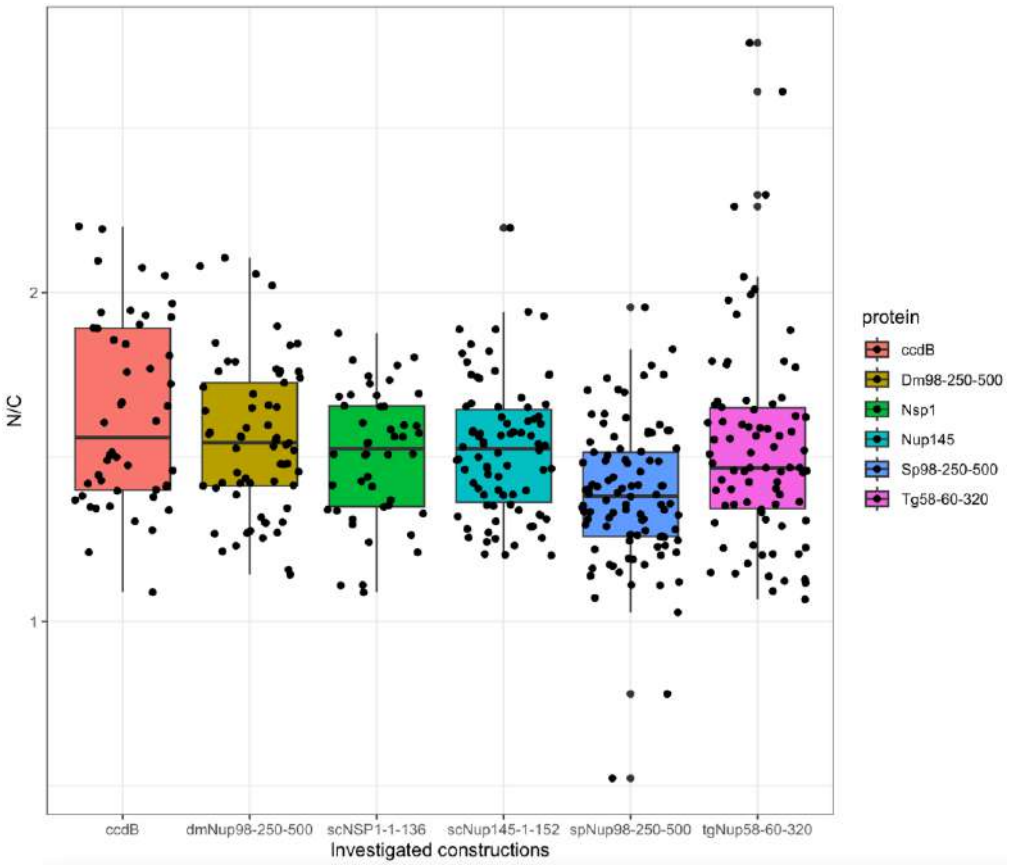

Figure 30-Overproduction of amyloidogenic regions of nucleoporins of different species leads to disruption of nuclear import in the strain with the [*pin*$^-$] prion. The graph shows the ratios of signals from NLS-GFP in the nucleus and cytoplasm (N/C). The presence of differences between the groups was revealed with the subsequent application of the Wilcoxon test with the Benjamin Hochberg correction for multiple comparisons.

A similar experiment was performed for the prion-carrying strain [*PIN*$^+$]. As a result, we observed a decrease in nuclear cytoplasmic transport for all constructs in comparison with the control samples (ccdB was used as a control), as well as in comparison with fragments of yeast nucleoporins $Nsp1_{1\text{-}136}$ and $Nup145_{1\text{-}152}$ (Fig. 32). The Wilcoxon test adjusted for multiple comparisons by Benjamin Hochberg was used for comparison. The obtained values of significance levels for each pair of comparisons are shown in Table 11.

Table 11-Results of the Wilcoxon test with the Benjamin Hochberg correction for comparing the effect on nuclear cytoplasmic transport in a strain with the [*PIN*$^+$] prion

Comparing pair	**p-value**
ccdB – $dmNup98_{250\text{-}500}$	$< 2*10^{-16}$
ccdB – $spNup98_{20\text{-}500}$	$< 2*10^{-16}$
ccdB – $tgNup58_{60\text{-}320}$	$< 2*10^{-16}$
ccdB-$scNsp1_{1\text{-}136}$	$< 2*10^{-16}$
ccdB-$scNup145_{1\text{-}152}$	$< 2*10^{-16}$

Nsp1 – dmNup98$_{250-500}$	$1.5*10^{-11}$
Nsp1 – spNup98$_{20-500}$	$< 2*10^{-16}$
Nsp1 – tgNup58$_{60-320}$	$1.9*10^{-6}$
Nup145 – dmNup98$_{250-500}$	$< 2*10^{-16}$
Nup145 – spNup98$_{20-500}$	$< 2*10^{-16}$
Nup145 – tgNup58$_{60-320}$	$4.2*10^{-11}$

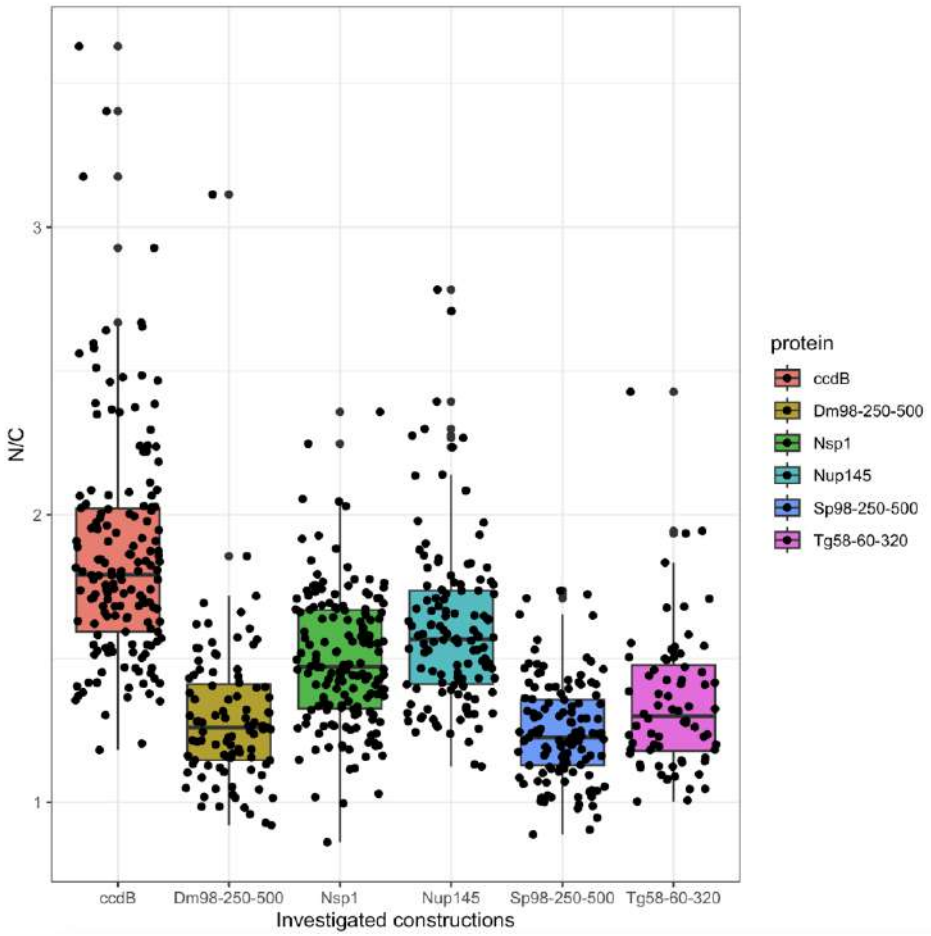

Figure 31-Overproduction of amyloidogenic regions of nucleoporins of different species leads to disruption of nuclear import in the strain with the [*PIN*$^+$] prion. The graph shows the ratios of signals from NLS-GFP in the nucleus and cytoplasm (N/C).
The presence of differences between the groups was revealed with the subsequent application of the Wilcoxon test with the Benjamin Hochberg correction for multiple comparisons.

The results obtained suggest that the presence of the prion [*PIN*$^+$] may affect the processes of nuclear-cytoplasmic transport. For this purpose, an additional analysis was performed, namely, we checked whether the efficiency of nuclear-cytoplasmic transport differs for nucleoporin fragments. As a result of the analysis, it was shown for the protein spNup98$_{250-500}$ that the presence of the prion [*PIN*$^+$] affects the transport effect shown (Fig. 31, Table 11). As a result of the Wilcoxon test, it was shown that the presence of the prion [*PIN*$^+$] leads to a

stronger decrease in nuclear cytoplasmic transport (p-value = 4.959 * 10-8^{-8}). The presence of the [*PIN*$^{+}$] prion also affects the strength of reduced nuclear-cytoplasmic transport in the case of overproduction of dmNup98$_{250-500}$ (p-value = 2.549*10-11^{-11}) and tgNup58$_{60-320}$ (p-value = 2.438*10-5^{-5}) nucleoporin fragments. Thus, we can say that the presented system for evaluating nuclear cytoplasmic transport depends on the presence of the [*PIN*$^{+}$] factor, and the presence of this prion can affect nuclear cytoplasmic transport in yeast cells. The experiments in this section were conducted jointly with T. M. Rogoza.

CHAPTER 4. Discussion

4.1 Amyloid properties of human protein NUP58

The results obtained in this study demonstrate for the first time that the human protein NUP58 can form amyloids in *vitro* and *in vivo*. To prove that the protein is amyloidogenic, it is necessary that the structure under consideration meets several criteria:: binding to specific dyes, the formation of fibrils that are resistant to ionic detergents and proteases in *in vivo* and in vitro systems *in vitro*[3]. We have shown that the NUP58 protein forms SDS-resistant aggregates (Figures 9 and 11), which are also resistant to treatment with proteinase K (Figure 13). The resulting fibrils of this protein were also stained with amyloid-specific dyes (Thioflavin T and Congo red) and showed characteristic properties: increased fluorescence (Figure 15) and apple-green birefringence, respectively (Figure 14). An interesting fact is that two forms of NUP58 aggregates were found in the solution, which differ in size. At the same time, large aggregates were sensitive to BME treatment, which reduces disulfide bonds, and therefore they can be called polymers (Figure 12). We assume that two cysteine residues in NUP58 at positions 252 and 521, located outside the predicted amyloidogenic region, are responsible for this (1-213 aa, Figure 5). However, it should be noted that *S. cerevisia* aggregation of the protein fragment from 215 to 599 amino acid residues is observed in S. cerevisia yeast cells. Despite the fact that this fact is consistent with the predictions of the ArchCandy program (Figure 5), this assumption requires additional verification and refinement.

The human protein NUP58 also exhibits amyloid properties in the bacterial C-DAG system, and also forms fluorescent glow foci in yeast cells. Cells producing full-length NUP58 or its amyloidogenic part $NUP58_{1-213}$can form amyloid aggregates on the surface. This is confirmed by the red color of colonies on a medium containing the Congo red dye (Fig. 16), apple-green birefringence of cells in polarized light (Fig. 18), and protein fibrils on the surface detected by TEM (Fig. 17). Since both cysteines are located outside the NUP58 $fragment_{1-213}$, which forms amyloids in the C-DAG system, we conclude that these residues are not essential for protein amyloidogenesis. Therefore, we have suggested that small oligomers detected *in vitro* in the presence of BME are also amyloids. Among the already described amyloids, there is an example – β2-microglobulin, the formation of aggregates of which also occurs due to the formation of disulfide bridges [44]. Partial deletion analysis of the NUP58 protein showed that its $NUP58_{1-95}$ fragment also exhibits amyloid properties in both the C-DAG system and the yeast system, which is consistent with ArchCandy's predictions (Figure 5). This is also consistent with the assessment of the conservativeness of amyloid properties, the analysis of which showed the

presence of a conservative region with amyloid properties in the 95 amino acid region (Figure 6). However, additional checks are necessary for unambiguous localization of the domain responsible for aggregation of the NUP58 protein. First, we observe aggregation of the $NUP58_{215-599}$ fragment in *S. cerevisiae* cells, but we do not observe the formation of fibrils and binding to the Congo red dye in the C-DAG system. Although the C-terminus of the protein has an increased content of FG repeats, which may contribute to aggregation in yeast cells. Secondly, according to the ArchCandy program predictions (Fig. 5), the maximum cumulative score (amyloidogenicity estimate) is observed for the region from 175 to 213 amino acids, which is also consistent with the estimate of conservativeness of amyloid properties (Fig. 6).

The described characteristics of the human protein NUP58 allow us to consider it a new amyloid. Bioinformatic analysis of the NUP58 protein orthologs showed that all of them are potential amyloids (Fig. 6) [30]. This analysis also revealed a protein fragment that is amyloidogenic in many orthologs and is located outside the region of FG repeats, which are supposed to play a key role in the formation of a selective barrier inside the nuclear pore [48, 90, 116]. It is noteworthy that the conservativeness of the protein sequence in this fragment is lower than the conservativeness of amyloidogenic properties [30]. This fact may indicate that the formation of amyloids inside the NPC is functional and necessary for the regulation of nuclear-cytoplasmic transport. A similar idea was put forward earlier on the basis of evidence for the formation of amyloids by human and yeast nucleoporins [104]. Thus, we suggest that the identified NUP58 fragment with a conservative tendency to aggregation may play an important role in the formation of a selective barrier in NPC.

4.2 Conservativeness of amyloid properties of nucleoporins

In the course of our work, we have shown that according to bioinfomatic predictions, amyloid properties are found in almost all orthologs of the human protein NUP58. It is also worth noting that the group of nucleoporin proteins has a certain sequence conservativeness. For this reason, it was logical to expect the preservation of amyloid properties. This is partially confirmed by studying the prion domains of yeast proteins. For example, Nsp1, Nup42, Nup49, Nup57, Nup100, and Nup116 formed aggregates *in vivo*. In almost all cases, these aggregates were resistant to SDS (with the exception of the Nup57 protein), and only aggregates of Nup100 and Nup116 fragments were stained with Thioflavin T *in vitro* [10]. Therefore, an important step in this work was to analyze the amyloid properties of nucleoporin proteins from different taxonomic groups. Bioinformatic analysis has shown that many nucleoporins from different taxonomic groups are potential amyloids (Figure 24). Moreover, for the orthologs of the Nup49, Nup57, Nup159, and Nsp1 proteins, we identified conserved regions that had amyloid properties

according to bioinformatic predictions (Figure 24). The preservation of amyloid properties among orthologs is also described for other proteins that are functional amyloids: for example, the CPEB protein [148], FXR1 [147], and proteins containing RHIM motifs [74].

Further experimental tests showed that fragments of yeast nucleoporins $Nsp1_{1-136}$ and $Nup100_{1-400}$ exhibit amyloid properties in the C-DAG system: red coloration of colonies on a dye-containing medium (Fig. 26) and interaction with the dye Congo red with subsequent apple-green birefringence (Fig. 27). This is consistent with earlier experimental data. Thus, the yeast protein fragment $Nsp1_{1-175}$ forms detergent-resistant aggregates in yeast cells during overproduction, and the corresponding aggregates obtained *in vitro*are stained with the dye Thioflavin T [10]. Also, the sequence from 1 to 601 amino acids of the protein forms a hydrogel *in vitro* [54], which contains intermolecular β-sheets, which is a characteristic feature of amyloid aggregates [119]. Similar results were obtained for $Nsp1_{2-277}$ [4]. It was shown that the yeast fragment $Nup100_{1-592}$ forms detergent-resistant aggregates in cells and forms aggregates *in vitro*that are stained with Thioflavin T [10]. Further analysis of this protein showed that shorter fragments of $Nup100_{1-200}$ and $Nup100_{201-400}$ protein are capable of aggregation in yeast, and $Nup100_{300-400}$ forms fibrils that are stained with Thioflavin T [59].

Most orthologs of yeast nucleoporins (for which amyloid properties were demonstrated [10]) demonstrated amyloid properties according to bioinformatic predictions. We selected several nucleoporin proteins for further analysis, and performed experimental tests in the C-DAG system and in the yeast system. These tests showed that fragments of only two nucleoporins that are orthologs of yeast, namely $dmNup98_{250-500}$ and $spNup98_{250-500}$, showed amyloid properties (Table 8). They were characterized by an apple-green glow when stained with Congo red dye (Fig. 27), the formation of fibrils on the cell surface (Fig. 28), and the formation of fluorescent glow foci in yeast cells (Fig. 29). Yeast nucleoporin fragments $scNup100_{1-400}$ and $scNSP1_{1-136}$ also exhibit similar properties, which is consistent with the described data [4, 10, 59]. At the same time, the nucleoporin fragment $tgNup58_{60-320}$ and the nucleoporin protein fragment $scNup145_{1-152}$ demonstrate amyloid properties only in the C-DAG system (Fig. 26). The results obtained on the amyloid properties of nucleoporins do not allow us to draw an unambiguous conclusion about the prevalence of amyloid properties among all nucleoporins. Undoubtedly, such properties are inherent in a large number of representatives, but this requires more experimental checks. Also, for such tests, it is necessary to expand the list of systems used (for example, add human cell cultures) for more reliable results, since post-translational modifications can affect protein aggregation [134].

4.3 Effect of nucleoporin aggregation on the import of macromolecules into the nucleus

Nucleoporin proteins with FG repeats form a selective barrier within the YAP. This occurs due to the filling of the central channel of the nuclear pore with unstructured domains. It is worth noting that the presence of such domains is characteristic of amyloid proteins. Small molecules easily pass this filter, but large loads require interactions with specific nuclear transport receptors to pass through the barrier due to the ability to interact with FG repeats. Previously, it was assumed that FG repeats of yeast Nsp1 and other Nups form a stable hydrogel inside the YPC [4, 86, 135, 155]. Further studies have shown the presence of intermolecular β-sheets characteristic of amyloids in hydrogels [155]. Amyloid fibrils presumably play an important role in the formation of hydrogels due to the FG repeat regions of yeast Nup49 and human NUP153 [104].

Presumably, aggregation of nucleoporin proteins can lead to disruption of nuclear-cytoplasmic transport. When evaluating the effect of nucleoporin aggregation on nuclear-cytoplasmic transport in this study, we obtained results that fragments of yeast nucleoporins $Nsp1_{1\text{-}136}$ and $Nup145_{1\text{-}152}$ affect the import of macromolecules into the nucleus in a strain with the [*PIN*$^+$] prion. Next, we analyzed the effect of orthologs of yeast nucleoporins Nup145 and Nsp1 from other organisms on nuclear-cytoplasmic transport. For the study, we used $tgNup58_{60\text{-}320}$, $spNup98_{250\text{-}500}$, and $dmNup98_{250\text{-}500}$, for which amyloid properties were shown in this study. In the course of our work, we found that all nucleoporin fragments are characterized by a decrease in the efficiency of macromolecule transport from the cytoplasm to the cell nucleus in the presence of [*PIN*$^+$] factor (Fig. 30 and Fig. 31). This can be explained by the fact that Rnq1 protein aggregates include fragments of nucleoporin proteins, which in turn lead to the inclusion of proteins responsible for nuclear-cytoplasmic transport. In the absence of the [*PIN*$^+$] prion in the strain, we observed an effect on transport for only one nucleoporin fragment, namely $spNup98_{250\text{-}500}$. For some neurodegenerative diseases (Huntington's disease), cases of sequestering of proteins responsible for nuclear-cytoplasmic transport into Htt protein aggregates have been described [52]. These inclusions include the RanGAP1, Nup62, and Nup88 proteins, which form intranuclear inclusions together with the HTT protein [57]. It was also shown that during the development of various neurodegenerative diseases, a complex effect is observed on the disruption of mRNA transport to the nucleus. This is due to the inclusion of proteins responsible for the transport of mRNA into the nucleus in aggregates, which in turn leads to a violation of cellular homeostasis [19, 37]. It is possible that similar processes are observed in the case of overproduction of fragments of nucleoporin proteins. During this process, cellular homeostasis is disrupted, some of the proteins responsible for importing macromolecules into the

nucleus bind to fragments and do not participate in transport, as a result, we observe a decrease in the level of import of macromolecules into the nucleus.

The data obtained on the effect of overproduction of nucleoporin fragments on the import of macromolecules into the nucleus do not allow us to draw an unambiguous conclusion. On the one hand, there is literature evidence that nucleoporin proteins exhibit amyloid properties and can form hydrogels. It is possible that the assembly and disassembly of aggregates in the lumen of the nuclear pore maybe a system for regulating the intensity of transport. On the other hand, overproduction of the nucleoporin protein fragment tgNup58$_{60\text{-}320}$ led to a decrease in the import of macromolecules into the nucleus, although it did not aggregate in yeast cells. This fact may indicate that changes in the level of individual nucleoporin proteins can also affect the processes of nuclear-cytoplasmic transport. This is due to a change in the number of functional proteins responsible for this. Thus, to date, there is no unambiguous mechanism of the effect of nucleoporin aggregation on nuclear-cytoplasmic transport. Most likely, irreversible aggregation of nucleoporins is rather an abnormal process and affects nuclear-cytoplasmic transport due to the inclusion of proteins that provide transport in the aggregates.

Conclusions

1. Human protein NUP58 has amyloid properties both *in vitro* and in model systems.

2.The N-terminal fragment of the protein is responsible for aggregation of the NUP58, and the first 95 amino acids are sufficient for this process.

3. Fragments of Nup98 nucleoporins from *Homo sapiens*, *Schizosaccharomyces pombe*, and *Drosophila melanogaster* demonstrate amyloid properties in model systems.

4. Overproduction of nucleoporin amyloidogenic fragments of *Saccharomyces cerevisiae*, as well as other species, leads to disruption of macromolecule transport to the nucleus in yeast cells in the presence of the prion [PIN^+].

List of literature

1. Galkin, A. P. Identification and analysis of the interaction of prions and amyloids in the yeast *Saccharomyces cerevisiae proteome*: dis. ... doct. biol. nauk: 03.02.07. - SPb., 2015. - 205 p.
2. Inge-Vechtomov, S. G. Selective systems for obtaining recessive ribosomal suppressors in saccharomyces yeast / S. G. Vechetomov, O. N. Tikhodeev, T. S. Karpova // Genetics. - 1988. - Vol. 24. - No. 7. - pp. 1159-1165.
3. Nizhnikov A. A., Antonets K. S., Inge-Vechtomov S. G. Amyloids: from pathogenesis to function. - 2015. - Vol. 80. - No. 9. - pp. 1356-1375.
4. Ader, C. Amyloid-like interactions within nucleoporin FG hydrogels / C. Ader C., S. Frey, W. Maas, H. B. Schmidt, D. Görlich, M. Baldus // Proceedings of the National Academy of Sciences. – 2010. – Vol. 107. – No. 14. – P. 6281– 6285.
5. Aguzzi, A. Molecular Mechanisms of Prion Pathogenesis / A. Aguzzi, C. Sigurdson, M. Heikenwaelder // Annual Review of Pathology-mechanisms of Disease. – 2008. – Vol. 3. – No. 11. – P. 67–97.
6. Ahmed, A. B. A structure-based approach to predict predisposition to amyloidosis / A. B. Ahmed, N. Znassi, M. T. Château, A. V. Kajava // Alzheimer's and Dementia. – 2015. – Vol. 11. – No. 6. – P. 681–690.
7. Ahmed, A. B. Breaking the amyloidogenicity code: Methods to predict amyloids from amino acid sequence / A. B. Ahmed, A. V. Kajava // FEBS Letters. – 2013. – Vol. 587. – No. 8. – P. 1089 –1095.
8. Aimanianda, V. The dual activity responsible for the elongation and branching oa β-(1,3)-glucan in the fungal cell wall / V. Aimanianda, C. Simenel, C. Garnaud, C. Clavaud, R. Tada, L. Barbin, I. Mouyna, C. Heddergott, L. Popolo, Y. Ohya, M. Delepierre, J. Latge // MBio. – 2017. – Vol. 8. – No. 3. – P. 1–14.
9. Alber, F. The molecular architecture of the nuclear pore complex / F. Alber, S. Dokudovskaya, L.M. Veenhoff, W. Zhang, J. Kipper, D. Devos, A. Suprapto, O. Karni-Schmidt, R. Williams, B.T. Chait, A. Sali, M. P. Rout // Nature. – 2007. – Vol. 450. – No. 7170. – P. 695-701.
10. Alberti, S. A systematic survey identifies prions and illuminates sequence features of prionogenic proteins / S. Alberti, R. Halfmann, O. King, A. Kapila, S. Lindquist // Cell. – 2009. – Vol. 137. – P. 146–158.
11. Alteri, C. J. *Mycobacterium tuberculosis* produces pili during human infection / C. J. Alteri, J. Xicohténcatl-Cortes, S. Hess, G. Caballero-Olín, J. A.Giron, R. L. Friedman //

Proceedings of the National Academy of Sciences of the United States of America. — 2007. – Vol. 104. – No. 12. – P. 5145–5150.

12. Antonets, K.S. Accumulation of storage proteins in plant seeds is mediated by amyloid formation / K.S. Antonets, M.V. Belousov, A.I. Sulatskaya, M.E. Belousova, A.O. Kosolapova, M.I. Sulatsky // PLoS Biology. – 2020. – Vol. 18. – No 7. – P. e3000564.
13. Barbitoff, Y.A. Chromosome-level genome assembly and structural variant analysis of two laboratory yeast strains from the Peterhof Genetic Collection lineage / Y.A. Barbitoff, A.G. Matveenko, A.B. Matiiv, E.M. Maksiutenko, S.E. Moskalenko, P.B. Drozdova, D.E. Polev, A.Y. Beliavskaia, L.G. Danilov, A.V. Predeus, G.A. Zhouravleva //G3 Genes|Genomes|Genetics. – 2021. – Vol. 11. – P. jkab029.
14. Barnhart, M. M. Curli biogenesis and function / M. M. Barnhart, M. R. Chapman // Annual review of microbiology. – 2006. – Vol. 60. – P. 131–147.
15. Bates, G. P. et al. Huntington disease / G.P. Bates, R. Dorsey, J. F. Gusella, M. R. Hayden, C. Kay, B. R. Leavitt, M. Nance, C.A. Ross, R. I. Scahill, R. Wetzel, E. J. Wild, S. J. Tabrizi // Nature Reviews Disease Primers. – 2015. – Vol. 1. – P. 1–21.
16. Baxa U. Structural basis of infectious and non-infectious amyloids / U. Baxa // Current Alzheimer research. – 2008. – Vol. 5. – No. 3. – P. 308–18.
17. Bian Z., Normark S. Nucleator function of CsgB for the assembly of adhesive surface organelles in *Escherichia coli* / Z. Bian, S. Normark // The EMBO Journal. – 1997. – Vol. 16. – No. 19. – P. 5827– 5836.
18. Birsa, N. Cytoplasmic functions of TDP-43 and FUS and their role in ALS / N. Birsa, M.P. Bentham, P. Fratta // Seminars in Cell and Developmental Biology. – 2020. – Vol. 99. – P. 193-201.
19. Bitetto, G. Nucleo–cytoplasmic transport defects and protein aggregates in neurodegeneration / G. Bitetto, A. Di Fonzo // Translational Neurodegeneration. – 2020. – Vol. 9. – No. 1. – P. 25.
20. Bradford, M. A rapid and sensitive method for the quantitation of microgram quantities of protein utilizing the principle of protein-dye binding / M. Bradford// Analityc Biochemistry. – 1976. – Vol. 72. – P. 248–54.
21. Bondarev, S.A. Protein Co-Aggregation Related to Amyloids: Methods of Investigation, Diversity, and Classification / S.A. Bondarev, K.S. Antonets, A.V. Kajava, A.A. Nizhnikov, G.A. Zhouravleva // International Journal of Molecular Sciences. – 2018. – Vol. 19. – No. 8. – P. 2292.
22. Bondarev, S.A. Structure-based view on [*PSI*$^{+}$] prion properties / S.A. Bondarev, G.A. Zhouravleva, M.V. Belousov, A.V. Kajava // Prion. – 2015. – Vol. 9. – No. 1. – P.190-

199.

23. Cao, Q. Amyloid precursor proteins anchor CPEB to membranes and promote polyadenylation-induced translation / Q. Cao, Y.-S. Huang, M.-C. Kan, J. D. Richter // Molecular and cellular biology. – 2005. – Vol. 25. – No. 24. – P. 10930–10939.
24. Chabelskaya, S. Inactivation of NMD increases viability of *sup45* nonsense mutants in *Saccharomyces cerevisiae* / S. Chabelskaya, V. Gryzina, S. Moskalenko, C. Le Goff, G. Zhouravleva // BMC molecular biology. – 2007. – Vol. 8. – P. 71.
25. Chandramowlishwaran, P. Mammalian amyloidogenic proteins promote prion nucleation in yeast / P. Chandramowlishwaran, M. Sun, K. L. Casey, A. V. Romanyuk, A. V. Grizel, J. V. Sopova, A. A. Rubel, C. Nussbaum-Krammer, I. M. Vorberg, Y. O. Chernoff // Journal of Biological Chemistry. – 2018. – No. 293. – P. 3436–3450.
26. Chapman, M. R. Role of *Escherichia coli* curli operons in directing amyloid fiber formation / M. R. Chapman, L. S. Robinson, J. S. Pinkner, R. Roth, J. Heuser, M. Hammar, S. Normark, S. J. Hultgren // Science. – 2002. – Vol. 295. – No. 5556. – P. 851–855.
27. Chiti, F. Protein misfolding, functional amyloid, and human disease / F. Chiti, C.M. Dobson // Annual Review of Biochemistry. – 2006. – Vol. 75. – P. 333-366.
28. Chou, C.C. TDP-43 pathology disrupts nuclear pore complexes and nucleocytoplasmic transport in ALS/FTD / C.C.Chou, Y. Zhang, M.E. Umoh // Nature Neuroscience. – 2018. – Vol. 21. – P. 228–239.
29. Coustou, V. The protein product of the Het-s heterokaryon incompatibility gene of the fungus *Podospora anserina* behaves as a prion analog / V. Coustou, C. Deleu, S. Saupe, J. Begueret // Proceedings of the National Academy of Sciences. – 1997. – Vol. 94. – No. 18. – P. 9773–9778.
30. Danilov, L.G. The Human NUP58 Nucleoporin Can Form Amyloids In Vitro and In Vivo / L.G. Danilov, S.E. Moskalenko, A.G. Matveenko, X.V. Sukhanova, M.V. Belousov, G.A. Zhouravleva, S.A. Bondarev // Biomedicines. – 2021. – Vol. 9. – P. 1451.
31. Danilov, L.G. Identification of New FG-Repeat Nucleoporins with Amyloid Properties / L.G. Danilov, X.V. Sukhanova, T.M. Rogoza, E.Y. Antonova, N.P. Trubitsina, G.A. Zhouravleva, S.A. Bondarev // International Journal of Molecular Science. – 2023. – Vol. 24 – P. 8571.
32. Dawson, H. N. Loss of Tau elicits axonal degeneration in a mouse model of Alzheimer's disease / H. N. Dawson, V. Cantillana, M. P. Vitek, D. M. Wilcock, J. R. Lynch, D. T. Laskowitz // Neuroscience. – 2010. – V. 169. – No. 1. – P. 516-531.

33. Denning, D.P. Disorder in the nuclear pore complex: the FG repeat regions of nucleoporins are natively unfolded / D.P. Denning, S.S. Patel, V. Uversky, A.L. Fink, M. Rexach // Proceedings of the National Academy of Sciences. – 2003. – V.100. – No. 5. – P. 2450-2455.
34. DePace, A.H. A critical role for amino-terminal glutamine/asparagine repeats in the formation and propagation of a yeast prion / A.H. DePace, A. Santoso, P. Hillner, J.S. Weissman // Cell. – 1998. – Vol. 93. – No. 7. – P. 1241-1252.
35. Derkatch, I. L. Genesis and variability of [*PSI*$^{+}$] prion factors in *Saccharomyces cerevisiae* / I. L. Derkatch, Y. O. Chernoff, V. V. Kushnirov, S. G. Inge-Vechtomov, S. W. Liebman // Genetics. – 1996. – Vol. 144. – No. 4. – P. 1375-1386.
36. Derkatch, I. L. Prions affect the appearance of other prions: the story of [PIN+] / I. L. Derkatch, M. E. Bradley, J. Y. Hong, S. W. Liebman // Cell. – 2001. – Vol. 106. – No. 2. – P. 171–182.
37. Ding, B. Nucleocytoplasmic Transport: Regulatory Mechanisms and the Implications in Neurodegeneration / B. Ding, M. Sepehrimanesh // International Journal of Molecular Sciences. – 2021. – Vol. 22. – No.8. – P. 4165.
38. Dosztányi, Z. IUPred: Web server for the prediction of intrinsically unstructured regions of proteins based on estimated energy content / Z. Dosztányi, V. Csizmok, P. Tompa, I. Simon // Bioinformatics. – 2005. – Vol. 21. – No. 16. – P. 3433-3434.
39. Dueholm, M. S. Functional amyloid in *Pseudomonas* / M. S. Dueholm, S. V. Petersen, M. Sønderkær, P. Larsen, G. Christiansen, K. L. Hein, … & D. E. Otzen // Molecular Microbiology. – 2010. – Vol. 77. – No. 4. – P. 1009-1020.
40. Dultz, E. Live imaging of single nuclear pores reveals unique assembly kinetics and mechanism in interphase / E. Dultz, J. Ellenberg // Journal of Cell Biology. – 2010. – Vol. 191. – No. 1. – P. 15-22.
41. Ed, H. Towards understanding nuclear pore complex architecture and dynamics in the age of integrative structural analysis / H. Ed, B. Martin // Current Opinion in Cell Biology. – 2015. – Vol. 34. – P. 31–38.
42. Edgar, R. C. MUSCLE: Multiple sequence alignment with high accuracy and high throughput / R.C. Edgar // Nucleic Acids Research. – 2004. – Vol. 32. – No. 5. – P. 1792–1797.
43. Ehud, C. Opposing activities protect against age onset proteotoxicity / C. Ehud, B. Jan, M. P. Rhonda, W. K. Jeffery, D. Andrew // Science. – 2006. – Vol. 313. – P. 1604-1610.
44. Eichner, T. Understanding the complex mechanisms of β2-microglobulin amyloid

assembly / T. Eichner, S.E. Radford // The FEBS Journal. – 2011. – Vol. 278. – P. 3868–3883.

45. Elliot, M. A. The chaplins: A family of hydrophobic cell-surface proteins involved in aerial mycelium formation in *Streptomyces coelicolor* / M. A. Elliot, N. Karoonuthaisiri, J. Huang, M. J. Bibb, S. N. Cohen, C. M. Kao, M. J. Buttner // Genes and Development. – 2003. – Vol. 17. – No. 14. – P. 1727-1740.
46. Feoktistova, M. cIAPs Block Ripoptosome Formation, a RIP1/Caspase- 8 Containing Intracellular Cell Death Complex Differentially Regulated by cFLIP Isoforms / M. Feoktistova, P. Geserick, B. Kellert, D. Dimitrova, C. Langlais, M. Hupe, K. Cain, M. MacFarlane, G. Häcker, M. Leverkus // Molecular Cell. – 2011. – Vol. 43. – No. 3. – P. 449-463.
47. Fowler, D. M. Functional amyloid formation within mammalian tissue / D. M. Fowler, A. V. Koulov, C. Alory-Jost, M. S. Marks, W. E. Balch, J. W. Kelly // PLoS Biology. – 2006. – Vol. 4. – No. 1. – P. 100-107.
48. Fragasso, A. A designer FG-Nup that reconstitutes the selective transport barrier of the nuclear pore complex / A. Fragasso, H.W. de Vries, J. Andersson, E.O. van der Sluis, E. van der Giessen, A. Dahlin, P.R. Onck, C. Dekker // Nature Communications. – 2021. – Vol. 12. – P. 2010.
49. Frey, S. A saturated FG-repeat hydrogel can reproduce the permeability properties of nuclear pore complexes / S.Frey, D. Görlich // Cell. – 2007. – Vol. 130. – No. 3. – P. 512-523.
50. Frey, S. FG-rich repeats of nuclear pore proteins form a three-dimensional meshwork with hydrogel-like properties / S. Frey, R.P. Richter, D. Görlich // Science. – 2006. – Vol. 314. – P. 815–817.
51. Gasset-Rosa, F. Cytoplasmic TDP-43 De-mixing Independent of Stress Granules Drives Inhibition of Nuclear Import, Loss of Nuclear TDP-43, and Cell Death / F. Gasset-Rosa, S. Lu, H. Yu, C. Chen, … & D.W. Cleveland //Neuron – 2019. – Vol. 102. – No. 2. – P. 339-357.
52. Gasset-Rosa, F. Polyglutamine-Expanded Huntingtin Exacerbates Age-Related Disruption of Nuclear Integrity and Nucleocytoplasmic Transport / F. Gasset-Rosa, C. Chillon-Marinas, A. Goginashvili, R.S. Atwal, … & C. Lagier-Tourenne // Neuron. – 2017. – Vol. 94. – No. 1. – P. 48-57.
53. Gibson, D. L. AgfC and AgfE facilitate extracellular thin aggregative fimbriae synthesis in *Salmonella Enteritidis* / D. L. Gibson, A. P. White, C. M. Rajotte, W. W. Kay // Microbiology. – 2007. – Vol. 153. – No. 4. – P. 1131-1140.

54. Goedert, M. 100 years of Lewy pathology / M. Goedert, M. G. Spillantini, K. D. Tredici, H. Braak // Nature Reviews Neurology. – 2013. – Vol. 1. – P. 13–24.
55. Gour, S. Antimicrobial peptide (CnAMP2) from liquid endosperm of Cocos nucifera forms amyloidlike fibrillar structure / S. Gour, V. Kaushik, V. Kumar, P. Bhat, S.C.Yadav, J.K. Yadav // The Journal of Peptide Science. – 2016. – Vol. 22. – No. 4. – P. 201–207.
56. Goyal, P. Structural and mechanistic insights into the bacterial amyloid secretion channel CsgG / P. Goyal, P. V. Krasteva, N. Van Gerven, F. Gubellini, I. Van den Broeck, A. Troupiotis-Tsaïlaki, ... & H. Remaut // Nature. – 2014. – Vol. 516. – No. 7530. – P. 250-253.
57. Grima, J.C. Mutant Huntingtin Disrupts the Nuclear Pore Complex / J.C. Grima, J.G. Daigle, N. Arbez, K.C. Cunningham, … & J.D. Rothstein. // Neuron. – 2017. – Vol. 94. – No. 1. – P. 93-107.
58. Halfmann, R. Screening for amyloid aggregation by Semi-Denaturing Detergent-Agarose Gel Electrophoresis / R. Halfmann, S. Lindquist // Journal of visualized experiments: JoVE. – 2009. – Vol. 17. – No. 2008. – P. 1-4.
59. Halfmann, R. Prion formation by a yeast GLFG nucleoporin / R. Halfmann, J.J.R. Wright, S. Alberti, S. Lindquist, M. Rexach //Prion. – 2012. – Vol. 6. – P. 391–399.
60. Hammar, M. Nucleator-dependent intercellular assembly of adhesive curli organelles in *Escherichia coli* / M. Hammar, Z. Bian, S. Normark // Proceedings of the National Academy of Sciences of the United States of America. – 1996. – Vol. 93. – No. 13. – P. 6562–6566.
61. Hartono, Nucleoporin Nup58 localizes to centrosomes and mid-bodies during mitosis / Hartono, M. Hazawa, K. S. Lim, F. R. Dewi, A. Kobayashi, R. W. Wong // Cell Division. – 2019. – Vol. 14. – No. 1. – P. 1-13.
62. Hee, J. Melanosomal formation of PMEL core amyloid is driven by aromatic residues / J. Hee, S. Mitchell, X. Liu, R. Leonhardt // Science Report. – 2011. – Vol. 7. – No. 1. – P. 1-12.
63. Hoelz, A. The Structure of the Nuclear Pore Complex / A. Hoelz, E. W. Debler, G. Blobel // Annual Review of Biochemistry. – 2011. – Vol. 80. – No. 1. – P. 613-643.
64. Hofer, S. Studying Huntington's Disease in Yeast: From Mechanisms to Pharmacological Approaches / S. Hofer, K. Kainz, A. Zimmermann, M.A. Bauer, T. Pendl, M. Poglitsch, F. Madeo and D. Carmona-Gutierrez // Frontiers in Molecular Neuroscience. – 2018. – V. 11. – P. 318.
65. Huerta-Cepas J., eggNOG 5.0: a hierarchical, functionally and phylogenetically

annotated orthology resource based on 5090 organisms and 2502 viruses / J. Huerta-Cepas, D. Szklarczyk, D. Heller, A. Hernández-Plaza, S. K. Forslund, H. Cook, D. R. Mende, I. Letunic, T. Rattei, L. J. Jensen, C. von Mering and P. Bork // *Nucleic Acids Research. – 2019. – Vol. 47. – No. 1. – P.* 309–314.

66. Humenik, M. Ion and seed dependent fibril assembly of a spidroin core domain / M. Humenik, A. M. Smith, S. Arndt, T. Scheibel // Journal of Structural Biology. – 2015. – Vol. 191. – No. 2. – P. 130-138.
67. Iconomidou, V.A. Amyloids protect the silkmoth oocyte and embryo / V.A. Iconomidou, G. Vriend, S.J. Hamodrakas // FEBS Letters. – 2000. – Vol. 479. – No. 3. – P. 141–145.
68. Isgro, T. A. Cse1p-Binding Dynamics Reveal a Binding Pattern for FG- Repeat Nucleoporins on Transport Receptors / T. A. Isgro, K. Schulten // Cell Press. – 2007. – Vol. 15. – No. 8. – P. 977-991.
69. IUPAC-IUB JCBN. IUPAC-IUB Joint Commission on Biochemical Nomenclature (JCBN). Nomenclature and symbolism for amino acids and peptides. Recommendations 1983 // The Biochemical journal. – 1984. – Vol. 219. – No. 2. – P. 345-73.
70. Jackson, M.P. Why are Functional Amyloids Non-Toxic in Humans? / M.P. Jackson, E.W Hewitt // Biomolecules. – 2017. – Vol. 7. – No. 4. – P. 71.
71. Jeener, J. Investigation of exchange processes by two-dimensional NMR spectroscopy / J. Jeener, B. H. Meier, P. Bachmann, R. R. Ernst // The Journal of Chemical Physics. – 1979. – Vol.71. – No. 11. – P. 4546–4553.
72. Kaiser C., Michaelis S., Mitchell A. Methods in Yeast Genetics. – NY: CSHL PRESS, 1994. – 234 pp.
73. Kajava, A. V. B-Arcades: Recurring Motifs in Naturally Occurring and Disease-Related Amyloid Fibrils / A. V. Kajava, U. Baxa, A. C. Steven // The FASEB Journal. – 2010. – Vol. 24. – No. 5. – P. 1311-1319.
74. Kajava, A.V. Evolutionary link between metazoan RHIM motif and prion-forming domain of fungal heterokaryon incompatibility factor HET-s/HET-s / A.V. Kajava, K. Klopffleisch, S. Chen, K. Hofmann // Scientific Reports. – 2014. – Vol. 4. – P. 7436.
75. Kalebina, T. Amyloid-like properties of *Saccharomyces cerevisiae* cell wall glucantransferase Bgl2 / T. Kalebina, T. Plotnikova, A. Gorkovskii, I. Selyakh, O. V. Galzitskaya, E. Bezsonov, G. Gellissen, I. Kulaev // Prion. – 2008. – Vol. 2. – No. 2. – P. 91–96.
76. Kayed, R. Molecular mechanisms of amyloid oligomers toxicity / R. Kayed, C. A. Lasagna-Reeves // Journal of Alzheimer's Disease. – 2013. – Vol. 33. – No. 1. – P. S67-

S78.

77. Kelley, J. B. Fluorescence-based quantification of nucleocytoplasmic transport / J. B. Kelley, B. M. Paschal // Methods. – 2019. – Vol. 157 – P. 106-114.
78. Khan, A. U. Role of Nucleoporins and Transport Receptors in Cell Differentiation / A. U. Khan, R. Qu, J. Ouyang, J. Dai // Frontiers in Physiology. – 2020. – P. 239-251.
79. Knowles, T. P. J. The amyloid state and its association with protein misfolding diseases / T. P. J. Knowles, M. Vendruscolo, C. M. Dobson // Nature reviews: Molecular cell biology. – 2014. – Vol. 15. – No. 6. – P. 384-396.
80. Koh, J. Allosteric regulation in gating the central channel of the nuclear pore complex / J. Koh, G. Blobel // Cell. – 2015. – Vol. 161. – No. 6. – P. 1361–1373.
81. Kryndushkin, D. S. Yeast [*PSI* $^{+}$] prion aggregates are formed by small Sup35 polymers fragmented by Hsp104 / D. S. Kryndushkin, I. M. Alexandrov, M. D. Ter-Avanesyan, V. V. Kushnirov // The Journal of biological chemistry. – 2003. – Vol. 278. – No. 49. – P. 49636-49643.
82. Kryndushkin, D. Non-targeted identification of prions and amyloid-forming proteins from yeast and mammalian cells / D. Kryndushkin, N. Pripuzova, B. G. Burnett, F. Shewmaker // Journal of Biological Chemistry. – 2013. – Vol. 288. – No. 38. – P. 27100-27111.
83. Kushnirov, V. V. Nucleotide sequence of the SUP2 (SUP35) gene of Saccharomyces cerevisiae / V. V. Kushnirov, M. D. Ter-Avanesyan, M. V. Telckov, A. P. Surguchov, V. N. Smirnov, S. G. Inge-Vechtomov // Gene. – 1988. – Vol. 66. – No. 1. – P. 45–54.
84. Kushnirov, V. V. Purification and analysis of prion and amyloid aggregates / V. V. Kushnirov, I. M. Alexandrov, O. V. Mitkevich, I. S. Shkundina, M. D. Ter-Avanesyan // Methods. – 2006. – Vol. 39. – No. 1. – P. 50-55.
85. Kushnirov, V. V. Structure and replication of yeast prions / V. V. Kushnirov, M. D. Ter-Avanesyan // Cell. – 1998. – Vol. 94. – No. 1. – P. 13-16.
86. Labokha, A.A. Systematic analysis of barrier-forming FG hydrogels from Xenopus nuclear pore complexes / A.A. Labokha, S. Gradmann, S. Frey, B.B. Hülsmann, H. Urlaub, M. Baldus, D. Görlich, // The EMBO Journal. – 2013. – Vol. 32. – P. 204–218.
87. Lasagna-Reeves, C. A. Alzheimer brain-derived tau oligomers propagate pathology from endogenous tau / C. A. Lasagna-Reeves, D. L. Castillo-Carranza, U. Sengupta, M. J. Guerrero-Munoz, T. Kiritoshi, V. Neugebauer, G. R. Jackson, R. Kayed // Scientific Reports. – 2012. – Vol. 2. – No. 1. – P. 700.
88. Lee, C. Y. D. Genetic manipulations of mutant huntingtin in mice: new insights into Huntington's disease pathogenesis / C. Y. D. Lee, J. P. Cantle, X. W. Yang // The FEBS

journal. – 2013. – Vol. 280. – No. 18. – P. 4382-4394.

89. Li, J. The RIP1/RIP3 Necrosome Forms a Functional Amyloid Signaling Complex Required for Programmed Necrosis / J. Li, T. McQuade, A. B. Siemer, J. Napetschnig, K. Moriwaki, Y. S. Hsiao, ... & H. Wu // Cell. – 2012. – Vol. 150. – No. 2. – P. 339-350.
90. Li, C. The selective permeability barrier in the nuclear pore complex / C. Li, A. Goryaynov, W. Yang // Nucleus. – 2016. – Vol. 7. – P. 430–446.
91. Liang, Y. Dynamic Association of NUP98 with the Human Genome / Y. Liang, T. M. Franks, M. C. Marchetto, F. H. Gage, M. W. Hetzer // PLOS Genetics. – 2013. – Vol. 9. – No. 2. – P. 1-14.
92. Liebman, S. W. Prions in yeast / S. W. Liebman, Y. O. Chernoff // Genetics. – 2012. – Vol. 191. – No. 4. – P. 1041-1072.
93. Louros, N.N. A common ―aggregationpronell interface possibly participates in the selfassembly of human zona pellucida proteins / N.N. Louros, E.D. Chrysina, G.E. Baltatzis, E.S. Patsouris, S.J. Hamodrakas, V.A. Iconomidou // FEBS Letters. – 2016. – Vol. 590. – No. 5. – P. 619–630.
94. Ma, J. Super-resolution 3D tomography of interactions and competition in the nuclear pore complex / J. Ma, A. Goryaynov, W. Yang // Nature Structural and Molecular Biology. – 2016. – Vol. 23. – No. 3. – P. 239-247.
95. Mackenzie, I.R. Molecular neuropathology of frontotemporal dementia: insights into disease mechanisms from postmortem studies / I.R. Mackenzie, M. Neumann // Journal of Neurochemistry. – 2016. – Vol. 138. – Suppl.1. – P. 54-70.
96. Majumdar, A. Critical role of amyloid-like oligomers of Drosophila Orb2 in the persistence of memory / A. Majumdar, W. C. Cesario, E. White-Grindley, H. Jiang, F. Ren, L. Li, ... & K. Si // Cell. – 2012. – Vol. 148. –No. 3. – P. 515-529.
97. Matiiv, A.B. Amyloid and amyloid-like aggregates: Diversity and the term crisis / A.B. Matiiv, N.P. Trubitsina, A.G. Matveenko, Y.A. Barbitoff, G.A. Zhouravleva, S.A. Bondarev // Biochemistry. – 2020. – Vol. 85. – P. 1011-1034.
98. Matveenko, A. G. SFP1-mediated prion-dependent lethality is caused by increased Sup35 aggregation and alleviated by Sis1 / A. G. Matveenko, P. B. Drozdova, M. V. Belousov, S. E. Moskalenko, S. A. Bondarev, Y. A. Barbitoff, A. A. Nizhnikov, G. A. Zhouravleva // Genes to Cells. – 2016. – Vol. 21. – No. 12. – P. 1290-1308.
99. McLaurin, J. Review: modulating factors in amyloid-□ fibril formation / J. McLaurin, D. Yang, C. M. Yip, P. E. Fraser // Journal of Structural Biology. – 2000. – Vol. 130. – No. 2/3. – P. 259-270.

100. Medina, M. The role of extracellular tau in the spreading of neurofibrillary pathology / M. Medina, J. Avila // Frontiers in cellular neuroscience. – 2014. – Vol. 8. – P. 113.

101. Meyer-Luehmann, M. Exogenous induction of cerebral ß-amyloidogenesis is governed by agent and host / M. Meyer-Luehmann, J. Coomaraswamy, T. Bolmont, S. Kaeser, C. Schaefer, E. Kilger, ... & M. Jucker // Science. – 2006. – Vol. 313. – No. 2006. – P. 1781-1784.

102. Meriin, A. B. Endocytosis machinery is involved in aggregation of proteins with expanded polyglutamine domains / A. B. Meriin, X. Zhang, I. M. Alexandrov, A. B. Salnikova, M. D. Ter-Avanesian, Y. O. Chernoff, M. Y. Sherman // FASEB Journal. – 2007. – Vol. 21. – No. 8. – P. 1915-1925.

103. Michelitsch, M.D. A census of glutamine/asparagine-rich regions: implications for their conserved function and the prediction of novel prions / M.D. Michelitsch, J.S. Weissman // Proceedings of the National Academy of Sciences. – 2000. – Vol. 97. – No. 22. – P.11910-11915.

104. Milles, S. Facilitated aggregation of FG nucleoporins under molecular crowding conditions / S. Milles, K. Huy Bui, C. Koehler, M. Eltsov, M. Beck, E.A. Lemke // EMBO Reports. – 2013. – Vol. 14. – P. 178–183.

105. Milles, S. Single molecule study of the intrinsically disordered FG-repeat nucleoporin 153 / S. Milles, E.A. Lemke // Biophysical Journal. – 2011. – Vol. 101. – No. 7. – P. 1710-1719.

106. Morales, R. *De novo* induction of amyloid-β deposition *in vivo* / R. Morales, C. Duran-Aniotz, J. Castilla, L. D. Estrada, C. Soto // Molecular psychiatry. – 2012. – Vol. 17. – No. 12. – P. 1347-53.

107. Murakami, T. Experimental induction and oral transmission of avian AA amyloidosis in vaccinated white hens / T. Murakami, N. Muhammad, Y. Inoshima, T. Yanai, M. Goryo, N. Ishiguro // Amyloid. – 2013. – Vol. 20. – No. 2. – P. 80-85.

108. Nenninger, A. A. Localized and efficient curli nucleation requires the chaperone-like amyloid assembly protein CsgF / A. A. Nenninger, L. S. Robinson, S. J. Hultgren // Proceedings of the National Academy of Sciences. – 2009. – Vol. 106. – No. 3. – P. 900–905.

109. Nizhnikov, A. A. Proteomic screening for amyloid proteins / A. A. Nizhnikov, A. I. Alexandrov, T. A. Ryzhova, O. V. Mitkevich, A. A. Dergalev, M. D. Ter-Avanesyan, A. P. Galkin // PLoS ONE. – 2014. – Vol. 9. – No. 12. – P. 1-18.

110. Nouspikel T.When parsimony backfires: neglecting DNA repair may doom neurons in Alzheimer's disease / T. Nouspikel, P.C. Hanawalt // Bioessays. – 2003. – Vol. 25. –

No. 2. – P. 168-73.

111. Oh, J. Amyloidogenesis of type III-dependent harpins from plant pathogenic bacteria / J.Oh, J. G. Kim, E. Jeon, C. H. Yoo, S. M. Jae, S. Rhee, I. Hwang // Journal of Biological Chemistry. – 2007. – Vol. 282. – No. 18. – P. 13601-13609.

112. Okonechnikov, K. Unipro UGENE: A unified bioinformatics toolkit / K. Okonechnikov, O. Golosova, M. Fursov, & Ugene Team // Bioinformatics. – 2012. – Vol. 28. – No. 8. – P. 1166–1167.

113. Oli, M. W.. Functional amyloid formation by *Streptococcus mutans* / M. W. Oli, H. N. Otoo, P. J. Crowley, K. P. Heim, M. M. Nascimento, C. B. Ramsook, P. N. Lipke, L. J. Brady // Microbiology (United Kingdom). – 2012. – Vol. 158. – No. 12. – P. 2903-2916.

114. Olsén, A. The RpoS Sigma factor relieves H-NS-mediated transcriptional repression of csgA, the subunit gene of fibronectin- binding curli in *Escherichia coli* / A. Olsén, A. Arnqvist, M. R. Hammar, S. Sukupolvi, S. Normark // Molecular Microbiology. – 1993. – Vol. 7. – No. 4. – P. 523-536.

115. Olsén, A. Fibronectin binding mediated by a novel class of surface organelles on *Escherichia coli* / A. Olsén, A. Jonsson, S. Normark // Nature. – 1989. – Vol. 338. – No. 6217. – P. 652-655.

116. Onischenko, E. Natively unfolded FG repeats stabilize the structure of the nuclear pore complex / E. Onischenko, J.H. Tang, K.R. Andersen, K.E. Knockenhauer, P. Vallotton, C.P. Derrer, A. Kralt, C.F. Mugler, L.Y. Chan, T.U. Schwartz // Cell. – 2017. – Vol. 171. – P. 904–917.

117. Oughtred, R. The BioGRID database: A comprehensive biomedical resource of curated protein, genetic, and chemical interactions / R. Oughtred, J. Rust, C. Chang, B.J. Breitkreutz, C. Stark, … & Tyers M. // Protein Science. – 2021. – Vol. 30. – No. 1. – P. 187-200.

118. Patel, S.S. Natively unfolded nucleoporins gate protein diffusion across the nuclear pore complex / S.S. Patel, B.J. Belmont, J.M. Sante, M.F. Rexach // Cell. – 2007. – Vol.129. – No. 1. – P. 83-96.

119. Petri, M. Structural characterization of nanoscale meshworks within a nucleoporin FG hydrogel / M. Petri, S. Frey, A. Menzel, D. Gorlich, S. Techert // Biomacromolecules. – 2012. – Vol. 13. – P. 1882–1889.

120. Picken, M. M. The Pathology of Amyloidosis in Classification: A Review / M. M. Picken // Acta Haematologica. – 2020. – Vol. 60153. – P. 1-13.

121. Prusiner, S. B. Prions causing degenerative neurological diseases / S. B. Prusiner //

Annual review of medicine. – 1987. – Vol. 38. – P. 381-398.

122. Prusiner, S. B. Creutzfeldt-Jakob disease and scrapie prions / S. B. Prusiner // Alzheimer disease and associated disorders. – 1989. – Vol. 3. - No. 1/2. – P. 52-78.

123. R Core Team. R: A language and environment for statistical computing. R foundation for statistical computing [Electronic resource] / R Core Team / / R Found. Stat. Comput. URL: https://www.R-project.org/

124. Rencus-Lazar S. Yeast Models for the Study of Amyloid-Associated Disorders and Development of Future Therapy / Y. DeRowe, H. Adsi, E. Gazit, D. Laor // Frontiers in Molecular Biosciences. – 2019. – Vol. 6. – P. 15.

125. Riek, R. The HET-S/s Prion Motif in the Control of Programmed Cell Death / R.Riek, S. Saupe // Cold Spring Harbor Perspectives in Biology. – 2016. – Vol. 8. – No. 9. – P. 1-11.

126. Roche, D. B. Usage of a dataset of NMR resolved protein structures to test aggregation versus solubility prediction algorithms / D. B. Roche, E. Villain, A. V. Kajava // Protein Science. – 2017. – Vol. 26. – No. 9. – P. 1864–1869.

127. Romero, D. Amyloid fibers provide structural integrity to *Bacillus subtilis* biofilms / D. Romero, C. Aguilar, R. Losick, R. Kolter // Proceedings of the National Academy of Sciences. – 2010. – Vol. 107. – No. 5. – P. 2230-2234.

128. Romero, D. Functional amyloids in bacteria / D. Romero, R. Kolter // International Microbiology. – 2014. – Vol. 17. – No. 2. – P. 65-73.

129. Ruan Q.X. An investigation into the effect of potassium ions on the folding of silk fibroin studied by generalized two-dimensional NMR–NMR correlation and Raman spectroscopy / Q.X. Ruan, P. Zhou, B.-W. Hu, D. Ji // FEBS Journal. – 2008. – Vol. 275. – P. 219-232.

130. Rubel, A. Identification of PrP sequences essential for the interaction between the PrP polymers and A□ peptide in a yeast-based assay / A. Rubel, T. Ryzhova, K. S. Antonets, Y. Chernoff, A. Galkin // Prion. – 2013. – Vol. 7. – No. 6. – P. 469-476

131. Sambrook, J. Molecular cloning: a laboratory manual, second edition. — NY: Cold Spring Harbor Laboratory Press, Cold Spring Harbour, New York, 1989.

132. Sarantseva, S. Apolipoprotein E-mimetics inhibit neurodegeneration and restore cognitive functions in a transgenic drosophila model of Alzheimer's disease / S. Sarantseva, S. Timoshenko, O. Bolshakova, E. Karaseva, D. Rodin, A. L. Schwarzman, M. P. Vitek // PLoS ONE. – 2009. – Vol. 4. – No. 12. - P. e8191.

133. Schilling, G. Intranuclear inclusions and neuritic aggregates in transgenic mice expressing a mutant N-terminal fragment of huntingtin / G. Schilling, M. W. Becher, A.

H. Sharp, H. A. Jinnah, K. Duan, J. A. Kotzuk, ... & D. R. Borchelt // Human Molecular Genetics. – 1999. – Vol. 8. – No. 3. – P. 397-407.

134. Schaffert, L.N. Do Post-Translational Modifications Influence Protein Aggregation in Neurodegenerative Diseases: A Systematic Review / L.N. Schaffert, W.G. Carter // Brain Sciences. – 2020. – Vol. 10. – No. 4. – P. 232.

135. Schmidt, H.B. Transport selectivity of nuclear pores, phase separation, and membraneless organelles / H.B. Schmidt, D. Görlich // Trends in Biochemical Sciences. – 2016. – Vol. 41. – P. 46–61.

136. Schneider, C. A. NIH Image to ImageJ: 25 years of Image Analysis / C. A. Schneider, W. S. Rasband, K. W. Eliceiri // Nature Methods. – 2012. – Vol. 9. – No. 7. – P. 671–675.

137. Schwartz, K. Functional amyloids composed of phenol soluble modulins stabilize *Staphylococcus aureus* biofilms / K. Schwartz, A. K. Syed, R. E. Stephenson, A. H. Rickard, B. R. Boles // PLoS Pathogens. – 2012. – Vol. 8. – No. 6. – P. e1002744.

138. Selkoe, D. J. Alzheimer's Disease / D. J. Selkoe // Cold Spring Harbor Perspectives in Biology. – 2011. – Vol. 3. – No. 7. – P. 4457-4457.

139. Serio, T. R. Yeast prion [PSI^{+}] and its determinant, Sup35p / T. R. Serio, A.G. Cashikar, J. J. Moslehi, A. S. Kowal, S. L. Lindquist // Methods in Enzymology. – 1999. – Vol. 309. – P. 649-673.

140. Shahnawaz, M. Microcin amyloid fibrils A are reservoir of toxic oligomeric species / M. Shahnawaz, C. Soto // Journal of Biological Chemistry. – 2012. – Vol. 287. – No. 15. – P. 11665-11676.

141. Sharma, A. Ordered regions of channel nucleoporins Nup62, Nup54, and Nup58 form dynamic complexes in solution / A. Sharma, S. R. Solmaz, G. Blobel, I. Melčák // Journal of Biological Chemistry. – 2015. – Vol. 290. – No. 30. – P. 18370-18378.

142. Shewmaker, F. Structural Insights into Functional and Pathological Amyloid / F. Shewmaker, R. P. Mcglinchey, R. B. Wickner // The Journal of biological chemistry. – 2011. – Vol. 286. – No. 19. – P. 16533-16540.

143. Si, K. Aplysia CPEB can form prion-like multimers in sensory neurons that contribute to long-term facilitation / K. Si, Y. B. Choi, E. White-Grindley, A. Majumdar, E. R. Kandel // Cell. – 2010. – Vol. 140. – No. 3. – P. 421-435.

144. Siniukova, V.A. Search for functional amyloid structures in chicken and fruit fly female reproductive cells / V.A. Siniukova, J.V. Sopova, S.A. Galkina, A.P. Galkin // Prion. – 2020. – Vol. 14. – No. 1. – P. 278–282.

145. Sipe, J. D. Amyloid fibril proteins and amyloidosis: chemical identification and

clinical classification International Society of Amyloidosis 2016 Nomenclature Guidelines / J. D. Sipe, M. D. Benson, J. N. Buxbaum, S.-I. Ikeda, G. Merlini, M. J. M. Saraiva, P. Westermark // Amyloid. – 2016. – Vol. 23. – No. 4. – P. 209-213.

146. Sivanathan, V. A bacterial export system for generating extracellular amyloid aggregates / V .Sivanathan, A. Hochschild // Nature protocols. – 2013. – Vol. 8. – No. 7. – P. 1381–1390.

147. Sopova, J.V. RNA-binding protein FXR1 is presented in rat brain in amyloid form / J.V. Sopova, E.I. Koshel, T.A. Belashova, S.P. Zadorsky, A.V. Sergeeva, V.A. Siniukova, A.A. Shenfeld, M.E. Velizhanina, K.V. Volkov, A.A. Nizhnikov // Scientific Reports. – 2019. – Vol. 9. – P. 18983.

148. Stephan, J.S.The CPEB3 protein is a functional prion that interacts with the actin cytoskeleton / J.S. Stephan, L. Fioriti, N. Lamba, L. Colnaghi, K. Karl, I.L. Derkatch, E.R. Kandel // Cell Reports. – 2015. – Vol. 11. – P. 1772–1785.

149. Studier, F. Use of bacteriophage T7 RNA polymerase to direct selective high-level expression of cloned genes / F. Studier, B. A. Moffatt // Journal of Molecular Biology. – 1986. – Vol. 189. – No. 1. – P. 113-130.

150. Sugiyama, S. Self-propagating amyloid as a critical regulator for diverse cellular functions / S. Sugiyama, M. Tanaka // Journal of Biochemistry. – 2014. – Vol. 155. – No. 6. – P. 345-351.

151. Swinnen, B. The phenotypic variability of amyotrophic lateral sclerosis / B. Swinnen, W. Robberecht // Nature Reviews Neurology. – 2014. – Vol. 10. – No. 11. – P. 661-670.

152. Syed, A. K. Fold modulating function: Bacterial toxins to functional amyloids / A. K. Syed, B. R. Boles // Frontiers in Microbiology. – 2014. – Vol. 5. – P. 1-10.

153. Taylor, J.P. Decoding ALS: from genes to mechanism / J.P. Taylor, R.H. Jr. Brown, D.W. Cleveland // Nature. – 2016. – Vol. 539. – No. 7628. – P. 197-206.

154. Taylor, J.P. Toxic proteins in neurodegenerative disease / J.P. Taylor, J. Hardy, K.H. Fischbeck // Science. – 2002. – Vol. 296. – No. 5575. – P.1991-1995.

155. Terry, L.J. Flexible gates: dynamic topologies and functions for FG nucleoporins in nucleocytoplasmic transport / L.J. Terry, S.R Wente. // Eukaryotic Cell. – 2009. – Vol. 8. – No. 12. – P. 1814-1827.

156. Tipping, K. Amyloid Fibres: Inert EndStage Aggregates or Key Players in Disease? / K. Tipping, P. V. Oosten-Hawle, E. Hewitt, S. Radford // Trends in Biochemical Sciences – 2015. – Vol. 40. – No. 12. – P. 719-727.

157. Toombs, J.A. Compositional determinants of prion formation in yeast / J.A. Toombs,

B.R. McCarty, E.D. Ross // Molecular Biology of the Cell. – 2010. – V. 30. – No. 1. – P. 319-332.

158. Von Der Haar, T. Development of a novel yeast cell-based system for studying the aggregation of Alzheimer's disease-associated A□ peptides *in vivo* / T. Von Der Haar, L. Joss´e, P. Wright, J. Zenthon, M. F. Tuite // Neurodegenerative Diseases. – 2007. – Vol. 4. – No. 2/3. – P. 136-147.

159. Vonsattel, J. P. G. Huntington Disease / J. P. G. Vonsattel, M. Difiglia // Journal of Neuropathology & Experimental Neurology. – 1998. – Vol. 57. – No. 5. – P. 369-384.

160. Walczak, H. TNF and ubiquitin at the crossroads of gene activation, cell death, inflammation, and cancer / H. Walczak // Immunological Reviews. – 2011. – Vol. 244. – No. 1. – P. 9-28.

161. Wang, L. Empirical correlation between protein backbone 15N and 13C secondary chemical shifts and its application to nitrogen chemical shift re-referencing / L. Wang, J.L. Markley // Journal of Biomolecular NMR. – 2009. – Vol. 44. – No 2. – P. 95-99.

162. Westermark, G. T. Serum amyloid A and protein AA: Molecular mechanisms of a transmissible amyloidosis / G. T. Westermark, P. Westermark // FEBS Letters. – 2009. – Vol. 583. – No. 16. – P. 2685-2690.

163. Winklhofer, K. F. The two faces of protein misfolding: gain- and loss-of-function in neurodegenerative diseases / K. F. Winklhofer, J. Tatzelt, C. Haass // The EMBO Journal. – 2008. – Vol. 27. – No. 2. – P. 336-349.

164. Xu, L. Nucleoporin 35 regulates cardiomyocyte pH homeostasis by controlling Na+-H+ exchanger-1 expression / L. Xu, L. Pan, J. Li, B. Huang, J. Feng, C. Li, ... & Y. H. Chen // Journal of Molecular Cell Biology. – 2015. – Vol. 7. – No. 5. – P. 476-485.

165. Yang, J. Gating pluripotency via nuclear pores / J. Yang, N. Cai, F. Yi, G.H. Liu, J. Qu, J.C. Izpisua Belmonte // Trends in Molecular Medicine. – 2014. – Vol. 20. – No.1. – P. 1-7.

Acknowledgements

I would like to express my deep gratitude to Stanislav Alexandrovich Bondarev for his sensitive guidance, patient attitude, methodological advice, and comprehensive assistance in planning experiments, conducting them, and writing the paper.

I would like to thank Andrey Georgievich Matveenko for providing plasmids and strains, and Svetlana Yevgenyevna Moskalenko for providing theNUP58 protein repair kit, as well as for their help and advice in conducting experimental work. I would like to thank Mikhail Vladimirovich Belousov for his help in visualizing fibrils using transmission electron microscopy. I would like to thank Tatyana Mikhailovna Rogoza for her help with the construction of plasmids.

I would like to thank Natalia V. Loseva for her help with experiments on nuclear cytoplasmic transport. I would like to thank Ksenia Vladimirovna Sukhanova and Ekaterina Antonova for their help with the experiments and the design of the results. I would like to thank both Stanislav Alexandrovich Bondarev and Galina Anatolyevna Zhuravleva for their valuable methodological advice and materials. I would also like to thank Andrey Vilkhovich Kayav for providing the ArchCandy program.

I would like to thank Maria Velizhanina for her help in mastering the technique of staining proteins with Congo red dye and working with a polarizing microscope. For providing material for isolation of Danil V. Kachkin and Svetlana Anatolyevna Galkina for providing biomaterial for cDNA isolation. Yulia Viktorovna Sopova for repeatedly reviewing interim reports and providing valuable comments when reading my work.

I would like to express my gratitude to the entire staff of the Laboratory of Physiological Genetics for their support, warm attitude and creation of a wonderful working atmosphere.

I would also like to thank my wife, Alexandra Artemovna Danilova, for her boundless patience and great support in writing my dissertation. I would also like to express my gratitude to my parents for their support and advice during my postgraduate studies and when writing my dissertation.